**Title**
The mechanics and functional consequences of hyphal fusion in Neurospora crassa; from genes to nutrient and nuclear translocation



**Author**
Simonin, Anna Ruth

**Publication Date**
2011

Peer reviewed|Thesis/dissertation

# The mechanics and functional consequences of hyphal fusion in *Neurospora crassa;* from genes to nutrient and nuclear translocation

By

Anna Ruth Simonin

A dissertation submitted in partial satisfaction of the
requirements for the degree of

Doctor of Philosophy

In

Plant Biology

in the

Graduate Division

of the

University of California, Berkeley

Committee in charge:

Chair Professor N. Louise Glass
Professor Thomas Bruns
Professor Sheila McCormick
Professor Todd Dawson

Spring 2011

Abstract

The mechanics and functional consequences of hyphal fusion in *Neurospora crassa;* from genes to nutrient and nuclear translocation

By

Anna Ruth Simonin

Doctor of Philosophy in Plant Biology

University of California, Berkeley

N. Louise Glass, Chair

Cell-cell fusion is integral in many developmental processes in eukaryotic organisms. In filamentous fungi, such as *Neurospora crassa,* hyphal anastomoses within the mycelium allows for the development of an interconnected network, which is thought to be important for colony homeostasis. Hyphal anastomosis mutants have altered body plans, but it is unclear how this affects colony functions such as nuclear and nutrient movement. In this study we characterize two new hyphal anastomosis muntants, *ham-3* and *ham-4*. In addition we explore nuclear movement and mechanisms of nuclear dispersal in wild type colonies as well as a fusion mutant *soft*. Finally, we determine the influence of vegetative hyphal fusion on the movement of amino acids within a mycelium. Chapter one is a detailed review of the genetics and cell biology of hyphal fusion as well as the link between hyphal architecture and functionality in filamentous fungi.

In chapter two, novel *N. crassa* hyphal anastamosis mutants *ham-3* and *ham-4,* are identified and characterized. *ham-3* encodes a striatin - like homolog and *ham-4* encodes a protein that contains a forkhead-associated (FHA) domain. Deletions of both genes cause severe fusion frequency decreases in conidial germlings, similar to a previously identified fusion mutant *ham-2*. In both yeast and humans striatin homologs, *ham-2* homologs, and proteins containing FHA domains, interact in a complex which is thought to be involved in intracellular signalling and trafficking. We show that *ham-2, ham-3,* and *ham-4* all have similar fusion defects indicating they might act in the same complex or pathway. In addition to fusion defects, homozygous crosses of *ham-2, ham-3,* and *ham-4* exhibit aberrant meiosis resulting in abnormally shaped ascospores. *ham-2* and *ham-3* are female sterile, but *ham-4* is female fertile. All three mutants are male fertile, and can undergo trichogyne/condium sexual fusion as a female. We suspect that the HAM-2,3,and 4 interact in a larger complex with a phocein homolog, MOB-3, to facilitate vegetative fusion

and sexual development in *N. crassa.*

In chapter three, profiles of nuclear movement in *N. crassa* colonies were measured and described. Filamentous fungi have the ability to harbour multiple, genetically distinct nuclei in a common cytoplasm. These nuclei have free movement due to open septal pores large enough for nuclei to move through. In other fungal systems, this leads to sectoring of the population and single nuclear origin for homogeneous regions of expanding colonies. In *N. crassa* wild type colonies*,* we found that genetically different nuclei are well mixed through out the greater mycelium maintaining diversity of nuclear lineages. The distribution and nuclear velocities in a colony are maintained by a pressure source from growing hyphal tips driving nuclei through interconnected hyphae with different conductivities. When an alternative pressure, such as osmotic pressure is added to the system, nuclei can reverse flow toward the pressure source in a profile almost the mirror image of the forward movement profile. In addition nuclei toward the center of hyphae move faster relative to nuclei at the edges of the hypha indicating a pressure driven flow. We find that hyphal fusion also affects the flow profiles of *N. crassa* colonies. Fusion mutant *soft* has a nuclear velocity profile that reflects a hierarchical branching architecture where larger “feeder” hyphae supply nuclei to a multitude of tips.

Finally, in chapter four, the role of hyphal fusion in resource translocation is assessed. Nutrient translocation in fungi is necessary for biomass recycling in forest ecosystems, mycorrhizal associations, and substrate degradation. Maintenance of an interconnected network is thought to be necessary for intracolony communication and homeostasis. We tested whether the frequency of hyphal fusion influenced the translocation of $^{15}N$ and $^{14}C$ labeled 2-amino isobutyric acid (AIB) in *N. crassa* colonies. Two fusion mutants, *soft,* that has no vegetative hyphal fusion and *prm-1,* which has about a 50% fusion frequency as compared to wild type, were used to test amino acid translocation. Both *soft* and *prm-1* have similar maximum growth rates as wild type but only *soft* showed a severe defect in translocation of the tracers. In addition we found that there is little reverse translocation in all of the strains. All of the strains had a greater level of total percent N at the tips of the colonies compared to other parts of the colony and *soft* had a more negative natural abundance $^{13}C$. In addition we found that though germlings readily fuse and share resources, colonies greater than 0.5 cm in radius, cease to share resources. Developmental age affects resource sharing between colonies.

*To my husband, Kevin. You are an inspiration and I love you very much.*

* * *

*To my parents, my sister and her family, and all the friends and family who have provided love and support along the way.*

* * *

*To my grandparents, amazing people who inspired the pursuit of knowledge and education in their children and grandchildren*

Acknowledgments:

Thank you to everyone in the Glass lab for listening and providing feedback on presentations, papers, and projects. You made working in the lab a great experience and I will miss having such a wonderful community of scientists to work with. I want to thank Louise Glass for her mentoring, advice, and moral support during the last six years. I especially want to thank Betsy Hutschison, Charles Hall, Jian Ping Sun, Abby Leeder, Chauguong Tian, Takao Kasuga and Andre Fleissner for patiently answering all the 'stupid' questions I had to ask and for their insights and help on my projects. In addition I want to thank Marcus Roper for being an amazing collaborator and mentor. Who knew mathematics could be so interesting?

I want to thank my committee for all their mentoring and advice, the PMB staff who make our department run smoothly , and Steve Ruzin and Denise Schichnes at the CNR Bioimaging Facility.

I want to thank my friends and family for supporting my throughout my dissertation. First and foremost I want to thank my husband, Kevin, for being my best friend and greatest advocate. I wouldn't have been able to do this without you. You keep me laughing, sane, and enjoying life and I love you very much.

Thanks to all my friends in the lab, the department, and all over the country for listening. You are irreplaceable! Thanks to Betsy and our countless coffee breaks, long runs, and girls nights out. You are an amazing friend and I am so happy that we were able to complete our dissertations together, I can't imagine having a better companion. Thanks to Laurie for all the great television, books, and bottles of bubbly we've shared together over the years, you are a wonderful friend. Madelaine, thanks for being the voice of reason when I'm going crazy, and I always look forward to our chats, your crazy stories and lots of laughs. Abby, thanks for being both my science and cocktail buddy, you are always there to help out and I really appreciate it. Thanks to Elaine and Ksenia and the rest of the cookie club, I looked forward to seeing you all every week. Thanks to the bakery girls, Elise and Melanie for being such great friends when I first moved to Berkeley. Ryan, Krista, Curtis, SME, Dave and Sarah, thanks for all the fun Thanksgiving meals and Ryan and Krista for camping trips and dog watching.

I want to thank my parents for always believing in me and supporting me in all my endeavors. Thank you for introducing me to the natural world and science as a child, I love you and I hope I've made you proud. Thanks to my sister Jess for sticking with me even when I'm being a brat, you are a wonderful and supportive sister. Thanks to my bother-in-law Max and my nephews for keeping me laughing and smiling. Thanks to my in-laws the Simonins for welcoming me into their family, and supporting both Kevin and I through our dissertations. Beck, thanks for being like a sister to me through out my life and my dissertation, maybe one of these days we'll be back in the same state again! Until then....skype!

**Chapter One**: Cell fusion in the filamentous fungus,*Neurospora crassa*

This chapter was previously published in Methods in Molecular Biology under the following reference: Fleissner, A., Simonin, A.R., and Glass, N.L. (2008) Cell fusion in the filamentous fungus, *Neurospora crassa*. Methods Mol Biol *475*, 21-38. New sections were added after the acknowledgements of the published review.

**Summary**
Hyphal fusion occurs at different stages in the vegetative and sexual life cycle of filamentous fungi. Similar to cell fusion in other organisms, the process of hyphal fusion requires cell recognition, adhesion and membrane merger. Analysis of the hyphal fusion process in the model organism *Neurospora crassa* using fluorescence and live cell imaging as well as cell and molecular biological techniques has begun to reveal its complex cellular regulation. Several genes required for hyphal fusion have been identified in recent years. While some of these genes are conserved in other eukaryotic species, other genes encode fungal-specific proteins. Analysis of fusion mutants in *N. crassa* has revealed that genes previously identified as having non-fusion related functions in other systems, have novel hyphal fusion functions in *N. crassa*. Understanding the molecular basis of cell fusion in filamentous fungi provides a paradigm for cell communication and fusion in eukaryotic organisms. Furthermore, the physiological and/or developmental role of hyphal fusion is not understood in these organisms; identifying these mechanisms will provide insight into environmental adaptation.

## 1. Introduction

Filamentous ascomycete fungi, such as *Neurospora crassa,* typically form mycelial colonies consisting of a network of interconnected, multinucleate hyphae. Colonies grow by hyphal tip extension, branching and fusion (Buller 1933, Glass et al 2004). In filamentous ascomycete species, hyphal crosswalls or septa are incomplete and contain a single central pore. Septal pores allow cytoplasm and organelles, including nuclei, to move between hyphal compartments, thus making the fungal colony a syncytium. The syncytial, interconnected, organization of a fungal colony enables translocation of cellular contents, such as organelles, metabolites, nutrients or signaling compounds throughout the colony, presumably facilitating growth and reproduction.

Cell fusion events occur during all stages of the filamentous fungal lifecycle (Glass and Fleißner 2006). These fusion events serve different purposes during the establishment and development of fungal colonies. During vegetative growth, germling fusion events between germinating, and even apparently ungerminated, asexual spores (conidia) are correlated with faster colony establishment (Fig. 1-1A) (Kohler 1930, Rocca et al. 2003). Fusion between hyphal branches within a mature fungal colony results in the formation of a network of interlinked hyphae (Buller 1933, Rayner 1996) (Fig. 1B). Germling or hyphal fusion between genetically different, but heterokaryon-compatible individuals leads to the formation of colonies containing genetically different nuclei (heterokaryon). Within heterokaryons, non-meiotic or parasexual recombination can result in the formation of new genotypes (Potecorvo 1956), which possibly contribute to the high adaptability of fungal species that lack sexual reproduction. In the sexual phase of the life cycle, cell fusion between male and female reproductive structures is essential for mating in out-breeding species (Bistis 1981) (Fig. 1-1C). After mating, cell fusion is associated with ascus formation (Fig. 1-1D), the cell in which karyogamy and meiosis occur (Raju 1980). Whether common cell fusion machinery is involved in both sexual and vegetative fusion events in filamentous fungi remains an unsolved question.

Fusion processes in filamentous fungi are comparable to cell fusion events in other eukaryotic organisms. Examples include fertilization events between egg and sperm or somatic cell fusion that result in syncytia (e.g. between myoblasts during muscle differentiation, between macrophages in osteoclast and giant cell formation, and during placental development) (Chen and Olson 2004, Primakoff and Miles 2007, Dworak and Sink 2002, Potgens et al. 2002). Although cell fusion events occur in a diversity of species and cell types, they require very similar cellular processes, such as cell recognition, adhesion and membrane merger. Although in many cases cell types involved in fusion are genetically or physiologically different, such as cell fusion during mating in *N. crassa*, vegetative hyphal fusion occurs between genetically and probably physiologically identical cells. Understanding the molecular basis of hyphal fusion provides a paradigm for self-signaling in eukaryotic cells and provides a useful comparative model for somatic cell fusion events in other eukaryotes. The model organism *N. crassa* is methodically tractable (Davis 2000, Perkins et al. 2001, Colot et al. 2006), thus allowing the direct comparison of the molecular basis of

hyphal and cell fusion events during its life cycle.

## 2. Vegetative Cell Fusion

### 2.1 Germling Fusion

The life of a fungal individual often begins with the germination of an asexual spore, termed conidium. When multiple conidia are placed close to one another, numerous germling fusion events are observed (Roca et al. 2003, Roca et al. 2005). As a result, numerous individual germlings become one functional unit, which subsequently develops into a mycelial colony. Germinating conidia can fuse by germ tube fusion (Fig. 1-1A) or by the formation of small hyphal bridges ("Fusionshyphen" or "conidial anastomosis tubes (CATs)), which are significantly narrower than germ tubes (Kohler 1930, Roca et al. 2003, Pandey et al. 2004). Fusion events among conidia show a density- and nutrient-dependent function; fusion is suppressed on nutrient rich media. The merger of initially individual cells into functional units in response to environmental cues is not only found in fungi but also in other species such as the social amoeba of Dictyostelid slime molds (Manahan et al. 2004).

### 2.2 Hyphal Fusion

After germlings create a fused hyphal network, hyphal exploration extends outward from the conidia, thus taking on the morphological aspects of a typical fungal colony (Buller 1933, Glass et al 2004). In *N. crassa* and other filamentous ascomycete species, the frequency of hyphal fusion within a vegetative colony varies from the periphery to the interior of the colony (Hickey et al. 2002). At the periphery, hyphae grow straight out from the colony and exhibit avoidance (negative autotropism), presumably to maximize the outward growth of the colony (Trinci 1984). In the inner portion of a colony, hyphae show a different behavior. Instead of avoidance, certain hyphae or hyphal branches show attraction, directed growth and hyphal fusion (Buller 1933, Hickey et al. 2002, Kohler 1929) (Fig. 1-2). Similar to germling fusion, the frequency of hyphal fusion events depends on the availability of nutrients. Generally speaking the following rule applies: the fewer nutrients, the more fusion events (Kohler 1930, Ahmad and Miles 1970, Yokoyama and Ogoshi 1988). For example, addition of nitrogen to nutrient-poor media led to the largest decrease in hyphal fusion frequency in *Rhizoctonia sp.* (Yokoyama and Ogoshi 1988 ).

### 2.3 Mechanistic aspects of germling and hyphal fusion

Mechanistically, the process of germling and hyphal fusion can be divided into three steps: 1. pre-contact; 2. contact, adhesion and cell wall breakdown; 3. pore formation and cytoplasmic flow (Glass et al. 2004, Hickey et al. 2002, Glass et al. 2000) (Fig.1-2).

#### 2.3.1 Pre-contact

The observed attraction between conidial germlings or fusion hyphae suggests chemotropic interactions between the fusion partners. When the relative position of two germlings showing mutual attraction is changed by micromanipulation using optical tweezers, both individuals readjust their growth

towards each other to make contact and undergo fusion (Roca et al. 2005, Fleissner et al. 2005). During hyphal fusion, the presence of a fusion-competent hypha often results in either the alteration of growth trajectory or the formation of fusion branches in a receptive hypha (Buller 1933, Kohler 1930, Hickey et al. 2002) (Fig. 1-2).

The secretion of signaling molecules is a common theme in chemotactic and chemotropic cellular interactions. Instances of cell-cell communication by diffusible substances leading to cell fusion include mating in the unicellular yeast species, *Saccharomyces cerevisiae*, pollen tube growth to the ovary in plant species, or egg-sperm interaction in animals. Mating in *S. cerevisiae* requires two cells of opposite mating type. Haploid cells secrete mating-type specific pheromones, which bind to their cognate plasma membrane receptors in a partner of the opposite mating type (Kurjan 1993). Germinating pollen tubes are also thought to be guided by diffusible chemotropic substances, such as $Ca^{2+}$ or small heat stable molecules secreted by the style (Lord 2003, Mascaretihas 1993). Another diffusible substance that is released by synergid cells, guides the pollen tube once it reaches the ovary (Higashiyama et al. 2003). The eggs of many aquatic animal species also release chemotactic substances to attract sperm, for example, *Xenopus* egg jelly releases a cysteine-rich secretory protein, allurin, to attract sperm (Al-Anzi and Chandler 1998). In these examples, the fusion partners are genetically and/or physiologically distinct and either secret different signaling molecules (such as mating-type specific pheromones) or only one partner secretes a signal that results in the attraction of the other partner. While the involvement of secreted signals is not clear in other systems, such as in myoblast fusion during muscle development, in most cases the fusing cells are also different, such that one partner presents an extracellular or surface attractant and the other grows or migrates towards it. In *N. crassa,* there is no evidence that cells that undergo germling and hyphal fusion are genetically or physiologically different. Both cells show chemotropic interactions, indicating that both are secreting and responding to a chemotropic signal. This scenario is somewhat similar to cAMP signaling in *Dictyostelium discoideum*, where a gradient of cAMP mediates attraction of individual cells during the initiation of asexual sporulation (Manahan et al. 2004). However, in *D. discoideum*, all cells responds to the chemotactic signal, whereas in *N. crassa*, only cells/hyphae destined to fuse do so. The identity of the molecules that mediate chemotropic interactions during germling/hyphal fusion in any filamentous fungus, including *N. crassa*, remains enigmatic.

The chemotropic re-orientation of hyphae destined to fuse is associated with alterations in the position of the Spitzenkörper, or with the formation of a new Spitzenkörper associated with branch formation in the receptive hypha (Hickey et al. 2002) (Fig. 1-2A,B). The Spitzenkörper is a vesicle rich structure found in growing hyphal tips or at sites of branch initiation (Hickey et al. 2002, Riquelme et al. 1998). Localization of the Spitzenkörper in the hyphal apex has been associated with directionality of growth. In hyphae showing chemotropic interactions prior to hyphal fusion, the Spitzenkörper in the two partner hyphae continually re-orient toward each other until the point of contact (Fig. 1-2B, C).

Re-orientation of the Spitzenkörper and polar hyphal extension towards the fusion partner requires cellular mechanisms linking reception of the fusion signal to re-organization of the cytoskeleton. Adjustment of hyphal growth towards the fusion partner is comparable to cell polarization and schmoo formation during yeast mating (Kurjan 1993), directed pollen tube growth towards the ovary (Higashiyama et al. 2003) or the extension and/or stabilization of filopodia during myoblast fusion (Chen and Olson 2004).

### 2.3.2 Contact, adhesion and cell wall breakdown

After making contact, hyphae involved in fusion switch from polar to isotropic growth, resulting in swelling of hyphae at the fusion point. The two Spitzenkörpers of the fusion hyphae are juxtaposed at the point of contact (Fig. 1-2C) (Hickey et al. 2002). During chemotropic interactions, vesicles targeted to the Spitzenkörper are associated with hyphal growth. However, once contact occurs, vesicles secreted to the hyphal tips via the the Spitzenkörper must be involved in the cell wall degradation at the site of fusion. The localization of the two Spitzenkörpers in the fusion hyphae resembles the prefusion complexes found during myoblast fusion, in which vesicles line up at the sites of cell contact, forming pairs across the apposing plasma membranes (Dworak and Sink 2002). Interpretation of Spitzenkörper behavior during hyphal fusion as a component of the pre-fusion complex offers an interesting working hypothesis for further analysis.

Germlings and hyphae involved in fusion events tightly adhere to one another (Roca et al. 2005, Hickey et al. 2002), and extracellular electron dense material associated with fusing hyphae (Newhouse and MacDonald 1991) may be involved in adhesion of participating hyphae. Interaction between adhesive molecules during mating in *S. cerevisiae*, termed agglutinins, is required to hold mating pairs together during cell wall breakdown and plasma membrane fusion (Suzuki 2003). During prefusion complex formation in myoblast fusion extracellular electron-dense material is also found in the area between two aligning vesicles, but not at non-paired vesicles, suggesting a role for this extracellular material in aligning vesicles during fusion events (Doberstein et al. 1997).

### 2.3.3 Pore formation and cytoplasmic flow

After fusion of plasma membranes, the cytoplasm of the two participating hyphae mix. In *N. crassa,* the Spitzenkörper remains associated with the fusion pore as it enlarges (Hickey et al. 2002) (Fig. 1-2D/E). Dramatic changes in cytoplasmic flow are often associated with hyphal fusion. Organelles, such as mitochondria, vacuoles and nuclei are transferred between hyphae as a result of fusion (Fig.1-2E). Septum formation near the site of hyphal fusion is also often observed. Physiological changes associated with cytoplasmic mixing upon hyphal/germling fusion are unclear, but are presumed to occur; hyphae participating in fusion may be in different developmental states or be exposed to different nutritional conditions.

**3. Sexual Fusion**

Fusion is also essential for fertilization during mating in filamentous ascomycete species, such as *N. crassa* (Fig. 1-1C, D). Mating requires the production of a specialized female reproductive structure, termed a protoperithecium (Davis 2000). Reproductive hyphae, called trichogynes, protrude from the protoperithecia. Trichogynes are attracted by mating-type specific pheromones secreted by male cells (microconidia or macroconidia) of the opposite mating type (Bistis 1981, Kim and Borkovich 2006). After making physical contact, the tip of the female trichogyne fuses with the male cell (Fig. 1C). Following fusion, the nucleus from the male cell migrates through the trichogyne and into the protoperithecium. Following this fertilization event, opposite mating-type nuclei proliferate in a common cytoplasm within the developing perithecium. Opposite mating-type nuclei pair off and migrate into a hook-shaped structure called a crozier (Raju 1980) (Fig. 1-1D). In *N. crassa,* karyogamy occurs in the penultimate cell of the crozier, while hyphal fusion occurs between the terminal cell and the hyphal compartment nearest to the penultimate cell (Fig. 1-1D). Although fusion events occur during both vegetative growth and sexual reproduction in filamentous ascomycete species, it is unclear whether common signaling mechanisms and/or hyphal fusion machinery are common to both processes.

**4. Identification of fusion mutants**

Chemotropic interactions observed during hyphal and germling fusion suggests that receptors and signal transduction mechanism are involved. During mating in *S. cerevisiae*, binding of mating-type specific pheromones to their cognate receptors results in activation of the pheromone response MAP kinase pathway. Activation of this signaling pathway results in G1 growth arrest and transcriptional activation of genes associated with mating, such as *FUS1* and *PRM1* (Heiman and Walter 2000, McCafferey et al. 1987). Components of the MAP kinase pathway, such as the MAP kinase Fus3p, interact with proteins associated with cytoskeleton rearrangement and cell polarization, such as the formin Bni1p (Matheos et al. 2004). In *N. crassa,* mutations in homologs of components of the *S. cerevisiae* pheromone response pathway result in strains that cannot perform germling or hyphal fusion [19]. Strains containing mutations in the MAP kinase (MAPK) gene *mak-2,* the MAP kinase kinase gene (MAPKK) (NCU04612.3) or the MAP kinase kinase kinase gene (MAPKKK), *nrc-1* show similar phenotypes. In addition to a failure to undergo hyphal or germling fusion, these mutants show reduced growth rates, shortened, aerial hyphae, and failure to form female reproductive structures (protoperithecia) (Pandey et al. 2004, Kothe and Free 1998, Li et al. 2005). Similarly, an *Aspergillus nidulans* mutant disrupted in a MAPKKK *STE11* homolog, *steC*, fails to form heterokaryons (indicating a defect in hyphal fusion) and is also affected in formation of sexual reproductive structures (Wei et al. 2003). Because mutations in this MAP kinase pathway affect formation of sexual reproductive structures in filamentous fungi, its role in mating cell fusion has not been addressed.

Phosphorylation of MAK-2 is temporally associated with germling fusion events and is dependent on functional NRC-1 (Pandey et al. 2004). In *S. cerevisiae*, activation of the pheromone response pathway leads to activation of the transcription factor Ste12p. In *N. crassa,* a strain containing a mutation in the *Ste12* ortholog, *pp-1,* is very similar in phenotype to a *mak-2* mutant and is defective in hyphal and germling fusion (Li et al. 2005, D. J. Jacobson, A. Fleißner and N. L. Glass, unpublished results). Live cell imaging and microscopic observations of the *N. crassa nrc-1/mak-2/pp-1* mutants indicate that they are blind to self (mutants neither attract nor are attracted to hyphae/conidia in cases where germling fusion is common in wild type strains). Furthermore, the *nrc-1* and *mak-2* mutants do not form CATs (Roca et al. 2005). These data suggest that this MAP kinase pathway is either involved in early communication between the fusion partners or is required for rendering conidia and hyphae competent to undergo fusion.

In *S. cerevisiae,* the *SLT2* locus encodes a MAP kinase that is involved in cell wall integrity. The *SLT2* MAP kinase pathway is downstream of the *FUS3* MAP kinase pathway and is required for remodeling the cell wall during schmoo formation during mating (Buchier and Errede 1997). Initial data show that a mutant of the *SLT2* homolog in *N. crassa*, *mak-3*, is also hyphal fusion defective (A. Fleißner and N. L. Glass, unpublished results). Mutations in the *SLT2* ortholog in *Fusarium graminearum, MGV1,* resulted in a mutant that is female sterile, fails to form heterokaryons by hyphal fusion and is substantially reduced in virulence (Hou et al. 2002).

In numerous plant pathogenic filamentous fungi, homologs of components of the mating or cell wall integrity MAP kinase pathways are essential for pathogenic development despite their distinct infection strategies. For example, in *Magnaporthe grisea*, *Colletotrichum lagenarium* or *Cochliobolus heterostrophus*, strains containing mutations in *FUS3* homologs are defective in appressoria formation and fail to colonize host plants (Xu and Hamer 1996, Lev et al. 1999, Takano et al 2000). Mutations in the *FUS3* homolog of the biotrophic, non-appressorium-forming grass pathogen, *Claviceps purpurea,* results in the inability of the fungus to colonize rye-ovaries (Mey et al. 2002). Possible defects in hyphal fusion have not been addressed in most of these cases. Thus, a role for germling and hyphal fusion for colony development during invasion and growth within host tissue remains unanswered.

Cells recognize extracellular signaling molecules by different types of receptors. All eukaryotes use G-protein-coupled receptors (GPCR) for cell-cell communication and sensing of environmental stimuli. Examples are the mating pheromone receptors in *S. cerevisiae* (Kurjan 1993, Dohlman and Thorner 2001), cAMP receptors involved in cell-cell communication in *D. discoideum* (Manahan et al. 2004), or GPCRs involved in neuron guidance by extra cellular chemical cues (reviewed in (Xian et al. 2002)). Genome sequence analysis of the *N. crassa* genome has revealed at least ten, seven-transmembrane receptors within the GPCR family (Borkovich et al. 2004). The two mating-type specific pheromone receptors share homology with the *S. cerevisiae* pheromone receptors Ste2p and Ste3p (Kim and Borkovich 2004). In *N. crassa*, mutations in

the putative pheromone receptor gene, *pre-1*, result in female sterility. Female *pre-1* trichogynes are unable to detect and contact male cells of the opposite mating type, indicating a role of the PRE-1 receptor in pheromone signaling between mating partners. However, heterokaryon formation between two *pre-1* strains was comparable to wild-type strains, indicating that hyphal fusion in the *pre-1* mutant is normal (Kim and Borkovich 2004).

Binding of ligands to GPCRs results in the disassociation of an intracellular heterotrimeric G-protein (Gα, Gβ and Gγ) and subsequent activation of downstream processes (Dohlman and Thorner 2001). In the *N. crassa* genome, three Gα, one Gβ and one Gγ genes are present (Borkovich et al. 2004, Galagan et al. 2003). *gna-1* and *gnb-1* mutants do not show chemotropic interactions between a trichogyne and conidium, which is required for the initiation of the sexual cycle (Fig. 1C) (Kim and Borkovich 2004). However, G-protein mutants show no defects in vegetative germling or hyphal fusion (A. Fleißner and N. L. Glass, unpublished results), suggesting that G-protein coupled receptors are not involved in signaling vegetative fusion events. However, there is growing evidence to suggest that GPCRs could function in a G-protein independent manner (Brzkowski 2001). Together, these data indicate that signaling molecules and their receptors involved in mating cell fusion in *N. crassa* are different from those involved in vegetative germling/hyphal fusion.

### 4.1 Proteins mediating membrane fusion

Although cell fusion events are essential for the development of most eukaryotic organisms, the molecular basis of the final step of this process, the fusion of plasma membranes, is only poorly understood. In *S. cerevisiae,* one of the few proteins predicted to be involved in this process is Prm1p (Heiman and Walter 2000). *PRM1* encodes a plasma membrane protein and is found only in fungal species. *prm1* mutants show a significant fusion defect during mating, resulting in the accumulation of pre-zygotes. Preliminary data indicate that mutations in the *N. crassa prm-1* ortholog also results a fusion defect during germling and hyphal fusion (A. Fleißner, S. Diamond and N. L. Glass, unpublished results). Further studies will evaluate if *prm-1* is required for fusion of the female trichogyne with the male cell during sexual development. These experiments will reveal whether the different cell fusion events during the *N. crassa* life cycle, which are initiated by different cell-cell communication mechanisms, share the same membrane fusion machinery.

### 4.2 Genes of unknown function: *so* and *ham-2, ham-3* and *ham-4*

The *N. crassa so* mutant (allelic to *ham-1*) is deficient in both germling and hyphal fusion (Fleissner et al 2005) and exhibits an altered conidiation pattern and shortened aerial hyphae. The *so* locus encodes a protein of unknown function, which contains a WW domain predicted to be involved in protein-protein interactions. Homologs of *so* are present in the genomes of filamentous ascomycete fungi, but are absent in other eukaryotic species. These data indicate that some aspects of tip growth, polarization and germling/hyphal fusion require functions that are specific to filamentous fungi. Interestingly, the SO

protein accumulates at septal plugs of injured hyphae (Fleissner and Glass 2007); SO is not essential for wound sealing, but contributes to the speed of septal plugging. A possible connection between its function in germling/hyphal fusion and wound sealing is unclear.

The *so* mutant forms female reproductive structures (protoperithecia) and mating cell fusion between the *so* trichogynes and male cells is unimpaired. However, fertilization by a male cell does not result in entry into sexual reproduction (Fleissner et al 2005). Thus, the block in sexual reproduction in the *so* mutant occurs post-fertilization. It is possible that *so* may be required for development of the ascogenous hyphae and for the second sexual fusion event during ascus formation (Fig. 1-1D).

In *N. crassa,* the *ham-2* (hyphal anastomosis) locus encodes a putative transmembrane protein (Xiang et al. 2002). *ham-2* mutants show a pleiotropic phenotype, including slow growth, female sterility and homozygous lethality in sexual crosses. In addition, *ham-2* mutants fail to undergo both hyphal and germling fusion. Laser tweezer experiments showed that *ham-2* mutants are blind to self (fail to attract or be attracted to a wild-type during germling fusion events) (Roca et al. 2005), similar to the *mak-2* mutants described above. Subsequently, a function for a homolog of *ham-2* in *S. cerevisiae,* termed *FAR11,* was reported. Mutations in *FAR11* result in a mutant that prematurely recovers from G1 growth arrest following exposure to pheromone (Kemp and Sprague 2003). Far11p was shown to interact with five other proteins (Far3p, Far7p, Far8p, Far9p and Far10p). Mutations in any of these other genes give an identical phenotype as *far11* mutants. It was proposed that the Far11 complex is part of a checkpoint that monitors mating cell fusion in coordination with G1 cell cycle arrest. Apparent homologs of genes encoding several of the proteins which form a complex with Far11p in *S. cerevisiae* are lacking in *N. crassa*, including *FAR3* and *FAR7* (Glass et al. 2004). Preliminary data show that mutations in the homologs that are present *N. crassa, Far8* and *Far9/10* (*ham-3* and *ham-4*, respectively), result in phenotypes similar to the *ham-2* mutant, including defects during germling/hyphal fusion (C. Rasmussen, A. Fleißner, A. Simonin, M. Yang and N. L. Glass, unpublished results). These data indicate that homologs of proteins of the *S. cerevisiae* Far11 complex might also physically interact in *N. crassa* and that this interaction is essential for vegetative germling/hyphal fusion. Interestingly, HAM-3 shows significant similarity to proteins of the striatin family. In mammals, genes belonging to the striatin family are principally expressed in neurons (Benoist et al. 2006). Striatin proteins accumulate in dendritic spines in neurons at the point of cell-cell contact or synapses. Striatin family proteins act as scaffolding proteins that organize signaling complexes, e.g. formation of a complex between striatin and the estrogen receptor is required for estrogen-induced activation of a MAP kinase signal transduction pathway (Lu et al. 2006). In *Sordaria macrospora,* a species related to *N. crassa,* mutations in the *ham-3* homolog (*pro11*) result in a mutant unable to complete sexual development but full fertility was restored by expression of a striatin cDNA from mouse (Poggler and Kuck 2004). These data indicate that the homologous proteins carry out similar cellular functions in fungi

and animals. Further characterization of the function of HAM-3 in *N. crassa* will allow interesting comparisons between neuronal and hyphal signaling and might reveal conserved cellular mechanisms.

## 5.Physiological and Morphogenetic Consequences of Fusion

There are many advantages associated with hyphal fusion within a colony and between colonies, including increased resource sharing and translocation, increased colony cooperation, hyphal healing, and exchange of genetic material. For example, in *Colletotrichum lindemuthianum*, conidia that undergo fusion exhibit a higher rate of germination as compared to single unfused conidia (Roca et al. 2003). Also, conidia grown in low nutrient environments show an increased rate of fusion (Kohler 1930). These observations suggest that fusion between conidial germlings may serve to increase or pool resources that are important for colony establishment.

It is widely assumed that vegetative hyphal fusion within an established colony is important for intra-hyphal communication, cooperation, translocation of water and nutrients, and general homeostasis within a colony. Fusing to create a hyphal network could be important in influencing hyphal patterns of growth and morphogenesis in filamentous fungi. Formation of a connected network may also facilitate signaling within a colony (either by molecules, proteins or perhaps electric fields) (reviewed in (Gow and Morris 1995)), which may also affect behavior and development of a filamentous fungal colony. In nature, fungal colonies exploit diverse environments with unequal distributions and types of nutrient sources. The ability to form a hyphal network may be needed for coordinated behavior between the different parts of a fungal colony and nutrient transport from sources to sinks (Rayner 1996).

As well as facilitation of long-distance nutrient transport, vegetative hyphal fusion can function as a healing mechanism to repair hyphal connections when the fungal network has been damaged. Hyphal tips growing out from either side of damaged compartments will eventually find each other, fuse, and re-establish the hyphal network (Buller 1933). In fungi that are asexual, fusion between different individuals can be a means of exchanging genetic material through the formation of a heterokaryon (Potecorvo 1956, Giovannetti et al. 2001).

Fusion between different colonies has potential disadvantages. Hyphal fusion between individuals increases the risk of transfer of deleterious infectious elements, parasitism, or resource plundering, such as the competitive acquisition of resources by one colony from another (reviewed in (Glass and Dementhon 2006)). Many fungi have developed mechanisms for non-self recognition that result in programmed cell death (PCD), which is assumed to minimize the amount of exchange between individual colonies (Glass and Dementhon 2006, Glass and Kaneko 2003, Saupe 2000). Many of the non-self recognition mechanisms occur following hyphal fusion between genetically different colonies, raising the intriguing possibility that a link is present between the hyphal fusion and PCD machinery in filamentous fungi.

## 6. Conclusion

Cell fusion events are essential for the vegetative and sexual development of filamentous ascomycete fungi. Live cell imaging has revealed that the processes of cell-cell communication and cell fusion are complex and highly regulated. Characterization of the components required for sexual fertilization versus vegetative fusion indicates that upstream components of the signaling pathways differ. Future analyses will reveal if the machinery associated with fusion processes are similar between sexual and vegetative fusion events. *N. crassa* is an attractive model system to study the molecular basis of cell-cell communication and cell fusion in eukaryotes and to dissect similarities and differences in the processes of sexual and vegetative fusion: the genome has been sequenced and annotated (Glalagan et al. 2003), well-established molecular and cell biology techniques are available (Davis 2000)(see also: http://www.nih.gov/science/models/neurospora/), and whole genome microarrays (Kasuga et al. 2005) and knock-out mutants for every single gene are in progress (Colot et al. 2006). It is currently unclear what the adaptive role of germling and hyphal fusion is in filamentous fungi and what selective advantages it provides. Further analysis of these issues will provide significant insight into environmental adaptation and the evolution of form and function in multicellular microorganisms.

**Acknowledgements**

The work on germling/hyphal fusion in the N.L.G. laboratory is funded by a grant from the National Science Foundation (MCB-0131355/0517660). We thank Drs. Denise Schichnes and Steve Ruzin (CNR Biological Imaging Facility) for help with microscopy and Dr. Carolyn Rasmussen for helpful suggestions on the manuscript.

**8. Additional research on cell-cell fusion:**

After the above review was written, further roles of SO and MAK-2 in cell-cell communication were discovered. Fleissner et al. (2009) found that genetically identical *N. crassa* germlings rapidly switch between physiologically different states to send and receive communication between germlings. During this switch, fluorescently labeled SO and MAK-2 oscillate in opposition of each other in germling tips undergoing chemotropic interactions. The inhibition of MAK-2 kinase activity arrests the oscillation of both MAK-2 and SO indicating that phosphorylation is necessary for germling communication. These data show that SO is involved in cell response to chemotropic signal in the cell fusion pathway, and is dependent on a MAP kinase, MAK-2 to phosphorylate proteins (Fleissner et al. 2009). Another study has shown that human striatin is necessary for the localization of estrogen receptors to the plasma membrane and rapid induction of a MAP kinase (Qing et al 2004), suggesting a possible connection between HAM-3 (striatin homolog) and MAK-2 (MAP kinase) in *N. crassa*. Pieces of the signaling and fusion pathway of *N. crassa* are being revealed but future studies are needed to complete the puzzle.

**9. Nuclear and nutrient movement in fungi**

Filamentous fungi are essentially tubular systems connected through branches and fusions. The movement of the contents of these tubes is limited by the structure of the network, such as hyphal diameter, density, branching, fusions, and mesh size. In addition to structural boundaries there is an abundance of internal complexity that can limit both nutrient and organelle movement through this hyphal network. For example, septum size and type, vacuolar morphology, molecular motors and the cytoskeleton all contribute to the conductivity of hyphae. Often it is heterogeneous environmental conditions that drive the need to shift hyphal contents around within the mycelium. Movement can be induced by osmotic pressure and growth induced bulk flow, with any number of internal and external sources and sinks drawing hyphal contents in different directions.

**9.1 Nuclear positioning and flow**

Nuclear movement and positioning is controlled by microtubules and molecular motors in filamentous fungi, but there are other mechanisms driving nuclear movement as well. Microtubules perform functions such as anchoring and separating chromosomes during cell division, positioning nuclei at the tips of hyphae, and moving nuclei during migration (Gladfelter and Berman 2009, Plamann 1996, Uchida et al. 2008). Both dynein and kinesins are microtubular associated motor proteins that are involved in moving cargos both to the minus and plus ends respectively of microtubule filaments.

Dynein mutants, such as *ro-1*, in *N. crassa,* have a disrupted microtubule cytoskeleton, curvy/wavy hyphal morphology and aberrant nuclear positioning. Despite the clumpy and abnormal nuclear distribution, nuclei move through hyphae toward the tips (Plamann et al. 1994, Requilme et al. 2002). Nuclei in *N. crassa ropy* and kinesin mutants move at the speed of growth of hyphal tips. After the addition of benomyl, a microtubule disrupting agent, wild type nuclei moved forward with the rate of growth of hyphal tips indicating passive nuclear movement by bulk flow (Ramos-Garcia et al. 2009). The addition of benomyl led to less retrograde movement of nuclei and a tighter correlation between nuclear movement and growth, suggesting that mictrotubules are necessary for retrograde and fast anterograde nuclear movement. Though microtubules are necessary for correct nuclear positioning, these studies indicate that they are not required for the bulk flow of nuclear movement through hyphae.

At least two pressure gradients appear to drive mass flow in *N. crassa* hyphae. Internal turgor pressure is maintained by an osmotic gradient within the hypha leading to 0.4 to 0.6MPA in pressure (Lew et al. 2004). This turgor pressure can be abolished briefly by the addition of a hyperosmotic solution (Lew and Nasserifar 2009). The other pressure gradient comes from growing hyphal tips, and pressure is indicated by particle and injected oil droplet velocities that match tip growth velocities (Lew 2005). Both of these pressure gradients preclude the necessity of a cytoskeleton or cytoskeletal motors for particle movement within hyphae. Other pressure gradients such as heterogeneous nutrient sources, transpiration, and specialized hyphal structures like protoperithecia could lead to a dynamic flow of hyphal contents. Although the

cytoskeleton is involved in nuclear positioning and migration, exactly what parameters and processes limit flow in hyphae within the colony is unclear.

### 9.2 Functional consequence of nuclear movement

Fungi are different than most other Eukaryotes in that they contain multiple nuclei within a common cytoplasm and these nuclei can be genetically different. The ability to harbor multiple genomes in a shared environment can have potential disadvantages such as nuclear competition, and advantages such as nuclear cooperation and adaptability to heterogeneous environments. Basidiomycete and ascomycete species have different methods of maintaining nuclear ratios in the mycelium. Generally, basidiomycete fungi spend most of their life in a dikaryotic state. When two monokaryotic hyphae meet, there is a carefully orchestrated event where septal plugs are dissolved and nuclei of the opposite mating-type are spread through out the mycelium. To maintain this dikaryotic state many basidiomycete species use clamp connections to ensure there are two nuclei of compatible mating type per hyphal section. These fungi have very controlled numbers of nuclei of different genotypes residing in each section of their mycelium (Reviewed most recently in (Gladfelter and Berman 2009)).

However, ascomycete species and some basidiomycete species do not have a rigid 1:1 nuclear ratio and can harbor unbalanced ratios of genetically different nuclei in the same compartment. Recent research has shown that nuclear ratios can be much more dynamic than previously thought in basidiomycetes with the ability to maintain multinucleate cells (James et al. 2008). Some filamentous ascomycete species show rapid and dynamic nuclear movement due to septal pores large enough for nuclei to flow through, allowing for free movement of nuclei within the mycelium.

Some filamentous ascomycete species can rapidly change nuclear ratios in response to environmental conditions (Jinks 1952, Davis 1960) effectively changing allele frequencies in certain areas of the mycelium by changing nuclear abundance. These fungi must have a mechanism by which nuclear movement and/or division is controlled in response to external cues. Maintaining a plastic heterokaryon can lead to genomic conflict between genetically different nuclei due to selection acting on individual genotypes even to the possible detriment of colony fitness (James et al. 2008, Rayner 1991). On the other hand, there can be an advantage of quick adaptability to new environments resulting in greater fitness if an individual harbors multiple genomes mixed throughout the mycelium (Jinks 1952, Davis 1960). Eventually, if a colony can no longer maintain a heterokaryon, one nuclear lineage could become fixed in the population, leading to either genomic takeover (Rayner 1991) or sectoring (Hallatschek et al. 2007).

Though there is large body of research on cytoskeleton and molecular motor involvement in nuclear movement and some research on the functional consequence of nuclear ratios in a mycelium, there is little known about the dynamic nature of nuclear movement through out a colony and the mechanisms behind maintaining or losing a genetically well mixed heterokaryon.

## 9.3 Nutrient translocation in fungal colonies

Translocation of resources occurs across all phyla of fungi as a means to distribute nutrients for growth through out the growing mycelium, maintain homeostasis in a colony, establish symbiotic relationships with plants, and hydrate areas of the colony that are transpiring. The bidirectional translocation of nitrogen, carbon, and phosphorous has been observed in arbuscular mycorrhizal (AM) and ectomycorrhizal (EM) fungi as well as many cord (rhizomorph) forming fungi. Plant pathogens such a *Rhizoctonia solanii* have also been shown to translocate carbon form a source to a sink (Jacobs et al. 2004). In addition, a variety of radioactive tracers have been used to follow translocation in ascomycete and zygomycete fungi, for example *N. crassa* can translocate $^{86}$Rb (Thain et al. 1982) and *Phycomyces blakeseeanus* sporangiophores translocate $^{42}$K (Cowan et al. 1972). Although it is well known that fungi translocate resources, the mechanisms driving and limiting translocation are not well understood.

Many cord forming fungi and mycorrhizal fungi can translocate water and nutrients bidirectionally along gradients from sources to sinks, maintaining equilibrium within the mycelium (Rayner 1991, Boddy et al. 2009). For mycorrhizal fungi, this bidirectional translocation is integral to establishing a mutualistic symbiotic relationship with plant hosts, where nutrients from surrounding substrates are taken up by the fungus and translocated to the plant and photosynthate from the plant is translocated through out the fungus (Smith and Read 1997). Recent studies on mycorrhizal fungi and cord forming fungi have delved into the mechanisms and pathways of translocation. Some AM fungi convert inorganic N taken up by extraradical hyphae to arginine, which is translocated, presumably through the vacuolar system, and then converted back to ammonium at the plant/fungal interface (Cruz et al. 2007). The vacuolar systems of fungi are membrane-delineated compartments that can fuse to create a pathway for significant resource translocation, potentially in a different direction than cytoplasmic bulk flow. The diffusion rates in the vacuolar system of *P. velutina* are enough to supply N to areas of growth, suggesting vacuoles could play a major role in resource translocation within a colony (Fricker et al. 2008).

In many cord-forming fungi for example *Serepula lacrimins* and *Phanerochate velutina*, translocation occurs from high nutrient areas to low nutrient areas both from tip to origin of the colony and origin to tips (Tlalka et al. 2008). Translocation between sources and sinks in forest ecosystems is thought to help maintain efficient litter decomposition by connecting sources of nitrogen and sources of carbon that don't necessarily occur in the same proximity (Boberg et al. 2010, Lindahl et al. 2006, Boddy and Watkinson 1995). Mobile resources in cord forming fungi will concentrate around areas that are sinks and areas that require the nutrients to maintain homeostasis, for example, new growth is often a sink that draws nutrients (Tlalka et al. 2008).

Anastamosis can occur within a colony or between two different colonies, though often incompatibility reactions limit the ability of genetically different individuals from forming a heterokaryon. Fusion between germinating conidia in *Neurospora* and *Colletotrichum* has been shown to be beneficial and germlings

share nutrients and nuclei (Roca et al. 2005). There is some evidence that AM fungal colonies that have already established associations with plant hosts can translocate nutrients within and between colonies. AM fungal colonies will fuse and pass cytoplasm and organelles from one colony to another (Giovannetti et al.1999, and 2001). In addition, fusion between colonies of AM *Glomus* species facilitate the translocation of $^{32}P$ from one host plant to another (Mikkelson et al. 2008). This implies that mycorrhizal fungal colonies can fuse to create a common mycorrhizal network linking two plants that can then share resource through the network. Cord-forming fungi will also fuse to form a common mycelium. *P. velutina* colonies have a pulsatile movement of nutrients and when colonies fuse they oscillate in the same rhythm suggesting communication and equilibration between the colonies (Tlalka et al. 2003 and 2007).

Bidirectional translocation might not be needed or advantageous in many fungal colonies. Plant pathogens need to transport resources from their plant host from the site of infection to the rest of the mycelium, but would not benefit from providing nutrients to the plant. Saprotrophic fungi will often deplete resources in the center of the colony and rather than maintain metabolism, resulting in the interior of the fungus becoming vacuolated and shut off from the rest of the colony. Solely forward translocation might be beneficial to early colonizing fungi that invest in foraging mycelia as opposed to creating lasting structures for translocation such as cords or rhizomorphs. There are arguably many different strategies and mechanisms for nutrient translocation in different fungal species, but there is still much to learn about the intricacies of translocation.

### 9.4 Further research

Fungi have many different strategies and mechanism for translocating nutrients and organelles through out their mycelium. Nutrient and nuclear translocation is a dynamic process that can help maintain homeostasis and growth in a colony. Further research will lead to a better understanding of the mechanisms behind resource translocation, the pathways of translocation, and the translocation difference in fungal species with different foraging and growth strategies.

### References for original review:


Ahmad, S. S. and Miles, P. G. (1970) Hyphal fusions in *Schizophyllum commune*. 2. Effects on environmental and chemical factors. *Mycologia* 62, 1008–1017.

Al-Anzi, B. and Chandler, D. E. (1998) A sperm chemoattractant is released from *Xenopus* egg jelly during spawning. *Dev. Biol*. 198, 366–375.

Benoist, M., Gaillard, S. and Castets, F. (2006) The striatin family: a new signaling platform in dendritic spines. *J. Physiol. Paris* 99, 146–153.

Bistis, G. N. (1981) Chemotropic interactions between trichogynes and conidia of opposite mating-type in *Neurospora crassa. Mycologia* 73, 959–975.

Borkovich, K. A., Alex, L. A., Yarden, O., Freitag, M., Turner, G. E., Read, N. D., Seiler, S., Bell-Pedersen, D., Paietta, J., Plesofsky, N., Plamann, M.,

Goodrich-Tanrikulu, M., Schulte, U., Mannhaupt, G., Nargang, F. E., Radford, A., Selitrennikoff, C., Galagan, J. E., Dunlap, J. C., Loros, J. J., Catcheside, D., Inoue, H., Aramayo, R., Polymenis, M., Selker, E. U., Sachs, M. S., Marzluf, G. A., Paulsen, I., Davis, R., Ebbole, D. J., Zelter, A., Kalkman, E. R., O'Rourke, R., Bowring, F., Yeadon, J., Ishii, C., Suzuki, K., Sakai, W., and Pratt, R. (2004) Lessons from the genome sequence of *Neurospora crassa*: tracing the path from genomic blueprint to multicellular organism. *Microbiol. Mol. Biol. Rev*. 68, 1–108.

Brzostowski, J. A. and Kimmel, A. R. (2001) Signaling at zero G: G-protein–independent functions for 7-TM receptors. *Trends Biochem. Sci*. 26, 291–297.

Buehrer, B. M. and Errede, B. (1997) Coordination of the mating and cell integrity mitogen-activated protein kinase pathways in *Saccharomyces cerevisiae. Mol. Cell. Biol*. 17, 6517–6525.

Buller, A. H. R. (1933) *Researches on Fungi,* vol. 5. Longman, London.

Chen, E. H. and Olson, E. N. (2004) Towards a molecular pathway for myoblast fusion in *Drosophila. Trends Cell Biol*. 14, 452–460.

Colot, H. V., Park, G., Turner, G. E., Ringelberg, C., Crew, C. M., Litvinkova, L., Weiss, R. L., Borkovich, K. A., and Dunlap J. C. (2006) A high-throughput gene knockout procedure for *Neurospora* reveals functions for multiple transcription factors. *Proc. Natl. Acad. Sci. U.S.A*. 103, 10352–10357.

Davis, R. H. (2000) *Neurospora*: *Contributions of a Model Organism*. Oxford University Press, New York.

Doberstein, S. K., Fetter, R. D., Mehta, A. Y., and Goodman, C. S. (1997). Genetic analysis of myoblast fusion: blown fuse is required for progression beyond the
prefusion complex. *J. Cell Biol*. 136, 1249–1261.

Dohlman, H. G., and Thorner, J. (2001) Regulation of G protein–initiated signal transduction in yeast: paradigms and principles. *Annu. Rev. Biochem*. 70, 703–754.

Dworak, H. A. and Sink, H. (2002) Myoblast fusion in *Drosophila. Bioessays* 24, 591–601.

Fleißner, A., Sarkar, S., Jacobson, D. J., Roca, M. G., Read, N. D., and Glass N. L. (2005) The *so* locus is required for vegetative cell fusion and post-fertilization events in *Neurospora crassa. Eukaryot. Cell* 4, 920–930.

Fleißner, A. and Glass, N. L. (2007) SO, a protein involved in hyphal fusion in *Neurospora crassa*, localizes to septal plugs. *Eukaryot. Cell* 6, 84–94.

Galagan, J. E., Calvo, S. E., Borkovich, K. A., Selker, E. U., Read, N. D., Jaffe. D., FitzHugh, W., Ma, L. J., Smirnov, S., Purcell, S., Rehman, B., Elkins, T., Engels, R., Wang, S., Nielsen, C. B., Butler, J., Endrizzi, M., Qui, D., Ianakiev, P., Bell- Pedersen, D., Nelson, M. A., Werner-Washburne, M., Selitrennikoff, C. P., Kinsey, J. A., Braun, E. L., Zelter, A., Schulte, U., Kothe, G.O., Jedd, G., Mewes, W., Staben, C., Marcotte, E., Greenberg, D., Roy, A., Foley, K., Naylor, J., Stange-Thomann, N., Barrett, R., Gnerre, S., Kamal, M., Kamvysselis, M., Mauceli, E., Bielke, C., Rudd, S., Frishman, D., Krystofova, S., Rasmussen, C., Metzenberg, R. L., Perkins, D. D., Kroken, S., Cogoni, C., Macino, G., Catcheside, D., Li, W., Pratt, R. J., Osmani, S.

A., DeSouza, C. P., Glass, L., Orbach, M. J., Berglund, J. A., Voelker, R., Yarden, O., Plamann, M., Seiler, S., Dunlap, J., Radford, A., Aramayo, R., Natvig, D. O., Alex, L. A., Mannhaupt, G., Ebbole, D. J., Freitag, M., Paulsen, I., Sachs, M. S., Lander, E. S., Nusbaum, C., and Birren, B. (2003) The genome sequence of the filamentous fungus *Neurospora crassa. Nature* 422, 859–868.

Giovannetti, M., Fortuna, P., Citernesia, A. S., Morini, S., and Nuti, M. P. (2001) The occurrence of anastomosis formation and nuclear exchange in intact arbuscular mycorrhizal networks. *New Phytol*. 151, 717–724.

Glass, N. L. and Dementhon, K. (2006) Nonself recognition and programmed cell death in filamentous fungi. *Curr. Opin. Microbiol*. 9, 553–558.

Glass, N. L. and Fleißner, A. (2006) Re-wiring the network: understanding the mechanism and function of anastomosis in filamentous ascomycete fungi, I n *TheMycota* (Kues, Fischer, eds.). Springer-Verlag, Berlin, pp. 123–139.

Glass, N. L., Rasmussen, C., Roca, M. G., and Read, N. D. (2004) Hyphal homing,fusion and mycelial interconnectedness. *Trends Microbiol*. 12, 135–141.

Glass, N. L. and Kaneko, I. (2003) Fatal attraction: nonself recognition and hetero- karyon incompatibility in filamentous fungi. *Eukaryot. Cell* 2, 1–8.

Glass, N. L., Jacobson, D. J., and Shiu, P. K. (2000) The genetics of hyphal f fusion and vegetative incompatibility in filamentous ascomycete fungi. *Annu. Rev. Genet*.
34, 165–186.

Gow, N. A. R. and Morris, B. M. (1995) The electric fungus. *Bot. J. Scotl*. 47, 263–277.

Heiman, M. G. and Walter, P. (2000) Prm1p, a pheromone-regulated multispanning membrane protein, facilitates plasma membrane fusion during yeast mating. *J. Cell Biol*. 151, 719–730.

Hickey, P. C., Jacobson, D. J., Read, N. D., and Glass, N. L. (2002) Live-cell imaging of vegetative hyphal fusion in *Neurospora crassa. Fungal Genet. Biol*. 37, 109–119.

Higashiyama, T., Kuroiwa, H., and Kuroiwa, T. (2003) Pollen-tube guidance: beacons from the female gametophyte. *Curr. Opin. Plant Biol*. 6, 36–41.

Hou, Z., Xue, C., Peng, Y., Katan, T., Kistler, H. C., and Xu, J. R. (2002) A mitogen-activated protein kinase gene (MGV1) in *Fusarium graminearum* is required for female fertility, heterokaryon formation, and plant infection. *Mol. Plant–Microbe Interact*. 15, 1119–1127.

Kasuga, T., Townsend, J. P., Tian, C., Gilbert, L. B., Mannhaupt, G., Taylor, J. W., and Glass, N. L. (2005) Long-oligomer microarray profiling in Neurospora crassa reveals the transcriptional program underlying biochemical and physiological events of conidial germination. *Nucleic Acids Res*. 33, 6469–6485.

Kemp, H. A. and Sprague, G. F. (2003) Far3 and five interacting proteins prevent premature recovery from pheromone arrest in the budding yeast *Saccharomyces cerevisiae. Mol. Cell. Biol*. 23, 1750–1763.

Kim, H. and Borkovich, K. A. (2004) A pheromone receptor gene, *pre-1*, is essen-

tial for mating type-specific directional growth and fusion of trichogynes and female fertility in *Neurospora crassa. Mol. Microbiol*. 52, 1781–1798.
Kim, H. and Borkovich, K. A. (2006) Pheromones are essential for male fertility and sufficient to direct chemotropic polarized growth of trichogynes during matingin *Neurospora crassa. Eukaryot. Cell* 5, 544–554.
Köhler, E. (1929) Beiträge zur Kenntnis der vegetativen Anastomosen der Pilze I. *Planta* 8, 140–153.
Köhler, E. (1930) Zur Kenntnis der vegetativen Anastomosen der Pilze (II. Mitteilung). *Planta* 10, 495–522.
Kothe, G. O. and Free, S. J. (1998) The isolation and characterization of *nrc-1* and *nrc-2*, two genes encoding protein kinases that control growth and development in *Neurospora crassa. Genetics* 149, 117–130.
Kurjan, J. (1993) The pheromone response pathway in *Saccharomyces cerevisiae. Annu. Rev. Genet*. 27(4), 147–179.
Lev, S., Sharon, A., Hadar, R., Ma, H., and Horwitz, B. A. (1999) A mitogen-activated protein kinase of the corn leaf pathogen *Cochliobolus heterostrophus* is involved in conidiation, appressorium formation, and pathogenicity: diverse roles for mitogen-activated protein kinase homologs in foliar pathogens. *Proc. Natl. Acad. Sci. U.S.A*. 96, 13542–13547.
Li, D., Bobrowicz, P., Wilkinson, H. H., and Ebbole, D. J. (2005) A mitogen-activated protein kinase pathway essential for mating and contributing to vegetative growth in *Neurospora crassa. Genetics* 170, 1091–1104.
Lord, E. M. (2003) Adhesion and guidance in compatible pollination. *J. Exp. Bot*. 54, 47–54.
Lu, Q., Pallas, D. C., Surks, H. K., Baur, W. E. Mendelsohn, M. E., and Karas R. H. (2004) Striatin assembles a membrane signaling complex necessary for r apid, non- genomic activation of endothelial NO synthase by estrogen r eceptor alpha. *Proc. Natl. Acad. Sci. U.S.A*. 101, 17126–17131.
Manahan, C. L., Iglesias, P. A., Long, Y., and Devreotes, P. N. (2004) Chemoattractant signaling in *Dictyostelium discoideum. Annu. Rev. Cell Dev. Biol*. 20, 223–253.
Mascarenhas, J. P. (1993) Molecular mechanisms of pollen tube growth and differentiation. *Plant Cell* 5, 1303–1314.
Matheos, D., Metodiev, M., Muller, E., Stone, D., and Rose, M. D. (2004) Pheromone-induced polarization is dependent on the Fus3p MAPK acting through the formin Bni1p. *J. Cell Biol*. 165, 99–109
McCaffrey, G., Clay, F. J., Kelsay, K. and Sprague, G. F. (1987) Identification and regulation of a gene required for cell fusion during mating of the yeast *Saccharomyces cerevisiae. Mol. Cell. Biol*. 7, 2680–2690.
Mey, G., Oeser, B., Lebrun, M. H,. and Tudzynski, P. (2002) The biotrophic, non-appressorium–forming grass pathogen *Claviceps purpurea* needs a Fus3/Pmk1 homologous mitogen-activated protein kinase for colonization of rye ovarian tis- sue. *Mol. Plant–Microbe Interact*. 15, 303–312.
Newhouse, J. R. and MacDonald, W. L. (1991) The ultrastructure of hyphal anastomoses between vegetatively compatible and incompatible virulent and hypovirulent strains of *Cryphonectria parasitica. Can. J. Bot*. 69, 602–614.

Pandey, A., Roca, M. G., Read, N. D., and Glass, N. L. (2004) Role of a MAP kinase during conidial germination and hyphal fusion in *Neurospora crassa. Eukaryot. Cell* 3, 348–358.

Perkins, D. D., Radford, A., and Sachs, M. S. (2001) *The Neurospora Compendium:Chromosomal Loci*. Academic Press, San Diego.

Pöggeler, S. and Kück, U. (2004) A WD40 repeat protein regulates fungal cell differentiation and can be replaced functionally by the mammalian homologue striatin. *Eukaryot. Cell* 3, 232–240.

Pontecorvo, G.(1956) The parasexual cycle in fungi. *Annu. Rev. Microbiol*. 10, 393–400.

Potgens, A. J. G., Schmitz, U., Bose, P., Versmold, A., Kaufmann, P., and Frank, H. G. (2002) Mechanisms of syncytial fusion: a review. *Placenta* 23 (Suppl A, *Trophoblast Res*. 16), 107–113.

Primakoff, P. and Myles, D. G. (2007) Cell–cell membrane fusion during mammalian fertilization. *FEBS Lett*. (in press, corrected proof).

Vignery, A. (2005) Macrophage fusion: the making of osteoclasts and giant cells. *J. Exp. Med*. 202, 337–340.

Raju, N. B. (1980) Meiosis and ascospore genesis in *Neurospora. Eur. J. Cell Biol*. 23, 208–223.

Rayner, A. D. M. (1996) Interconnectedness and individualism in fungal mycelia, in *A Century of Mycology* (B.C. Sutton, ed.). University of Cambridge Press,Cambridge, England, pp. 193–232.

Riquelme, M., Reynaga-Peña, C. G., Gierz, G., and Bartnicki-García, S. (1998) What determines growth direction in fungal hyphae? *Fungal Genet. Biol*. 24, 101–109.

Roca, M. G., Davide, L. C., Mendes-Costa, M. C., and Wheals, A. (2003) Conidial anastomosis tubes in *Colletotrichum. Fungal Genet. Biol*. 40, 138–145.

Roca, M. G., Arlt, J., Jeffree, C. E., and Read, N. D. (2005) Cell biology of conidial anastomosis tubes in *Neurospora crassa. Eukaryot. Cell* 4, 911–919. Saupe, S. J. (2000) Molecular genetics of heterokaryon incompatibility in filamen- tous ascomycetes. *Microbiol. Mol. Biol. Rev*. 64, 489–502.

Suzuki, K. (2003) Roles of sexual cell agglutination in yeast mass mating. *Genes Genet. Syst*. 78, 211–219.

Takano, Y., Kikuchi, T., Kubo, Y., Hamer, J. E., Mise, K., and Furusawa, I. (2000) The *Colletotrichum lagenarium* MAP kinase gene CMK1 regulates diverse aspects of fungal pathogenesis. *Mol. Plant–Microbe Interact*. 13, 374–383.

Trinci, A.P.J. (1984) Regulation of hyphal branching and hyphal orientation, in *The Ecology and Physiology of the Fungal Mycelium* (D.H. Jennings and A.D.M. Rayner, eds.). Cambridge University Press: Cambridge, England, pp. 23–

Wei, H. J., Requena, N., and Fischer, R. (2003) The MAPKK kinase SteC regulates conidiophore morphology and is essential for heterokaryon formation and sexual development in the homothallic fungus *Aspergillus nidulans. Mol. Microbiol*. 47, 1577–1588.

Wilson, J. F. and Dempsey, J. A. (1999) A hyphal fusion mutant in *Neurospora crassa. Fungal Genet. Newslett*. 46, 31.

Xiang, Y., Li, Y., Zhang, Z., Cui, K., Wang, S., Yuan, X. B., Wu, C. P., Poo, M. M., and Duan, S. (2002) Nerve growth cone guidance mediated by G protein–coupled receptors. *Nat. Neurosci*. 5, 843–848.

Xiang, Q., Rasmussen, C., and Glass, N. L. (2002) The *ham-2* locus, encoding a putative transmembrane protein, is required for hyphal fusion in *Neurospora crassa. Genetics* 160, 169–180.

Xu, J. R. and Hamer, J. E. (1996) MAP kinase and cAMP signaling regulate infection structure formation and pathogenic growth in the rice blast fungus *Magnaporthe grisea. Genes Dev*. 10, 2696–2706.

Yokoyama, K. and Ogoshi, A. (1988) Studies on hyphal anastomosis of *Rhizoctonia solani* V. Nutritional conditions for anastomosis. *Trans. Mycol. Soc. Jpn*. 29, 125–1 32.

**References for additional review section:**

Boberg, J. B., Finlay, R. D., Stenlid, J., & Lindahl, B. D. (2010). Fungal C translocation restricts N-mineralization in heterogeneous environments. *Functional Ecology*, Fungal translocation and N-mineralization, *24*(2), 454-459.

Boddy, L. & Watkinson, S. C.(1995). WOOD DECOMPOSITION, HIGHER FUNGI, AND THEIR ROLE IN NUTRIENT REDISTRIBUTION. *Canadian Journal of Botany-Revue Canadienne De Botanique* 73, S1377-S1383.

Boddy, L., Hynes, J., Bebber, Daniel P, & Fricker, Mark D. (2009). Saprotrophic cord systems: dispersal mechanisms in space and time. *Mycoscience*, *50*(1), 9-19.

Cowan, M C, B G Lewis, and J F Thain. (1972) Uptake of potassium by the developing sporangiophore of Phycomyces blakesleeanus. *Transactions Of The British Mycological Society* 58, no. 1: 113-126.

Cruz, C., Egsgaard, H., Trujillo, C., Ambus, P., Requena, N., Martins-Loucao, M. A., & Jakobsen, I. (2007). Enzymatic Evidence for the Key Role of Arginine in Nitrogen Translocation by Arbuscular Mycorrhizal Fungi. *PLANT PHYSIOLOGY*, *144*(2), 782-792.

DAVIS, R. (1960). ADAPTATION IN PANTOTHENATE-REQUIRING NEUROSPORA .2. NUCLEAR COMPETITION DURING ADAPTATION. *American Journal Of Botany*, *47*(8), 648-654.

Fleissner, A., Leeder, A. C., Roca, M. G., Read, N. D., & Glass, N. L. (2009). Oscillatory recruitment of signaling proteins to cell tips promotes coordinated behavior during cell fusion. *Proceedings Of The National Academy Of Sciences Of The United States Of America*, *106*(46), 19393-19398.

Fricker, M D, Lee, J. A., Bebber, D. P., Tlalka, M., Hynes, J., Darrah, P. R., Watkinson, S. C., et al. (2008). Imaging complex nutrient dynamics in mycelial networks. *Journal Of Microscopy-Oxford*, *231*(2), 317-331.

Giovannetti, M., Azzolini, D., & Citernesi, A. (1999). Anastomosis formation and nuclear and protoplasmic exchange in arbuscular mycorrhizal fungi.

*Applied and Environmental Microbiology*, *65*(12), 5571-5575.
Giovannetti, M., Fortuna, P., Citernesi, A., Morini, S., & Nuti, M. (2001). The occurrence of anastomosis formation and nuclear exchange in intact arbuscular mycorrhizal networks. *New Phytologist*, *151*(3), 717-724.
Gladfelter, A., & Berman, J. (2009). Dancing genomes: fungal nuclear positioning. *Nature Reviews Microbiology*, *7*(12), 875-886.
Hallatschek, O., Hersen, P., Ramanathan, S., & Nelson, D. R. (2007). Genetic drift at expanding frontiers promotes gene segregation. *Proceedings Of The National Academy Of Sciences Of The United States Of America*, *104*(50), 19926-19930.
Jacobs, H., Boswell, G., Scrimgeour, C., Davidson, F., Gadd, G., & Ritz, K. (2004). Translocation of carbon by Rhizoctonia solani in nutritionally-heterogeneous microcosms. *Mycological Research*, *108*, 453-462.
James, T. Y., Stenlid, J., Olson, A., & Johannesson, H. (2008). Evolutionary significance of imbalanced nuclear ratios within heterokaryons of the basidiomycete fungus Heterobasidion parviporum. *Evolution*, *62*(9), 2279-2296.
JINKS, J. (1952). HETEROKARYOSIS - A SYSTEM OF ADAPTATION IN WILD FUNGI. *Proceedings Of The Royal Society Of London Series B-Biological Sciences*, *140*(898), 83-&.
Lew, R. (2005). Mass flow and pressure-driven hyphal extension in Neurospora crassa. *Microbiology-Sgm*, *151*, 2685-2692. doi:10.1099/mic.0.27947-0
Lew, R. R., & Nasserifar, S. (2009). Transient responses during hyperosmotic shock in the filamentous fungus Neurospora crassa. *Microbiology-Sgm*, *155*, 903-911.
Lew, R., Levina, N., Walker, S., & Garrill, A. (2004). Turgor regulation in hyphal organisms. *Fungal Genetics And Biology*, *41*(11), 1007-1015.
Lindahl, B. D., Ihrmark, K., Boberg, J., Trumbore, S. E., Högberg, P., Stenlid, J., & Finlay, R. D. (2006). Spatial separation of litter decomposition and mycorrhizal nitrogen uptake in a boreal forest. *New Phytologist*, *173*(3), 611-620.
Mikkelsen, B. L., Rosendahl, S., & Jakobsen, I. (2008). Underground resource allocation between individual networks of mycorrhizal fungi. *New Phytologist*, *180*(4), 890-898.
Plamann, M., Minke, P.F., Tinsley, J.H., Bruno, K.S., (1994). Cytoplasmic dynein and actin-related protein Arp1 are required for normal nuclear distribution in filamentous fungi. J. Cell Biol. 127, 139–149.
Plamann, M. (1996). Nuclear division, nuclear distribution and cytokinesis in filamentous fungi. *Journal Of Genetics*, *75*(3), 351-360.
Qing, L., Pallas, D., Surks, H., Baur, W., Mendelsohn, M., & Karas, R. (2004). Striatin assembles a membrane signaling complex necessary for rapid, nongenomic activation of endothelial NO synthase by estrogen receptor alpha. *Proceedings Of The National Academy Of Sciences Of The United States Of America*, *101*(49), 17126-17131.
Ramos-Garcia, S. L., Roberson, R. W., Freitag, M., Bartnicki-Garcia, S., & Mourino-Perez, R. R. (2009). Cytoplasmic Bulk Flow Propels Nuclei in

Mature Hyphae of Neurospora crassa. *Eukaryotic Cell*, *8*(12), 1880-1890.
Riquelme, M., R. W. Roberson, D. P. McDaniel, and S. Bartnicki-Garcia. 2002. The effects of ropy-1 mutation on cytoplasmic organization and intra- cellular motility in mature hyphae of Neurospora crassa. Fungal Genet. Biol. 37:171–179.
Rayner, A. (1991). THE CHALLENGE OF THE INDIVIDUALISTIC MYCELIUM. *Mycologia*, *83*(1), 48-71.
Roca, M., Read, N., & Wheals, A. (2005). Conidial anastomosis tubes in filamentous fungi. *Fems Microbiology Letters*, *249*(2), 191-198.
Smith, S. E. & Read, D. J. in *Mycorrhizal symbiosis* (Academic Press, San Diego, CA,
1997).
Thain, J. F. & Girvin, D. TRANSLOCATION THROUGH ESTABLISHED MYCELIUM OF
NEUROSPORA-CRASSA ON A NUTRIENT-FREE SUBSTRATE. *Transactions of the British Mycological Society* **89**, 45-49 (1987).
Tlalka, M., Bebber, D P, Darrah, P. R., Watkinson, S. C., & Fricker, M D. (2007). Emergence of self-organised oscillatory domains in fungal mycelia. *Fungal Genetics And Biology*, *44*(11), 1085-1095.
Tlalka, M., Bebber, D P, Darrah, P. R., Watkinson, S. C., & Fricker, M D. (2008). Quantifying dynamic resource allocation illuminates foraging strategy in Phanerochaete velutina. *Fungal Genetics And Biology*, *45*(7), 1111-1121.
Tlalka, M., Hensman, D., Darrah, P. R., Watkinson, S. C., & Fricker, M D. (2003). Noncircadian oscillations in amino acid transport have complementary profiles in assimilatory and foraging hyphae of Phanerochaete velutina. *New Phytologist*, *158*(2), 325-335.
Uchida, M., Mourino-Perez, R. R., Freitag, M., Bartnicki-Garcia, S., & Roberson, R. W. (2008). Microtubule dynamics and the role of molecular motors in Neurospora crassa *Fungal Genetics And Biology*, *45*(5), 683-692.

**Figure legend:**

Fig. 1-1. Stages in the life cycle of *Neurospora crassa* in which fusion occurs. **(A)** Conidia at sufficient cell density undergo fusion between germlings. **(B)** Hyphae within the interior of the colony show chemotropism and hyphal fusion. **(C)** The sexual cycle is initiated by cell fusion between a fertile receptive hyphae (trichogyne [t]) emanating from a female reproductive structure, the protoperithecia (out of view). The trichogyne shows chemotropism toward a conidium of the opposite mating type (c). Arrow indi- cates fusion point. **(D)** Following fertilization, nuclei of opposite mating type (*mat A* and *mat a*) proliferate in ascogenous hyphae. Opposite mating-type nuclei pair off and migrate into the crozier (cr). In *N. crassa*, karyogamy occurs in the penultimate cell of the crozier. Hyphal and nuclear fusion occurs between the terminal cell and the sub- tending cell of the crozier (fc). Karyogamy, meiosis, and an

additional mitotic division occurs in the ascus resulting in an eight-spored ascus. Asci, ascogenous hyphae and croziers treated with DAPI, a nuclear stain. Bar = 20μm.

Fig. 1- 2. Stages of hyphal fusion. **(A,B)** The presence of a fusion-competent hypha often results in the formation of a peg in the receptive hypha. Peg formation is asso- ciated with the formation of a Spitzenkörper at the tip of the new peg. **(C)** Contact between fusion hyphae is associated with a switch from polar to nonpolar growth, resulting in a swelling of the fusion hyphae at the point of contact. The Spitzenkörper is associated with the site of the future pore in both fusion hyphae (arrows). **(D)** Pore formation (arrow) is associated with cytoplasmic flow. Organelles such as nuclei and mitochondria pass through the fusion pore. Septation is also often associated with hyphal fusion events. **(E)** Fusion results in cytoplasmic mixing. Fusion between one hypha labeled with cytoplasmic GFP and one carrying dsRED-labeled nuclei result in hyphae exhibiting red nuclei in green cytoplasm. Hyphae stained with FM4-64. Bar = 10 μm. (A–D, adapted from (Hickey 2002))

Fig. 1-3. In *Neurospora crassa,* mutations in the mitogen-activated protein kinase pathway components *nrc-1, NCU04612.3, mak-2,* and *pp-1* result in mutants unable to undergo germling or hyphal fusion (Pandey et al 2004). In addition, mutations in *ham-2*, encod- ing a putative plasma membrane protein, *ham-3,* and *ham-4* result in strains unable to undergo both hyphal and germling fusion (Xiang et al. 2002). Mutations in *so* result in germling/ hyphal fusion-deficient strains (Fleissner et al. 2005). In *Fusarium graminearum,* a strain containing a mutation in the ortholog of *SLT2* fails to form a heterokaryon (Hou et al. 2002); the *N. crassa* ortholog of *SLT2* is called *mak-3*. The natures of the receptor and ligand involved in anastomosis are unknown. Prm1p mediates membrane fusion in *Saccharomyces cerevisiae* (Heiman et al. 2000). Preliminary data indicate a similar role of the *N. crassa prm-1* homolog in germling/ hyphal fusion. (A. Fleißner, S. Diamond, and N. L. Glass, unpublished data.)

Figure. 1-1

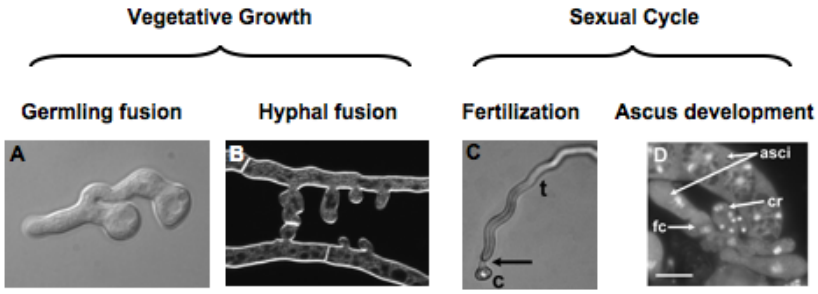
Vegetative Growth
Sexual Cycle
Germling fusion
Hyphal fusion
Fertilization
Ascus development
A
B
C
t
c
D
asci
cr
fc

Figure. 1-2

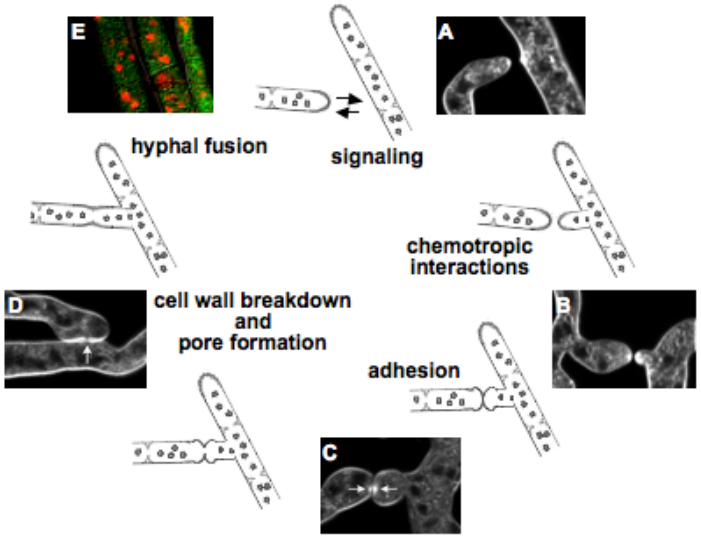
E
A
hyphal fusion
signaling
chemotropic
interactions
D
cell wall breakdown
and
pore formation
B
adhesion
C

Figure. 1-3

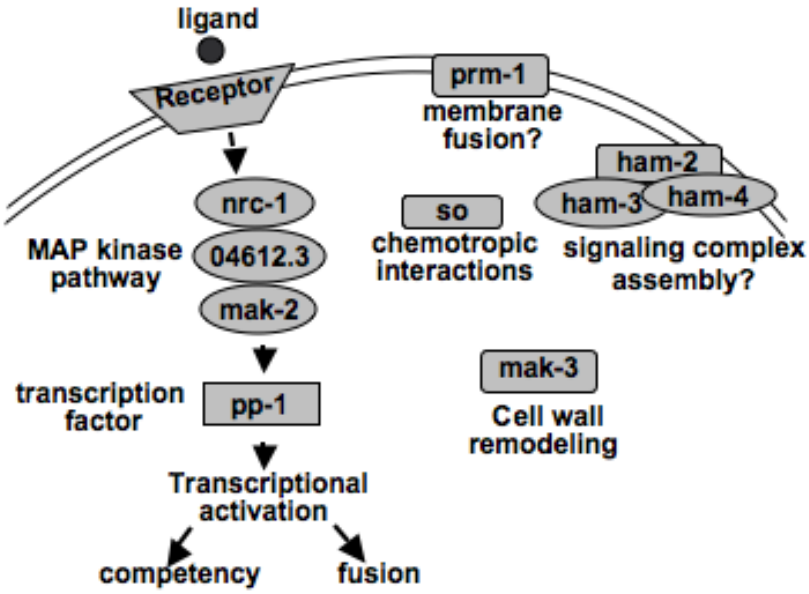
ligand
Receptor
prm-1
membrane fusion?
ham-2
ham-3
ham-4
nrc-1
so
chemotropic interactions
signaling complex assembly?
MAP kinase pathway
04612.3
mak-2
mak-3
transcription factor
pp-1
Cell wall remodeling
Transcriptional activation
competency
fusion

***Chapter 2:*** *Genes encoding a striatin-like protein (*ham-3*) and a Forkhead associated protein (*ham-4*) are required for hyphal fusion in* Neurospora crassa*.*

This chapter was previously published in Fungal Genetics and Biology under the reference: Anna R. Simonin, Carolyn G. Rasmussen, Mabel Yang, and N. Louise Glass. (2010) Genes encoding a striatin-like protein (ham-3) and a Forkhead associated protein (ham-4) are required for hyphal fusion in Neurospora crassa. Fungal Genetics and Biology. 47: 855–868. An addition to the end of the chapter highlights new data collected post publication.

**Abstract**

Cell-cell fusion during fertilization and between somatic cells is an integral process in eukaryotic development. In *Neurospora crassa*, the hyphal anastomosis mutant, *ham-2*, fails to undergo somatic fusion. In both humans and *Saccharomyces cerevisiae*, homologs of *ham-2* are found in protein complexes that include homologs to a striatin-like protein and a forkhead-associated (FHA) protein. We identified a striatin (*ham-3*) gene and a FHA domain (*ham-4*) gene in *N. crassa*; strains containing mutations in *ham-3* and *ham-4* show severe somatic fusion defects. However, *ham-3* and *ham-4* mutants undergo mating cell fusion, indicating functional differences in somatic versus sexual fusion events. The *ham-2* and *ham-3* mutants are female sterile, while *ham-4* mutants are fertile. Homozygous crosses of *ham-2, ham-3 and ham-4* mutants show aberrant meiosis and abnormally shaped ascospores. These data indicate that, similar to humans, the HAM proteins may form different signaling complexes that are important during both vegetative and sexual development in *N. crassa.*

## 1. Introduction

Cell signaling resulting in cell-cell fusion is integral to a multitude of eukaryotic processes. Examples include fertilization of an egg by sperm and osteoclast development in mammals (Primakoff and Myles, 2007; Vignery, 2008; Zeng and Chen, 2009), pollen tube and ovary fusion in plants (Higashiyama et al., 2003), and the development of filamentous colonies of fungi (Buller, 1933; Fleissner et al., 2008; Read et al., 2009). Unlike unicellular yeasts, such as *Saccharomyces cerevisiae* or *Schizosaccharomyces pombe*, where cell fusion is only associated with mating, in filamentous fungi, cell fusion also occurs between vegetative cells. Somatic cell fusion is important in colony establishment and development of the interconnected hyphal network characteristic of these organisms. Connectivity in fungal networks is presumed to be necessary for maintaining proper intercolony communication, resource exploitation, virulence in pathogens, and maintaining homeostasis (Reviewed in (Read et al. 2010, Fleissner et al., 2008; Glass et al., 2004; Rayner, 1991; Rayner, 1996).

A number of mutants deficient in hyphal fusion and/or signaling have been characterized in the filamentous ascomycete fungus, *Neurospora crassa* (Read et al., 2010). Many of these mutants have a decreased growth rate and are female sterile. One gene required for vegetative and germling fusion in *N. crassa* is *ham-2,* which encodes a protein with multiple transmembrane domains and a C-terminal domain of unknown function that is conserved in fungi and animals, but not in plants (Xiang et al., 2002). The *ham-2* mutant does not form conidial anastomosis tubes (CATs) and neither attracts nor responds to the presence of a wild type germling (Roca et al., 2005).

Homologs of *ham-2* have been identified in protein complexes in both yeast and humans. Far11, a protein encoded by the *S. cerevisiae* homolog of *ham-2,* was shown to be part of a complex composed of Far3, Far7, Far8, Far9 and Far 10 (Kemp and Sprague, 2003; Uetz et al., 2000). Far proteins are required for maintenance of G1 cell cycle arrest after pheromone stimulation (Kemp and Sprague, 2003). In humans, homologs of *ham-2* have been identified in a complex that acts as a regulatory subunit to protein phosphatase 2A (PP2A), and which also includes a protein similar to Far8 (striatin), and a protein similar to Far9/10 (similar to sarcolemmal membrane-associated protein, SLMAP) which contains a forkhead-associated domain (Goudreault et al., 2008). In addition, this complex contains a MOB3 homolog. Intriguingly, *mob-3* mutants were shown to be hyphal fusion mutants in *N. crassa* (Maerz et al., 2009).

In addition to *ham-2*, a genome wide search revealed that only two additional homologs to the *S. cerevisiae FAR* genes were present in the *N. crassa* genome (Glass et al., 2004); a homolog of *FAR8* (similar to striatin) and a homolog of *FAR9/10* (SLMAP). No homologs of *FAR3* or *FAR7* were identified. In this study, we evaluate whether mutations in the *FAR8* and *FAR9/10* homologs in *N. crassa,* termed *ham-3* and *ham-4* respectively cause a similar cell fusion phenotype to that observed in *ham-2* mutants. We show that *ham-2, 3* and *4* mutants share a similar vegetative fusion defect, but undergo sexual cell fusion. However, the *ham* mutants show an abnormal meiosis phenotype as well as aberrant ascospore development. The phenotypic similarities between *ham-2,*

*3* and *4* mutants suggest they are in the same pathway and regulate diverse cellular processes during both vegetative growth and sexual reproduction in *N. crassa*.

## 2. Materials and Methods

### *2.1. Strains, growth media and conditions*

The strains used in this study are listed in Table 1. Strains were grown on Vogel's minimal medium (Vogel, 1956) with required supplements. BDES medium was used to induce colonial growth (Brockman and de Serres, 1963). Crosses were performed on Westergaards's medium (Westergaard and Mitchell, 1947). The *ham-4* (NCU00528; *Δham-4*) deletion strains, the *ham-3* (NCU08741; *Δham-3*) deletion strains, and the *ham-2* (NCU03727; *Δham-2*) deletion strain (Table 1) were obtained from The Fungal Genetics Stock Center (FGSC) (Colot et al., 2006; McCluskey, 2003). The strain FGSC 4564 strain was used as a helper for crosses when the female could not produce sexual structures (Perkins, 1984). Growth rates were assessed using the race tube method (Ryan et al., 1943). Electroporation was performed according to (Margolin et al., 1997) with 1.5kV setting.

### *2.2. Nucleic acid techniques*

Genomic DNA was isolated as described (Lee et al., 1988). Southern hybridization was performed as described (Sambrook and Russell, 2001). Sequencing was performed by the Berkeley DNA sequencing facility (http://mcb.berkeley.edu/barker/dnaseq). Oligonucleotides were obtained from MWG Biotech (www.mwg-biotech.com) and IDT (www.idt.com). The following primers were used: YDR200CFOR371 AGCAACAGCAGCCATCATCG, YDR200CREV2193 TTGTATCAACGCACGCTCCTG, vps64-16 FOR TCTAGACATGTTCATCTCGCAAAATCTCTTCAAC, vps64-16 REV TTAATTAAA TTCTTCGCCTGCGGCTGCCACC. Taq polymerase (Promega) was used for routine PCR and PfuTurbo (Stratagene) or Phusion (Finnzymes) was used for high fidelity PCR for cloning.

Repeat induced point (RIP) mutation (Selker, 2002), a naturally mutagenic process in *N. crassa* was used to create *ham-4* point mutation mutants. A fragment amplified by oligonucleotides YDR200CFOR371 and YDR200CREV2193 was cloned into pCB1004, and transformed into strain I-1-83 (Table 1). Hygromycin-resistant transformants were crossed to FGSC 988 to obtain RIP mutants. Progeny were screened for sensitivity to hygromycin (to insure loss of the ectopic transformed *ham-4* fragment and retention of the native mutated *ham-4* locus) and morphological defects. Resulting mutant progeny identified by short aerial hyphae (~24%) were screened for restriction length fragment polymorphisms (RFLPs) at the *ham-4* locus (NCU00528) using a PCR product amplified using oligonucleotides *vps64* 16 FOR and *vps64* 16 REV and digested with *Sau3A* (New England Biolabs).

Cassettes were kindly provided by Hildur Colot for knocking out *vps39* (NCU01539). Deletion strains were constructed as previously described (Colot et al., 2006) and Southern blotting was used to confirm correct integration of the

*hph* cassette (data not shown).

The striatin domain, WD repeats, and N221 like protein domain were identified according to Pfam (http://pfam.sanger.ac.uk/). Transmembrane sequences were identified using TopPred (http://mobyle.pasteur.fr/cgi-bin/MobylePortal/portal.py) and verified using TMPRED (http://www.ch.embnet.org/software/TMPRED_form.html). Coils (http://www.ch.embnet.org/software/COILS_form.html) and Paircoil2 (http://groups.csail.mit.edu/cb/paircoil2/paircoil2.html) were used to predict coiled-coil domains in the protein sequences. The calmodulin-binding motif was identified using The Calmodulin Target Database (http://calcium.uhnres.utoronto.ca/ctdb/pub_pages/search/search.htm). A caveolin-binding motif was found in the striatin domain of *ham-3*, which is consistent with the sequence of the striatin domain in *F. verticillioides* FSR-1 and *S. macrospora* PRO11 (Shim 2006).

*2.3. Quantitative heterokaryon and conidia formation test*

A heterokaryon test between mutant strains and a wild-type tester strain was performed to assess hyphal fusion frequency as previously described (Xiang et al., 2002). A conidial suspension of ~$10^7$ conidia of the heterokaryon tester strain FGSC 4564 was mixed with ~$10^3$ conidia of the strains CR16-7 (*ham-4*$^{RIP1}$), CR16-16 (*ham-4*$^{RIP3}$), AS2-4 (*his-3 ham-3::hph)*, AS1-40 (*his-3 ham-4::hph),* the negative control strain CR1-10 *(ham-2*$^{RIP1}$*)* and the wild-type positive control strain I-1-83 or FGSC 6103. The mixed conidial suspensions were plated on BDES minimal media and grown for six days. The colonies resulting from fusion events to form a heterokaryon were counted. The amount of viable conidia in each suspension was determined by germinating the conidia on BDES plates containing supplements (adenine and histidine) and counting the number of resulting colonies. This experiment was repeated three times with similar results.

The amount of conidia each strain produced was determined by inoculating conidia into Vogel's MM tubes and allowing strains to grow for 5 days at 25˚C. After 5 days, one ml of water was added to the tube and vigorously vortexed (30 seconds) to release conidia. The conidia were then counted using a hemacytometer. This experiment was repeated three times with similar results.

*2.4. Microscopy*

Conidial fusion was assessed using 3-5 day old cultures grown in Vogel's MM (Vogel, 1956) tubes at room temperature (~22˚C). One ml of water was added to the tubes and vigorously vortexed. Conidia were filtered through cheesecloth to remove mycelia, and plated on Vogel's MM solidified with 1.5% agar. 3ml of $10^7$/ml conidia were spread evenly across each plate. The plates were incubated for four to ten hours at 30˚C. Agar slices were removed from the plates, and conidia were examined by differential interference contrast (DIC) microscopy for fusion every two hours. Micrographs were taken with a Hamamatsu digital C4742-95 CCD camera (Hamamatsu, Japan) using the Openlab software program (Coventry, United Kingdom) and a Zeiss Axioskop II microscope. Micrographs taken using a Zeiss dissecting microscope were

captured using a Micropublisher 5.0 RTV camera using Q capture image software (Surrey, BC Canada). Fusion was measured by counting conidial germlings touching each other, and fusion pegs or CATs between these germlings. One hundred cells were counted for each replicate and three independent replicates were performed for each strain. The percent germling fusion for each strain was graphed using Excel (Microsoft).

Perithecia were dissected as previously described (Xiang et al., 2002). Trichogyne assays were performed as previously described (Bistis, 1983; Fleissner et al., 2005; Kim and Borkovich, 2004). Briefly, FGSC 988 (WT), FGSC 11300 (*Δham-3*), FGSC 12080 *(Δham-4)* and FGSC 12091 (*Δham-2)* were inoculated onto 2% water agar and incubated for 5 days at room temperature. Blocks of water agar with approximate dimensions 1.0cm X 1.0cm X 0.3 cm were placed on top of the protoperithecia. A microconidial suspension of the opposite mating type (FGSC 2489 and H1-GFP (R11-03, and R12-60); Table 1) was inoculated on top of the block followed by a 20 hr to eight-day incubation at room temperature. Data from three independent replicates were pooled to determine the percentage of conidia whose nuclei had disappeared as a result of trichogyne fusion. Protoperithecia and trichogynes were observed using a dry 40X objective.

To compare ascospore morphology, ascospores ejected from perithecia from homozygous and heterozygous crosses were collected. Ascospores were suspended in a 10% glycerol and water solution and observed under the microscope with a 40x objective. For each cross, ascospores from three independent replicates were pooled and approximately 100 spores were scored as either normal, abnormal and melanized or white.

Vacuoles were stained with 5,6-carboxy-fluorescein-diacetate (CFDA). CFDA was diluted from a stock solution of 2 mg/ml in DMSO to 0.2mg/ml in water and placed onto *N. crassa* strains grown on agar. After a ten-minute incubation, agar slices were placed on glass slides and conidia or hyphae were observed using a standard FITC filter.

*2.5. Acriflavine staining*

Acriflavine staining of asci resulting from homozygous and heterozygous crosses was performed according to the protocol developed by Raju and Perkins (Raju, 1980). Perithecia were collected at six to eight days post fertilization and were incubated at 30˚C in 4N hydrochloric acid for 30 min. The perithecia were then rinsed and incubated at 30˚C in acriflavine for 30 min. The acriflavine was removed and the samples were washed 3 times with an HCl-70% ethanol mixture (2:98 V/V) and then washed three times with water. Squashes of the perithecia were performed and micrographs were taken of the different stages of ascus development using a fluorescence microscope as described above using an EGFP filter (Chroma Technology Corp., Bellows Falls, Vermont USA).

## 3. Results

*3.1. Identifying ham-3 and ham-4*

In a previous study, we identified the *ham-2* gene, which represented the first molecularly characterized gene required for hyphal fusion in filamentous

fungi (Xiang et al., 2002), and which shows significant similarity to a protein encoded by *FAR11* in *S. cerevisiae.* Far11 was subsequently shown to be part of a complex that physically interacts with five other proteins: Far3, Far7, Far8, Far9 and Far10 (Kemp and Sprague, 2003). Blastp (Altschul et al., 1997) was used to search the *N. crassa* predicted proteins (http://www.broad.mit.edu/annotation/fungi/neurospora/) for homologs to FAR3, FAR7, FAR8, FAR9 and FAR10. Single homologs in the *N. crassa* genome to *FAR9/10* (NCU00528) and *FAR8* (NCU08741) were identified, but homologs of either *FAR3* or *FAR7* were not recovered (Glass et al., 2004). NCU08741 encodes a predicted protein of 854 aa that shows significant similarity to *S. macrospora* PRO11, *F. verticillioides* FSR-1 and *S. cerevisiae* FAR8. The predicted protein product of NCU08741 showed the conserved domain structure of the striatin family, whose founding member was isolated from rat neurons (Castets et al., 1996), including a calmodulin-binding domain, which is thought to allow striatin proteins to act as $Ca^{2+}$ sensors (Bartoli et al., 1998). The striatin domain of NCU08741 and most striatin-like proteins (including Pro11 and Fsr-1), contain a caveolin binding motif, a calmodulin binding domain, a coiled-coil domain and WD repeats, which are protein interaction domains (Smith et al., 1999) (Fig. 1A).

We hypothesized that strains containing a deletion of NCU08741 would have a similar phenotype to *ham-2* mutants. Strains containing a deletion of NCU08741 (FGSC 11300; Table 1) grew slowly (~3.5 cm/day as compared to wild-type FGSC 988 at ~7.5 cm/day), had very short aerial hyphae (Fig. 1B, tube 3) and produced ~100 times fewer conidia than the equivalently grown wild-type strain FGSC 988 (data not shown), a phenotype similar to a *ham-2* mutant (Xiang et al., 2002). We refer to NCU08741 as *hyphal anastomosis-3 (ham-3)* locus to reflect the requirement of this gene for cell fusion (see below).

NCU00528 encodes a predicted 761 aa protein, which showed significant similarity to both Far9 and Far10 (e -19). The NCU00528 protein has a predicted FHA domain at its N-terminus, a coiled-coil domain and a transmembrane domain at the C-terminus (Fig. 1A). FHA domains are regions of ~100 aa that fold into an 11-stranded beta sandwich and have been characterized as phosphopeptide recognition domains found in many diverse regulatory proteins.

Using Repeat Induced Point (RIP) mutation, a naturally mutagenic process in *N. crassa* (Selker, 2002), several mutant alleles of NCU00528 were recovered (CR16-7, CR16-8, and CR16-16; Table 1). NCU00528 was sequenced from CR16-7 and CR16-8; altered codons were S175L, A202T, V205I, P206L, and Q228STOP (CR16-7) and M143I, M163I, G178S, M194I, A203T and W226STOP (CR16-8) (Fig. 1A). The stop codons in the NCU00528 RIP alleles in both CR16-7 and CR16-8 would result in a truncated protein of ~200 amino acid residues and which still retains the N-terminal part of the FHA domain. Strains containing the mutant NCU00528 RIP alleles were characterized by slow growth and a tuft of conidia at the top of a tube (Fig. 1B, tube 5). The growth rate of a representative mutant, CR16-8 was reduced to ~5 cm/day as compared to the wild-type growth rate of ~7.5 cm/day.

We also evaluated the phenotype of a strain containing a deletion of NCU00528 (FGSC 12080; Table 1) to compare to the NCU00528 RIP mutants. The ΔNCU00528 strain grew more slowly than CR16-8 (only ~4 cm/day), but was otherwise phenotypically similar to the NCU00528 RIP mutants (short aerial hyphae and a characteristic tuft of conidia (Fig. 1B, tube 4). Also, similar to the *ham-2* mutant (Xiang et al., 2002), the ΔNCU00528 strain produced ~100 times fewer conidia than a wild-type strain (data not shown). Most importantly for this study, the strain containing a deletion of NCU00528 was also a hyphal fusion mutant (see below). We therefore refer to NCU00528 as the hyphal anastomosis-4 (*ham-4*) locus.

*3.2. Quantifying cell fusion in the Δham-2, Δham-3, and Δham-4 mutants.*

The previously characterized *ham-2* mutant has a severe homotypic fusion defect (Xiang et al., 2002). We therefore used a quantitative conidial fusion assay (Pandey et al., 2004) to assess the ability of the *ham-3* and *ham-4* mutant strains to undergo homotypic fusion. Homotypic fusion is defined as fusion between strains of identical genotype where as heterotypic fusion is between strains of different genotypes. Figure 2 shows the comparative ability of *Δham-3, Δham-4, ham-4*$^{RIP2}$ and WT conidial germlings to fuse between themselves over a time course from four to ten hours post-inoculation. The wild-type strain FGSC 988 showed a robust ability to undergo fusion (Fig. 2A). A representative micrograph of wild-type germling fusion at the four hour time point is shown in Figure 2B (note the interconnected nature of the conidial germlings). In contrast to WT, *Δham-3, Δham-4* and the *ham-4*$^{RIP2}$ mutant (CR16-8) showed a significantly reduced ability to undergo fusion. However, in contrast to the *Δham-4* strain, the *ham-4*$^{RIP2}$ mutant displayed ability to undergo self-fusion, especially at later time points. Thus, this mutation in *ham-4* (which retains much of the FHA domain) may represent a partial loss-of-function allele, consistent with its less severe self-fusion defect (Fig. 2A). The morphology of the germinating conidia in the *ham* mutants was strikingly different from that of WT germlings and similar to each other (Fig. 2B). The germ tubes of *ham* mutant strains grew away from the inoculation point, while in WT the germ tubes of germlings grew towards each other and ultimately underwent fusion. This germination phenotype is similar to what has been reported for *ham-2* mutants (Roca et al., 2005).

The conidial germling fusion assay tested the ability of strains to undergo homotypic fusion, but did not provide information about whether wild-type strains can respond to, and fuse with, *Δham-3, Δham-4* or *ham-4*$^{RIP}$ strains. Using a quantitative heterokaryon assay, it was previously shown that strains containing mutations in *ham-2* mutants have a 1000-fold reduction in the ability to fuse with a wild-type strain (Xiang et al., 2002). In this assay, conidia from the mutant strain and a wild-type fusion competent strain (FGSC 4564; Table 1), containing different auxotrophic markers, are mixed and plated on minimal media. Only those germlings/hyphae that have undergone fusion with FGSC 4564 and containing the complementary auxotrophic markers, are able to grow on minimal

media without additional supplements (heterokaryon test). Similar to strains containing a mutation in *ham-2*, both the *Δham-4* (AS1-40) and the *Δham-3* (AS2-4) deletion strains showed a severe heterotypic fusion defect, with no heterokaryotic colonies recovered (Table 2). By contrast, strains containing the point mutations in *ham-4* (CR16-7; *ham-4*$^{RIP1}$ and CR16-16; *ham-4*$^{RIP3}$) formed heterokaryons with the wild-type tester strain (FGSC 4564) at a similar frequency to the wild-type control (Table 2). These data suggest that *ham-4*$^{RIP}$ alleles that encode a truncated HAM-4 protein containing only the FHA domain is sufficient for both homotypic and heterotypic fusion.

*3.3 Vacuolar morphology of ham-2, ham-3 and ham-4 mutants.*

In a functional genomics study in *S. cerevisiae*, the *ham-2* homolog *ynl127w (FAR11)* and *ham-4* homolog, *vps64 (FAR 9)* were identified as vacuolar protein sorting (*vps*) mutants due to their improper CPY secretion (Bonangelino et al., 2002). We therefore tested potential *vps* defects of the *ham* mutants in *N. crassa* by observing vacuolar morphology. A *vps* positive control strain containing a deletion of *vps-39 (vps-39::hph (Δvps-39))* was constructed (see Materials and Methods) (Table 1). Vps39 (also known as Vam6) is the guanine nucleotide exchange factor for the Rab GTPase Ypt7, and is required for vacuole fusion and organization (Wurmser et al., 2000). In both *S. cerevisiae* and *Aspergillus nidulans, vps39/vam6/avaB* mutants have defective vacuolar morphology, including small and fragmented vacuoles (Bonangelino et al., 2002; Oka et al., 2004; Raymond et al., 1992). We stained germlings from the *ham* mutants and the *Δvps-39* strain using 5,6-carboxy-fluorescein di-acetate (CFDA), a fluorescent probe that specifically labels vacuoles. While germlings in the *Δvps-39* strain (CR65-1) had tubular and small vacuoles, as expected (Fig. 3), the relative size of vacuoles in all of the *ham* mutants were consistently larger than the wild-type strain FGSC 988 (Fig. 3C-F). The relatively large vacuoles seen in the *ham* mutants were also seen at later time points when the relative growth of germinating spores from the *ham* mutants was equivalent to the wild-type strain (data not shown). Fragmented as well as large vacuoles have been associated with protein sorting defects in *S. cerevisiae* (Raymond et al., 1992).

*3.4. The Δham-2, Δham-3 and Δham-4 mutants show delayed formation of protoperithecia.*

In addition to germling and hyphal fusion, which occur during vegetative growth, cell fusion is also required during mating in *N. crassa*. Upon nitrogen starvation, a strain of either mating type will produce female reproductive structures termed protoperithecia. Specialized hyphae called trichogynes grow out of the protoperithecia and chemotropic interactions between trichogynes and conidia of opposite mating type ultimately result in cell fusion between the two (Bistis, 1981, 1983). After cell fusion occurs, one or more nuclei from the conidium subsequently travels down the trichogyne and into the protoperithecium. After approximately four days, fertile ascogenous hyphae can be observed within the developing perithecium. A second cell fusion event is

associated with crozier development and ascus formation (where karyogamy and meiosis occur) (Davis, 2000; Raju, 1992).

Previous results suggested that hyphal fusion is required for formation of protoperithecia in *N. crassa* (Maerz et al., 2008; Xiang et al., 2002). For example, RIP mutations in *ham-2* resulted in a strain that failed to make protoperithecia (Xiang et al., 2002), a phenotype that could be complemented in a heterokaryon with a wild-type strain. We therefore evaluated whether strains containing a deletion of *ham-2*, *ham-3* or *ham-4* were capable of forming female reproductive structures. To our surprise, strains containing a full deletion of *ham-2* (*Δham-2*, FGSC 12091) formed wild-type looking protoperithecia, although at a later time point than that observed for a wild-type strain (FGSC 988) (Table 3). Similarly, *Δham-3* and *Δham-4* strains produced normal looking protoperithecia, but were 1-2 days delayed in protoperithecium formation (Fig. 5), possibly as a consequence of their slow growth rate. These data indicate that hyphal fusion is not required for the development of morphologically normal female reproductive structures.

*3.5 The ham mutants show chemotropic interactions during mating and undergo mating cell fusion.*

The *ham-2, ham-3* and *ham-4* mutants failed to show chemotropic interactions during germling fusion and are fusion defective (Fig. 2 and Table 2). Thus, we evaluated whether *Δham-2, Δham-3,* and *Δham-4* mutants were also affected in mating-cell chemotropic interactions or fertilization by performing a trichogyne-conidium mating assays. All three *ham* strains were delayed in protoperithecial and trichogyne production as compared to a wild-type strain (FGSC 988). Wild-type trichogynes reached microconidia within 40 hours, while *Δham-3* and *Δham-4* trichogynes took 7 days to reach microconidia of the opposite mating type. Despite severely reduced growth rate of trichogynes towards microconidia, the *Δham-3* and *Δham-4* trichogynes were attracted to and wrapped around microconidia of the opposite mating type in a manner indistinguishable from wild-type strain FGSC 988 (Fig. 4A). Unlike the results using the *Δham-3* and *Δham-4* mutants, trichogyne assays with the *Δham-2* mutant were inconclusive. Trichogynes were observed growing from protoperithecia through the agar block toward microconidia on top of the block. However, after 8 to 9 days, the *Δham-2* trichogynes still had not reached the microconidia. Vegetative hyphae began growing over the agar blocks, making imaging of trichogyne-conidium interactions impossible.

We then evaluated whether mating cell fusion was affected in the *Δham-3* and *Δham-4* mutants. We used microconidia from strains containing a histone-1-GFP (H1-GFP) construct (R19-22; Table 1 (Freitag et al., 2004) to determine whether nuclei traveled from the microconidium to the trichogyne as a consequence of trichogyne-conidium fusion. When trichogynes of wild type strain FGSC 2489 wrapped around nuclear H1-GFP labeled microconidia of the opposite mating type (R12-60), 87% of nuclei disappeared, indicating mating cell fusion had occurred (Fig. 4B). Of the *Δham-3* trichogynes that circled around

wild-type H1-GFP microconidia, 52% (n=33) underwent mating cell fusion, as assessed by loss of nuclear H1-GFP fluorescence in the microconidia. In *Δham-4*, 59% (n=149) of the trichogynes that circled around wild-type H1-GFP labeled microconidia underwent mating-cell fusion. These data show that although there is a reduction in both the speed and number of successful mating cell fusions, *Δham-4* and *Δham-3* mutants are capable of both sexual chemotropic interactions and sexual cell fusion, which results in nuclear migration through the trichogyne.

*3.6. The Δham-2 and Δham-3 mutants are blocked in female sexual development following fertilization*.

To test their ability to complete a mating cross as a female, *Δham-2, Δham-3* and *Δham-4* strains were grown on mating plates until they produced protoperithecia and then were crossed using *Sad-1* as a male (Fig. 5). *Sad-1* mutants suppress meiotic gene silencing of unpaired DNA (MSUD) (Shiu et al., 2001) and therefore eliminate silencing from affecting sexual development. The *Δham-4* crosses with *Sad-1* resulted in production of mature sexual structures (perithecia). Perithecia from the *Δham-4* x *Sad-1* crosses were indistinguishable from those of a wild-type cross and contained viable ascospores (Table 3), although the density of perithecia on mating plates was less than wild type (data not shown). In contrast, perithecia in *Δham-2* and *Δham-3* crosses with *Sad-1* failed to develop and remained immature (Fig. 5; Table 3). No sexual tissue (paraphyses, ascogenous hyphae, croziers or asci) were observed in these crosses. These results suggest a post-mating defect in *ham-3* mutants because trichogyne-conidium fusions were observed in *ham-3* crosses.

Crosses between *Sad-1* strains as a female (P1-54 *A* or P1-68 *a*; Table 1) and *Δham-2, Δham-3* or *Δham-4* strains as a male were fully fertile. The crosses resulted in wild-type looking perithecia, in which wild-type ascospores developed (Fig. 6). These data indicate that *ham-2* and *ham-3* mutants have a sexual defect that is female autonomous in development of perithecia. To test this hypothesis, we created heterokaryons of *Δham-2, Δham-3* and *Δham-4* with a helper strain $a^{m1}$ (FGSC 4564). The $a^{m1}$ mutant contains a mutation at the *mating type* locus such that this mutant still makes female reproductive structures, but cannot participate in a cross as either a female or male; $a^{m1}$ nuclei are not active in ascogenous hyphae (Perkins, 1984; Raju, 1992). Heterokaryons between *Δham-2, Δham-3* or *Δham-4* and the helper strain (*Δham-2* + $a^{m1}$); (*Δham-3* + $a^{m1}$); (*Δham-4* + $a^{m1}$) were fertile as females when crossed to a *Sad-1* or wild type strain FGSC 2489 (Table 3). These data indicate that *ham-2* and *ham-3* mutants have a defect in female sexual development following fertilization, but before ascogenous hyphae development.

*3.7. Δham-2, Δham-3 and Δham-4 mutants show abnormal meiosis and ascospore development.*

When *Δham-2, Δham-3,* and *Δham-4* strains were used as males in a cross with a wild-type female instead of a *Sad-1* female, we observed an unexpected phenotype. The ascospores from these crosses had unusual sizes and shapes (Fig. 7). These data indicated that MSUD silenced the unpaired *ham* genes in these crosses, suggesting that homozygous crosses between *ham* mutants would show similar ascospore defects. We therefore used the (*his-3*; *ham-2::hph a* + $a^{m1}$) heterokaryon as a female and crossed it to *Δham-2 A*. As predicted, the resulting perithecia contained a reduced number of ascospores per rossette (Fig. 6B) and 93.5% (n=91) of these spores were abnormal (Fig. 7), deviating either from the typical elliptical shape and/or the typical spore size. Similarly, *ham-3* homozygous crosses ((*his-3*; *ham-3::hph a* + $a^{m1}$) x *ham-3::hph A*) resulted in a severe decrease in ascospore production (Fig. 6B); ascospores from this cross were never ejected and we were unable to recover enough spores to analyze. By contrast, *ham-4* homozygous crosses ((*his-3; ham-4::hph A* + $a^{m1}$ ) x *ham-4::hph a)* (Fig. 6B) showed a much less severe ascospore phenotype. Only 64.5% (n=124) of the ascospores were abnormal, although the number of ascospores per rosette was similar to that of wild type (Fig. 7).

Heterozygous crosses, using the *ham-2, 3, or 4* + $a^{m1}$ heterokaryons as female and crossed with a wild type male strain, showed a slightly less severe ascospore phenotype as compared to the homozygous crosses (Fig. 7B). Most notably ((*ham-3::hph* + $a^{m1}$) x WT) crosses resulted in ascospores (Fig. 7A), whereas *ham-3* homozygous crosses were completely sterile. The ascospore phenotypes of the (*Δham-2, 3,* or *4* + $a^{m1}$) x WT crosses were completely suppressed when the *Sad-1* strain was used as a male, with all three crosses resulting in only ~4-7% abnormal ascospores, a value comparable to a wild-type cross with *Sad-1* ((FGSC 6103+ $a^{m1}$) x *Sad-1*; 3.0% (n=100) abnormal ascospores).

*3.8 Nuclear staining in developing asci*

Mutants showing abnormal or delayed meiosis often result in wide range of ascospore phenotypes including barren asci, incorrect spore delimitation, abnormal spore size and shape, and a decreased number of spores per ascus (reviewed in Raju 1991). In order to determine if a defect in meiosis occurs in the *ham* mutants, we used acriflavine to stain nuclei at different stages of developing asci from *ham* homozygous crosses (Raju 1982). Normal ascus development after crozier formation includes karyogamy (one nucleus), meiosis I (two nuclei), meiosis II (four nuclei), mitosis I (eight nuclei), spore delimitation and mitosis II (two nuclei per ascospore) (Raju, 1980). A number of further mitoses then occur within the delimited ascospores, resulting in up to 32 or more nuclei in mature ascospores. All stages of meiosis and mitosis can be seen in Figure 8 during the development of a wild type ascus from a ((FGSC 6103 + $a^{m1}$) x *Sad-1*) cross. In homozygous crosses with *ham-2* ((*his-3; ham-2::hph a* + $a^{m1}$) x *ham-2::hph A), ham-3* ((*his-3; ham-3::hph a* + $a^{m1}$) x *ham-3::hph A),* and *ham-4* ((*his-3 ham-4::hph A* + $a^{m1}$) x *ham-4::hph a)*, many asci containing a single nucleus were found in developing perithecia (Fig. 8). These observations indicate successful crozier formation resulting in karyogamy. However, the *ham* homozygous

crosses appeared to be delayed in meiosis I as compared to a wild type cross. This is particularly evident in *ham-2* and *ham-3* homozygous crosses, where a single nucleus was observed in an ascus that would usually contain two or four nuclei in a wild type cross. By contrast, asci with two nuclei were eventually observed in all the *ham* homozygous crosses. A meiotic malfunction is even more evident during meiosis II and mitosis I in asci of the homozygous *ham* crosses, where spore delimitation occurred, but where fewer than eight nuclei were present in the ascus (Fig. 8B-D). This results in a variable number of large ascospores within one ascus and aborted ascospores lacking nuclei. Heterozygous crosses between the *ham* mutants and wild type ((*ham* mutant + $a^{m1}$) x WT) also often exhibited aberrant meiosis resulting in asci with various numbers of large ascospores (Fig. 6A). In contrast, the *ham-4* homozygous crosses often proceeded in the correct developmental order and resulted in eight-spored asci, although many of the spores were abnormally shaped. The phenotype of abnormal meiosis and ascospore development was present in all *ham* mutant homozygous crosses.

Ascospores produced from the *ham* homozygous and heterozygous crosses showed a variety of shapes and sizes but often had an extra appendage or tail (Fig. 7). In addition, the cell wall and/or the ability to maintain a correct osmotic potential is compromised such that when the ascospores are suspended in water they burst. This phenomenon is alleviated when the spores are suspended in 5% FIGS or in a 10% glycerol solution. As with wild type crosses, heat shock was required for ascospore germination, and many of the ascospores germinated despite their abnormalities (data not shown).

**4. Discussion**

Based on human and *S. cerevisiae* data, we interrogated the *N. crassa* genome for homologs of proteins in the STRIPAK and FAR complexes. We found single homologs of both *S. cerevisiae FAR8* (striatin) and *FAR9/10* (SLMAP) in the *N. crassa* genome, which we named *hyphal anastomosis mutants 3* and *4.* Mutations in *ham-3* and *ham-4* result in strains that lack vegetative hyphal fusion, similar to the previously identified *ham-2* mutant. In contrast to the pleiotropic phenotype of the *ham* mutants in *N. crassa*, the *S. cerevisiae FAR* mutants (even the sixtuple mutant) have a subtle-G1 arrest phenotype, but no apparent defect in mating cell fusion (Kemp and Sprague, 2003), the only type of fusion in yeast. As with *S. cerevisiae*, the *N. crassa ham* mutants can also undergo sexual cell fusion. These data indicate that there are differences between the signal transduction pathways involved in sexual and vegetative fusion in *N. crassa*. However, a *N. crassa* strain containing a deletion of a gene (*Prm1*), which was shown to be required for plasma membrane fusion during mating cell fusion in *S. cerevisiae* (Heiman and Walter, 2000), has a nearly identical cell fusion defect during both mating and vegetative fusion in *N. crassa* (Fleissner et al., 2009a) showing that some machinery is required for both cell fusion processes. In addition to vegetative fusion defects, the *ham* mutants showed growth and conidiation defects, as well as vacuolar and meiotic/ascospore abnormalities, suggesting that the HAM proteins are involved

in biological processes in addition to vegetative cell fusion.

We predict that HAM-2, HAM-3 and sometimes HAM-4 work in a complex involved in cell-cell signaling between germlings and between vegetative hyphae to promote cell fusion. In humans, striatin (*ham-3*) interacts with STRIP1/2 (*ham-2*), mob3 (*mob-3*), the CCM3 and GCK-III kinases, but only sometimes with SLMAP (*ham-4*) (BAILLAT et al., 2001; Castets et al., 2000; Goudreault et al., 2008). Mutations in *N. crassa mob-3* result in mutants that fail to undergo hyphal fusion (Maerz et al., 2009). These data suggest that MOB-3 may also interact with HAM-3 and/or HAM-4. In human endothelial cells, striatin (similar to HAM-3) is responsible for localizing estrogen receptors to caveolae on the cell membrane, inducing the rapid activation of a MAP kinase (Qing et al., 2004). A MAP kinase, MAK-2, is required for vegetative cell fusion in *N. crassa* (Pandey et al., 2004). Recent work has shown that MAK-2 oscillates between the fusion tip and the cytoplasm in germlings undergoing chemotropic interactions (Fleissner et al., 2009b). A second protein, SO, oscillates in opposition to MAK-2; *so* mutants are also fusion defective (Fleissner et al., 2005). Similar to *mak-2* and *so* mutants, *ham* mutants lack any chemotropic interactions (Roca et al., 2005) (this study). We hypothesize that HAM-3 and other HAM proteins play an important role in facilitating the rapid oscillation of MAK-2 and SO proteins at the two opposing sites of cell fusion.

Striatin has been implicated in other signal transduction and cellular processes in mammalian cells, including vesicular trafficking, endocytosis and epithelial cell sheet movement (reviewed in (Benoist et al., 2006). Striatin is involved in a $Ca^{2+}$ signal transduction pathway in which calcium binds striatin via calmodulin; in the absence of calcium, striatin binds directly to caveolin, but moves to the cytoplasm upon stimulation by $Ca^{2+}$ (Gaillard et al., 2001). It has been shown that calcium signaling is involved in fungal hyphal tip growth and establishment (Torralba and Heath, 2001). We predict that calcium signaling will also be required for hyphal fusion through and interaction between calmodulin and HAM-3. Further research will elucidate interactions between HAM-3, calcium signaling, hyphal fusion and MAK-2 activation.

In *S. macrospora*, a close relative to *N. crassa*, mutations in the striatin-like protein *Pro11* resulted in a block in perithecial development (Poggeler and Kuck, 2004). These observation are consistent with our findings in *N. crassa* where mating cell fusion was observed in *ham-3* crosses, but subsequent perithecial development was blocked, a phenotype that was complemented in a heterokaryon with $a^{m1}$. Similar to *N. crassa ham-3* and *S. macrospora* (Pro11) mutants, FSR-1 (a striatin like protein) mutants in *Fusarium verticilliodies* and *F. graminarium* (Shim et al., 2006) also showed defects in female fertility. Both the *ham-3* and *ham-2* mutants show a similar defect in perithecial development following fertilization, while the *ham-4* mutants did not, and were indistinguishable from WT in this regard.

SLMAP, Far9/10 and HAM-4 proteins contain an FHA domain, a phosphoprotein interaction domain, which binds specific phospho-threonine epitopes and is found in many proteins with diverse functions (many involved in cell cycle control) (Durocher and Jackson, 2002). Based on analysis of the *ham-4*

RIP mutants, the FHA domain of HAM-4 is sufficient for cell fusion, albeit at a reduced efficiency, suggesting that HAM-4 may recognize a phosphorylated protein during the hyphal fusion process. In humans, SLMAP (*ham-4)*, is necessary for myoblast cell fusion during muscle development (Guzzo et al., 2004). Our results showing the inability of *ham-4* deletion mutants to undergo hyphal fusion raise the possibility of a conserved or similar function between SLMAP and *ham-4* in cell fusion.

In *S. cerevisiae*, the Far mutants cannot maintain cell cycle arrest when exposed to mating pheromone but they are unaffected in ascospore development (Kemp and Sprague, 2003). In contrast, all of the *ham* mutants in *N. crassa* show defects in meiotic progression during ascospore formation. Acriflavine staining of developing asci showed that mutations in *ham-2, 3* and *4* affect nuclear division during ascus development, suggesting that the HAM proteins could also be involved in cell cycle regulation. However, the defect of the *ham* mutants appears to be specific to meiosis, as staining of nuclei in mitotic vegetative cells failed to reveal any differences from WT (data not shown).

Many mutants aberrant in meiosis, ascus development, and ascospore formation have been identified and characterized in *N. crassa* (reviewed in (Raju, 1992). Of particular interest and relevance are mutants where meiosis and ascospore delimitation are decoupled, such as those identified in *P. anserina* (Zickler and Simonet, 1980) and *S. cerevisiae* (Moens et al., 1974). When meiosis is uncoupled from ascospore formation, the resulting cross produces a reduced number of spores per ascus and often misshapen spores or spores of the wrong size. For example, an *N. crassa* mutant called *fourspore* (*fsp*) is delayed in mitosis after meiosis II and spores delimit around the four nuclei resulting in only four spores (Raju, 1986), although occasionally only three spores develop resulting in one large spore and two smaller ones. This phenotype is similar to some of the asci and ascospores from the *ham* homozygous crosses where a decreased number of ascospores per ascus and larger than normal ascospores were observed. However, ascospores from *ham* homozygous crosses often had tails or appendages, and were osmotically sensitive, phenotypes that have not been reported in any other meiotic mutants. Our discovery of a new intron in ham-2 suggests that ham-2 might have multiple roles during the development of N. crassa. As has been shown, ham-2 is involved in both hyphal fusion and ascospore development. However, further research into the role of this alternative species of ham-2 is necessary before any ….. of their function can be made.

In addition to meiotic/ascospore defects and hyphal fusion defects, the *ham* mutants show aberrant vacuolar morphology. Two of the FAR mutants, *far11* and *far9,* where identified in *S. cerevisiae* using a genome – wide screen for mutants that aberrantly secrete vacuolar-localized carboxy peptidase Y (Bonangelino et al., 2002). Vacuolar morphology has been described in several ascomycete species (Raymond et al., 1992) (Oka et al., 2004; Tarutani et al., 2001) (Shoji et al., 2006) and the mycorrhizal basidiomycete species *Pisolithus tinctorius* (Allaway and Ashford, 2001). Interestingly, while *vps* mutants do not affect the cellular shape of *S. cerevisiae*, mutations in homologs of *vps* genes in

filamentous fungi impact morphology; several *vps* mutants in *A. nidulans* and *A. oryzae* grow slowly or have altered conidiation or branching patterns (Ohneda et al., 2005; Oka et al., 2004). In filamentous fungi, different cell types also display different vacuolar morphology. For example, large vacuoles are found in older hyphae, while small vacuoles are observed in conidia (Shoji et al., 2006). The aberrant vacuoles found in the *ham* mutants, which serve as a storage compartment of $Ca^{2+}$ in fungi (Miller et al., 1990), may be due to sorting defects or a defect in $Ca^{2+}$ signaling, which appears to involve striatin (Gaillard et al. 2001).

The ER could be a potential location of a hypothesized ham - 2, 3, 4 and mob-3 complex in N. crassa. This would be consistent with our idea that this complex is involve in intracellular signal trafficking. Our results showing that mob-3 colocalizes with a known ER protein suggests an ER localization of mob-3 and potentially the ham proteins as well. At this point more evidence is needed to support this hypothesis and future tagging and colocalization studies are needed.

Our phenotypic analysis of the *ham-2, 3* and *4* mutants supports the hypothesis that these proteins function together to regulate germling and hyphal fusion, perhaps in conjunction with MOB-3. Similar to STRIPAK complex identified in humans, it is likely that these proteins form complexes with different sets of proteins to regulate growth, hyphal fusion and sexual development, consistent with the complex pleiotropic phenotype associated with the *ham* mutants. Further genetic and biochemical analyses are required to define the function of these signaling complexes in growth and reproduction in filamentous fungi.

**Acknowledgements**

We thank Dr. Andre Fleissner for preliminary analysis of the *ham-3::hph* mutant and preliminary trichogyne assay analysis in the *ham-3* and *ham-4* mutants. We also thank Dr. Abigail Leeder for help with the figures and thank the members of the Glass lab for their helpful insights and comments. This work was funded by a National Science Foundation Grant to N.L.G. (MCB-0817615).

**Additional Research Post-publication:**

**5. Alternate splicing in ham-2 transcription**

Sequencing of ham-2 transcipts from a 16hr old FGSC 2489 colony (provided by Charles Hall) revealed the potential of a previously unannotated intron. The new intron was predicted to be located around nucleotide 1071 and ending around nucleotide 1171 placing it between introns 1 and 2. We suspected this might be an intron due to lack of sequence coverage in this area. In order to determine if this was an actual intron or just poor coverage in sequencing, we designed primers for regions up and down stream of the suspected novel intron. Primers used to amplify the region containing both intron 1 and the suspected new intron were 5'-AGACGACCTTGAGGATATGG-3' and 5'-

GGAACACATGGTAATCGAGC-3'. We then amplified this region using wild type cDNA (supplied by Jian Ping Sun) made from RNA extracted from hyphae of a 16hr old colony. The size of the fragment amplified from our primers should be 400bp from genomic DNA, a 343bp amplification from cDNA according to the annotation which includes intron 1, and 238bp from cDNA if the new intron is also present. A PCR of cDNA using these primers revealed what appeared to be products of two different sizes both smaller than the 400bp gDNA PCR product. These products were cloned into a zero TOPO blunt plasmid, then transformed into E.coli One shot cells. Six transformants were harvested, and miniprepped for plasmid extraction. Plasmid DNA was digested using EcoR1. We found DNA fragments of two different sizes between 200 and 350bp. Two plasmids were sent for sequencing, one of each different size fragment. We found two different sequences, one containing the predicted annotated sequence between our two primer regions, and a sequence consistent containing a 66bp gap from nucleotide 1072 to 1138 in the region of the predicted new intron. An intron of 66bp in this region would not cause a frame shift but the intron is in the middle of a predicted pFam N1221 like protein domain, and a transmembrane domain. Based on these findings it appears that *ham-2* has alternative splicing leading to two different gene products that are both present in hyphae. The difference in function between these two products is entirely unknown and requires further investigation.

**6. Localization of MOB-3**

StrA, a homolog of HAM-3, has been shown to localize to the ER in *Aspergillus nidulans* (Wang et al. 2010) and the mob-3 (NCU07674) deletion in *N. crassa* has been shown to be a hyphal fusion mutant (Maerz et al. 2009). As described above, we hypothesize that MOB-3 is a member of a greater complex in *N. crassa* including HAM-2, HAM-3, and HAM-4 and is scaffolded by PP2A. We predicted that MOB-3 would localize to the ER similar to STRA. To determine the localization of MOB-3 in *N. crassa* we first performed a PCR of mob-3 using Phusion HF DNA polymerase (New England Biolabs) from FGSC2489 genomic DNA extracted using forward and reverse primers containing an Xba-1 digestion sequence before the start codon of mob-3, 5'-TCTAGAATGTCGCTTCCCCCGAG-3', and an Xma-1 digestion site in place of the stop codon of mob-3, 5'-CCCGGGTGCTGAGCAGGTCGCA-3'. The PCR product was run on an agarose gel, purified using a gel extraction kit (Qiagen), digested with enzymes Xma-1 and Xba-1 (New England Biolabs), and ligated using T4 ligase (Invitrogen) into vector pMF 272 between the Xba1 and Xma1 digestion sites. The vector was then sequenced to verify the correct mob-3 sequence. This vector was then transformed into FGSC 6103, and transformants that could grow on minimal media without supplements were selected. Three transformants were recovered and one showed GFP fluoresence. All images were obtained using a Deltavision Spectris DV4 deconvolution microscope (Applied Precision Instruments). SVI Huygens Professional and Bitplane Imaris were used to deconvolve and process the images. We found that GFP tagged MOB-3 appeared to be localizing to the ER (Fig 2-9A), as MOB-3 does in *A.*

*nidulans*. To determine whether this was true a heterokaryon was made with the mob-3::gfp strain and a grp-76::dsRed strain (Bowman et al. 2009). GRP-76 is a calcium transporter protein, which has been shown to localize to the ER in *N. crassa* (Bowman et al. 2009). Germlings of the heterokaryon were then imaged revealing MOB-3::GFP colocalization with GRP-76::dsRED. Though MOB-3 appears to localize to the ER, there were also areas of both MOB-3::GFP and GRP-76::dsred that were not colocalized indicating other sites of MOB-3 localization within the cell (Fig. 2-9 C) . Further research is needed to understand the interactions, function, and localization of MOB-3 in *N. crassa*.

## 7. References


Allaway, W.G., and Ashford, A.E. (2001). Motile tubular vacuoles in extramatrical mycelium and sheath hyphae of ectomycorrhizal systems. Protoplasma *215*, 218-225.

Altschul, S., Madden, T., Schaffer, A., Zhang, J., Zhang, Z., Miller, W., and Lipman, D. (1997). Gapped BLAST and PSI-BLAST: a new generation of protein database search programs. Nucleic Acids Res *25*, 3389-3402.

Baillat, G., Moqrich, A., Castets, F., Baude, A., Bailly, Y., Benmerah, A., and Monneron, A. (2001). Molecular cloning and characterization of phocein, a protein found from the Golgi complex to dendritic spines. Mol Biol Cell *12*, 663-673.

Bartoli, M., Monneron, A., and Ladant, D. (1998). Interaction of calmodulin with striatin, a WD-repeat protein present in neuronal dendritic spines. J Biol Chem *273*, 22248-22253.

Benoist, M., Gaillard, S., and Castets, F. (2006). The striatin family: A new signaling platform in dendritic spines. J Physiol-Paris *99*, 146-153.

Bistis, G.N. (1981). Chemotropic interactions between trichogynes and conidia of opposite mating-type in *Neurospora crassa.* Mycologia *73*, 959-975.

Bistis, G.N. (1983). Evidence for diffusable mating-type specific trichogyne attactants in *Neurospora crassa*. Exp Mycol *7*, 292-295.

Bonangelino, C., Chavez, E., and Bonifacino, J. (2002). Genomic screen for vacuolar protein sorting genes in *Saccharomyces cerevisiae*. Mol Biol Cell *13*, 2486-2501.

Brockman, H.E., and de Serres, F.J. (1963). "Sorbose toxicity" in *Neurospora*. Am J Bot *50*, 709-714.

Buller, A.H.R. (1933). *Researches on fungi.* Vol. 5., Vol 5 (London, Longman).

Castets, F., Bartoli, M., Barnier, J., Baillat, G., Salin, P., Moqrich, A., Bourgeois, J., Denizot, F., Rougon, G., Calothy, G.*, et al.* (1996). A novel calmodulin-binding protein, belonging to the WD-repeat family, is localized in dendrites of a subset of CNS neurons. J Cell Biol *134*, 1051-1062.

Colot, H.V., Park, G., Turner, G.E., Ringelberg, C., Crew, C.M., Litvinkova, L., Weiss, R.L., Borkovich, K.A., and Dunlap, J.C. (2006). A high-throughput gene knockout procedure for *Neurospora* reveals functions for multiple transcription factors. Proc Natl Acad Sci USA *103*, 10352-10357.

Davis, R.H. (2000). Neurospora: Contributions of a model organism (New York, Oxford University Press).

Durocher, D., and Jackson, S. (2002). The FHA domain. FEBS Lett *513*, 58-66.

Fleissner, A., Diamond, S., and Glass, N.L. (2009a). The *Saccharomyces cerevisiae PRM1* homolog in *Neurospora crassa* is involved in vegetative and sexual cell fusion events but also has postfertilization functions. Genetics *181*, 497-510.

Fleissner, A., Leeder, A.C., Roca, M.G., Read, N.D., and Glass, N.L. (2009b). Oscillatory recruitment of signaling proteins to cell tips promotes coordinated behavior during cell fusion. Proc Natl Acad Sci USA *106*, 19387-19392.

Fleissner, A., Sarkar, S., Jacobson, D.J., Roca, M.G., Read, N.D., and Glass, N.L. (2005). The *so* locus is required for vegetative cell fusion and postfertilization events in *Neurospora crassa*. Eukaryot Cell *4*, 920-930.
Fleissner, A., Simonin, A.R., and Glass, N.L. (2008). Cell fusion in the filamentous fungus, *Neurospora crassa*. Methods Mol Biol *475*, 21-38.
Freitag, M., Hickey, P.C., Raju, N.B., Selker, E.U., and Read, N.D. (2004). GFP as a tool to analyze the organization, dynamics and function of nuclei and microtubules in *Neurospora crassa***.** Fungal Genet Biol *41*, 897-910.
Gaillard, S., Bartoli, M., Castets, F., and Monneron, A. (2001). Striatin, a calmodulin-dependent scaffolding protein, directly binds caveolin-1. FEBS Lett *508*, 49-52.
Glass, N.L., Rasmussen, C., Roca, M.G., and Read, N.D. (2004). Hyphal homing, fusion and mycelial interconnectedness. Trends Microbiol *12*, 135-141.
Goudreault, M., D'Ambrosio, L.M., Kean, M.J., Mullin, M., Larsen, B.G., Sanchez, A., Chaudhry, S., Chen, G.I., Sicheri, F., Nesvizhskii, A.I.*, et al.* (2008). A PP2A phosphatase high-density interaction network identifies a novel striatin-interacting phosphatase and kinase complex linked to the cerebral cavernous malformation 3 (CCM3) protein. Mol Cell Proteomics *8,* 157-171.
Guzzo, R., Wigle, J., Salih, M., Moore, E., and Tuana, B. (2004). Regulated expression and temporal induction of the tail-anchored sarcolemmal-membrane-associated protein is critical for myoblast fusion. Biochem J *381*, 599-608.
Heiman, M.G., and Walter, P. (2000). Prm1p, a pheromone-regulated multispanning membrane protein, facilitates plasma membrane fusion during yeast mating. J Cell Biol *151*, 719-730.
Higashiyama, T., Kuroiwa, H., and Kuroiwa, T. (2003). Pollen-tube guidance: beacons from the female gametophyte. Curr Opin Plant Biol *6*, 36.
Kemp, H., and Sprague, G. (2003). Far3 and five interacting proteins prevent premature recovery from pheromone arrest in the budding yeast *Saccharomyces cerevisiae*. Mol Cell Biol *23*, 1750-1763.
Kim, H., and Borkovich, K. (2004). A pheromone receptor gene, *pre-1*, is essential for mating type-specific directional growth and fusion of trichogynes and female fertility in *Neurospora crassa*. Mol Microbiol *52*, 1781-1798.
Lee, S.B., Milgroom, M.G., and Taylor, J.W. (1988). A rapid, high yield mini-prep method for isolation of total genomic DNA from fungi. Fungal Genet Newslett *35*, 23-24.
Maerz, S., Dettmann, A., Ziv, C., Liu, Y., Valerius, O., Yarden, O., and Seiler, S. (2009). Two NDR kinase-MOB complexes function as distinct modules during septum formation and tip extension inNeurospora crassa. Mol Microbiol *74,* 707-723.
Maerz, S., Ziv, C., Vogt, N., Helmstaedt, K., Cohen, N., Gorovits, R., Yarden, O., and Seiler, S. (2008). The nuclear Dbf2-related kinase COT1 and the mitogen-activated protein kinases MAK1 and MAK2 genetically interact to

regulate filamentous growth, hyphal fusion and sexual development in *Neurospora crassa*. Genetics *179*, 1313-1325.
Margolin, B.S., Freitag, M., and Selker, E.U. (1997). Improved plasmids for gene targeting at the *his-3* locus of *Neurospora crassa* by electroporation. Fungal Genet Newslett *44*, 34-36.
McCluskey, K. (2003). The Fungal Genetics Stock Center: from molds to molecules. Adv Appl Microbiol *52*, 245-262.
Miller, A.J., Vogg, G., and Sanders, D. (1990). Cytosolic calcium homeostasis in fungi: roles of plasma membrane transport and intracellular sequestration of calcium. Proc Natl Acad Sci USA *87*, 9348-9352.
Moens, P., Esposito, R., and Esposito, M. (1974). Aberrant nuclear behavior at meiosis and anucleate spore formation by sporulation-deficient (SPO) mutants of *Saccharomyces cerevisiae.* Exp Cell Res *83*, 166-174.
Ohneda, M., Arioka, M., and Kitamoto, K. (2005). Isolation and characterization of *Aspergillus oryzae* vacuolar protein sorting mutants. Appl Environ Microbiol *71*, 4856-4861.
Oka, M., Maruyama, J., Arioka, M., Nakajima, H., and Kitamoto, K. (2004). Molecular cloning and functional characterization of *avaB*, a gene encoding Vam6p/Vps39p-like protein in *Aspergillus nidulans*. FEMS Microbiol Lett *232*, 113-121.
Pandey, A., Roca, M.G., Read, N.D., and Glass, N.L. (2004). Role of a mitogen-activated protein kinase pathway during conidial germination and hyphal fusion in *Neurospora crassa*. Eukaryot Cell *3*, 348-358.
Perkins, D.D. (1984). Advantages of using the inactive-mating-type $a^{m1}$ strain as a helper component in heterokaryons. Fungal Genet Newsl *31*, 41-42.
Poggeler, S., and Kuck, U. (2004). A WD40 repeat protein regulates fungal cell differentiation and can be replaced functionally by the mammalian homologue striatin. Eukaryot Cell *3*, 232-240.
Primakoff, P., and Myles, D.G. (2007). Cell-cell membrane fusion during mammalian fertilization. FEBS Lett *581*, 2174-2180.
Qing, L., Pallas, D., Surks, H., Baur, W., Mendelsohn, M., and Karas, R. (2004). Striatin assembles a membrane signaling complex necessary for rapid, nongenomic activation of endothelial NO synthase by estrogen receptor alpha. Proc Natl Acad Sci USA *101*, 17126-17131.
Raju, N.B. (1980). Meiosis and ascospore genesis in *Neurospora*. Eur J Cell Biol *23*, 208-223.
Raju, N.B. (1986). Ascus development in two temperature-sensitive *four-spore* mutants of *Neurospora crassa*. Can J Genet Cytol *28*, 982-990.
Raju, N.B. (1992). Genetic control of the sexual cycle in *Neurospora*. Mycol Res *96*, 241-262.
Raymond, C.K., Howald-Stevenson, I., Vater, C.A., and Stevens, T.H. (1992). Morphological classification of the yeast vacuolar protein sorting mutants: evidence for a prevacuolar compartment in class E *vps* mutants. Mol Biol Cell *3*, 1389-1402.
Rayner, A. (1991). The challenge of the individualistic mycelium. Mycologia *83*, 48-71.

Rayner, A.D.M. (1996). Interconnectedness and individualism in fungal mycelia (Cambridge, Cambridge University Press).
Read, N.D., Fleißner, A., Roca, M.G., and Glass, N.L. (2010). Hyphal fusion. In Cellular and Molecular Biology of Filamentous Fungi, K.A.B.a. D.Ebbole, ed. (American Society of Microbiology), pp. 260-273.
Read, N.D., Lichius, A., Shoji, J.Y., and Goryachev, A.B. (2009). Self-signalling and self-fusion in filamentous fungi. Curr Opin Microbiol *12*, 608-615.
Roca, M., Arlt, J., Jeffree, C., and Read, N. (2005). Cell biology of conidial anastomosis tubes in *Neurospora crassa*. Eukaryotic Cell *4*, 911-919.
Ryan, F., Beadle, G., and Tatum, E. (1943). The tube method of measuring the growth rate of *Neurospora*. Am J Bot *30*, 784-799.
Sambrook, J., and Russell, D.W. (2001). Molecular cloning: A Laboratory Manual (Cold Spring Harbor, Cold Spring Harbor Laboratory Press).
Selker, E.U. (2002). Repeat-induced gene silencing in fungi. Adv Genet *46*, 439-450.
Shim, W.B., Sagaram, U.S., Choi, Y.E., So, J., Wilkinson, H.H., and Lee, Y.W. (2006). FSR1 is essential for virulence and female fertility in *Fusarium verticillioides* and *F. graminearum*. Mol Plant Microbe Interact *19*, 725-733.
Shiu, P.K.T., Raju, N.B., Zickler, D., and Metzenberg, R.L. (2001). Meiotic silencing by unpaired DNA. Cell *107*, 905-916.
Shoji, J.Y., Arioka, M., and Kitamoto, K. (2006). Vacuolar membrane dynamics in the filamentous fungus *Aspergillus oryzae*. Eukaryot Cell *5*, 411-421.
Smith, T., Gaitatzes, C., Saxena, K., and Neer, E. (1999). The WD repeat: a common architecture for diverse functions. Trends Biochem Sci *24*, 181-185.
Tarutani, Y., Ohsumi, K., Arioka, M., Nakajima, H., and Kitamoto, K. (2001). Cloning and characterization of *Aspergillus nidulans vpsA* gene which is involved in vacuolar biogenesis. Gene *268*, 23-30.
Torralba, S., and Heath, I. (2001). Cytoskeletal and Ca2+ regulation of hyphal tip growth and initiation. Curr Top Dev Biol *51*, 135-187.
Uetz, P., Giot, L., Cagney, G., Mansfield, T., Judson, R., Knight, J., Lockshon, D., Narayan, V., Srinivasan, M., Pochart, P.*, et al.* (2000). A comprehensive analysis of protein-protein interactions in *Saccharomyces cerevisiae*. Nature *403*, 623-627.
Vignery, A. (2008). Macrophage fusion: molecular mechanisms. Methods Mol Biol *475*, 149-161.
Vogel, H.J. (1956). A convenient growth medium for *Neurospora*. Microbiol Genet Bull *13*, 42-46.
Westergaard, M., and Mitchell, H.K. (1947). Neurospora V. A synthetic medium favoring sexual reproduction. Amer J Bot *34*, 573-577.
Wurmser, A., Sato, T., and Emr, S. (2000). New component of the vacuolar class C-Vps complex couples nucleotide exchange on the Ypt7 GTPase to SNARE-dependent docking and fusion. J Cell Biol *151*, 551-562.

Xiang, Q., Rasmussen, C., and Glass, N.L. (2002). The *ham-2* Locus, encoding a putative transmembrane protein, is required for hyphal fusion in *Neurospora crassa*. Genetics *160*, 169-180.

Zeng, Z.-Y., and Chen, J.-M. (2009). Cell-cell fusion: human multinucleated osteoclasts. Cent Eur J Biol *4*, 543-548.

Zickler, D., and Simonet, J. (1980). Identication of gene-controlled steps of ascospore development in *Podospora anserina.* Exp Mycol *4*, 191-206.

**References for additional sections:**

Bowman, Barry J, Marija Draskovic, Michael Freitag, and Emma Jean Bowman. Structure and Distribution of Organelles and Cellular Location of Calcium Transporters in Neurospora crassa. *Eukaryotic Cell* 8, no. 12 (2009): 1845-1855.

Maerz, S., Dettmann, A., Ziv, C., Liu, Y., Valerius, O., Yarden, O., and Seiler, S. (2009). Two NDR kinase-MOB complexes function as distinct modules during septum formation and tip extension in Neurospora crassa. Mol Microbiol *74,* 707-723.

Wang, C.L., Shim, W.B., and Shaw, B.D. (2010) *Aspergillus nidulans* striatin (StrA) mediates sexual development and localizes to the endoplasmic reticulum. *Fungal Genet Biol*.

**Table 2-1.** Strains used in this study

| Strain | Genotype | Origin |
|---|---|---|
| FGSC 988 | ORS 8-1 *a* | FGSC |
| FGSC 2489 | 74 OR23 *A* | FGSC |
| FGSC 6103 | *his-3 A* | FGSC |
| FGSC 4564 | *ad-3B cyh-1 a$^{ml}$* | FGSC |
| FGSC 11299 | *ham-3::hph A* | FGSC |
| FGSC 11300 | *ham-3::hph a* | FGSC |
| FGSC 12081 | *ham-4::hph A* | FGSC |
| FGSC 12080 | *ham-4::hph a* | FGSC |
| FGSC 12091 | *ham-2::hph A* | FGSC |
| I-1-83 | *ad-3A his-3 A* | Gift from A. J. Griffiths |
| AS2-4 | *his-3; ham-3::hph a* | FGSC 11300 X FGSC 6103 |
| AS1-40 | *his-3 ham-4::hph A* | FGSC 12080 X FGSC 6103 |
| AS3-1 | *his-3; ham-2::hph a* | FGSC 12091 X FGSC6103 |
| CR16-7 | *ad-3A his-3 ham-4$^{RIP1}$ a* | FGSC 988 x I-1-83 (*ham-4$^{RIP1}$*) |
| CR16-8 | *ham-4$^{RIP2}$ a* | FGSC 988 x I-1-83 (*ham-4$^{RIP2}$*) |
| CR16-16 | *ad-3A his-3 ham-4$^{RIP3}$ A* | FGSC 988 x I-1-83 (*ham-4$^{RIP3}$*) |
| CR1-10 | *pyr-4; ham-2$^{RIP1}$ A* | (Xiang et al., 2002) |
| CR3-17 | *ham-2$^{RIP}$ A* | (Xiang et al., 2002) |
| CR65-1 | *vps39::hph A* | *mus-51* (*NCU01539::hph*) x FGSC 988 |
| P1-54 | *his-3 Sad-1$^{RIP78}$ mep A* | Gift from P. Shiu |
| P1-68 | *his-3 Sad-1$^{RIP141}$ mep a* | Gift from P. Shiu |
| R11-03 | *H1::GFP A* | Gift from D. Jacobson |
| R12-60 | *H1::GFP a* | Gift from D. Jacobson |

**Table 2-2. Frequency of heterokaryon formation in *ham* mutants versus wild type.**

| Strain | Viable conidia | Heterokaryotic colonies | Percent heterokaryon formation |
|---|---|---|---|
| FGSC6103 (WT) | 570 ± 53* | 104 ± 2 | 18.3 ± 2** |
| CR16-07 (*ham-4$^{RIP1}$*) | 810 ± 81 | 123.7 ± 10 | 15.3 ± 2 |
| CR16-16 (*ham-4$^{RIP3}$*) | 590 ± 52 | 108.7 ± 7 | 18.4 ± 2 |
| AS1-40 (*his-3 ham-4::hph A*) | 496 ± 24 | 0 | 0 |
| AS2-4 (*his-3; ham-3::hph a*) | 553 ± 129 | 0 | 0 |
| CR1-10 (*pyr-4; ham-2$^{RIP1}$*) | 652 ± 45 | 0 | 0 |
| FGSC 4564 | 4.26 x $10^6$ ± 9 | NA | NA |

* Standard error is shown for experiments done in triplicate

** Percent fusion error was calculated using Gaussian error propagation.

**Table 2-3. Summary of crosses**

| | **Male parent** | | | | | | |
|---|---|---|---|---|---|---|---|
| | | x WT | | x *Sad-1* | | x *ham* homozygous | |
| **Female parent** | Protoperith-ecia | perithecia | Ascosp-ores | Perithe-cia | Ascospo-res | Perith-ecia | Ascosp-ores |
| WT (FGSC 2489) | + | + | + | + | + | ND | ND |
| *Ham-2::hph* | +* | - | - | - | - | - | - |
| *Ham-3::hph* | +* | - | - | - | - | - | - |
| *Ham-4::hph* | +* | + | +$^{ab}$ | + | + | + | +$^{ab}$ |
| FGSC 6103 + *a$^{m1}$* | + | + | + | + | + | ND | ND |
| *ham-2::hph* + *a$^{m1}$* | + | + | +$^{ab}$ | + | + | + | +$^{ab}$ |
| *ham-3::hph* + *a$^{m1}$* | + | + | +$^{ab}$ | + | + | + | - |
| *ham-4::hph* + *a$^{m1}$* | + | + | +$^{ab}$ | + | + | + | +$^{ab}$ |

*= delayed $^{ab}$= abnormal ascospores

**Figure legends**

**Figure 2-1**. **A**. Domain structure of HAM-2, 3, and 4. The altered amino acid residues of CR16-7 *(ham-4$^{RIP1}$)* and CR16-8 *(ham-4$^{RIP2}$)* are depicted with black dashes and the location of the new stop codon is a vertical dashed line. The original amino acids that were altered are written in gray and the resulting amino acids after RIP are written in black with an asterisk representing a stop codon. TMD - transmembrane domain, CBM - calmodulin binding motif, FHA - forkhead associated domain, **B.** The macroscopic morphology of the *Δham-3* and *Δham-4* strains is similar to *ham-2* mutants. 1) FGSC 988 (WT) grown in a slant tube has typical extensive aerial hyphae and conidiation 2) CR3-17 (*ham-2$^{RIP}$*) has short aerial hyphae and makes a tuft of conidia at the top of the slant tube. 3) FGSC 11300 (*Δham-3)* has a similar macroscopic phenotype. 4) FGSC 12080 *(Δham-4)*. 5) CR16-8 *(ham-4$^{RIP2}$)* also makes a tuft of conidia at the top of the slant tube.

**Figure 2-2.** Germling fusion in *ham* mutants. **A.** Graph of germling fusion frequency. An aliquot of 300ul of $10^7$/ml conidia was inoculated onto Vogel's MM for four to ten hrs. Fusion rates were measured by counting the number of fused cells in the total number of cells (See white arrows in 2B for examples). All samples had >90% germination except FGSC 12080 (*Δham-4)* at 4 hrs (89%), and FGSC 11300 (*Δham-3)* at 4 hrs (82%). Fusion in FGSC 988 (WT) could not be measured at ten hrs because of over growth. **B.** Representative morphology of germlings. 1) FGSC 988 (WT) grown for four hrs shows fusion. 2) FGSC 988 (WT) at six hrs. 3) FGSC 988 (WT) at eight hrs. Examples of fusion indicated by arrows. 4) CR16-8 (*ham-4$^{RIP-2}$)* at eight hrs. Typically, conidial germlings touch each other, but rarely fuse. 5) FGSC 12080 (*Δham-4)* at eight hrs. Conidial germlings rarely fuse. 6) FGSC 11300 (*Δham-3)* at eight hrs. Conidial germlings rarely fuse and look similar in both *ham-4* mutants tested. Bar = 60 μm.

**Figure 2-3**. Vacuolar staining of *ham-2, Δham-3, Δham-4, and ham-4$^{RIP2}$* germlings. Comparative vacuolar morphology of conidia grown for four hrs at 30° C and stained with (0.2 mg/ml) 5,6 carboxy fluorescein di-acetate (CFDA). Left panels are DIC micrographs and right panels are the fluorescent micrographs of the same samples. All samples are the same relative size, with the scale bar =10 μm. **A**) FGSC 988 (WT) has small regularly sized vacuoles. **B**) CR65-1 (*vps-39::hph)* positive control strain for vacuolar protein sorting has small, tubular vacuoles. **C**) CR3-17 (*ham-2).* **D**) CR16-8 (*ham-4$^{RIP2}$).* **E**) FGSC 12080 (*Δham-4).* **F**) FGSC 11300 (*Δham-3)*. *ham* mutants have larger vacuoles.

**Figure 2-4.** *Δham-3* and *Δham-4* both undergo trichogyne-conidium fusion but are delayed in trichogyne development compared to wild-type. **A**) Wild type (FGSC 2489) trichogyne (arrow) approaches and circles a conidium of the opposite mating type, indicated by an arrowhead, after 16 hrs of incubation **B**) *Δham-3 A* (FGSC 11299) trichogyne wraps around a conidium of the opposite mating type after 3 days of incubation **C**) *Δham-4 A* (FGSC 12081) trichogyne wraps around a conidium after 2 days of incubation **D**) Percentage of nuclei from

a H1::GFP conidium that were transported into the trichogyne as a result of fertilization. Wild type fusion was measured over 40 hrs, n=67, *Δham-3* was measured over 7 days, n=33, and *Δham-4* was measured over 7 days n=149. Bar = 15 μm.

**Figure 2-5.** *Δham-2, Δham-3,* and *Δham-4* used as females crossed with *Sad-1* strains of the opposite mating type. Protoperithecial development (indicated by arrows) in **A**) *Δham-2,* **B**) *Δham-3,* **C**) *Δham-4* and **D**) wild type (FGSC 2489). **E-H** were taken thirteen days post fertilization. Perithecia resulted from the **G**) *Δham-4* x *Sad-1* and **H**) FGSC 6103 x *Sad-1* crosses. Squashes from the resulting perithecia were **I**) *Δham-4* x *Sad-1;* **J)** FGSC 6103 x *Sad-1*. The *Δham-2* and *Δham-3* crosses lacked any sexual tissue, including paraphyses, ascogenous hyphae and asci. Scale bars for A-H are 0.5 mm. Scale bar for squashes (I, J) equals 130 μm.

**Figure 2-6.** *Δham-2, Δham-3* and *Δham-4* crosses when used as males and crossed with either *Sad-1* or a wild type strain of the opposite mating type. **A**. Perithecia developed when *Sad-1* was crossed with 1) *Δham-2,* 2) *Δham-3,* 3) *Δham-4* and 4) wild type. Panels 5-8, respectively, are rosettes recovered from these crosses. Panel 9 is a rosette recovered from wild type crossed with *Δham-2,* panel 10 is a rosette resulting from wild type crossed with *Δham-3* and panel 11 is a rosette from wild type crossed with *Δham-4.* Scale bar for panels 1-4 equals 0.5 mm. The scale bars for 5-12 represent approximately 130 μm. **B**. Squashes from homozygous crosses **1**) *(Δham-2* + FGSC 4564) x *Δham-2*); **2**) *(Δham-3*+ FGSC 4564) x *Δham-3*) and **3**) (*Δham-4* + FGSC 4564) x *Δham-4*). The scale bars for 1-3 represent 130 μm.

**Figure 2-7**. Examples of ascospores recovered from crosses. **A. 1**) (*Δham-4* + FGSC 4564) x FGSC 2489; **2**) *(Δham-4* + FGSC 4564) x *Δham-4)*; **3**) (*Δham-3* + FGSC 4564) x FGSC 2489 and **4**) (*Δham-2* + FGSC 4564) x *Δham-2).* **5**) A wild type ascospore from an (FGSC 6103 + FGSC 4564) x *Sad-1* cross. Scale bar equals 15 μm. **B**. Graph showing the percentage of abnormal ascospores (white bars) collected after ejection from perithecia and percentage of abnormal ascospores that are melanized (black bars).

**Figure 2-8**. Acriflavine staining of the nuclei in developing asci. **A**) Stages of ascus development from (FGSC 6103 + FGSC 4564) x *Sad-1,* first panel shows a rosette with croziers and early asci indicated with arrows. The second panel shows a diploid nucleus in prophase (arrow), the third panel shows two nuclei after meiosis I, the fourth panel shows four nuclei after meiosis II, the fifth panel shows eight nuclei after the first mitotic division and the sixth panel shows spore delimitation and a second mitotic division resulting in two nuclei per ascospore (arrow). **B**) (*Δham-2* + FGSC 4564) x *Δham-2* shows normal karyogamy (first

panel) but results in abnormal subsequent meiotic and mitotic divisions as well as spore delimitation. The second panel shows the beginning of spore delimitation (arrow) but only two nuclei in the ascus, and the third panel shows only four large spores already delimited within the ascus containing one nucleus each (example indicated by arrow) **C**) (*Δham-3* + FGSC 4564) x *Δham-3* the first panel shows normal karyogamy, the second panel shows spore formation (arrows) with only four nuclei in the ascus, and the third panel depicts asci with incorrect numbers of ascospores that are large and have abnormal morphologies (arrows) **D**) (*Δham-4* +FGSC 4564) x *Δham-4* the first panel shows normal karyogamy, panel two shows abnormal spore delimitation, and panel three shows an ascus with eight ascospores that have aberrant morphologies and orientations (arrow points to an ascospore with a tail) **E**) (*Δham-4* + FGSC 4564) x R15-7 shows that some asci that develop normally from this cross. Scale bar represents 30 μm.

**Figure 2-9. A)** *MOB-3*-gfp localization in a (*mob3*::GFP + *Δgrp-76*::dsRed) heterokaryon, B) GRP-*76*-dsRed localization in the same heterokaryon, C) merged image to show MOB-3-GFPand GRP-76-dsRed colocalization. Scale bar equals 5um.

Figure 2-1.

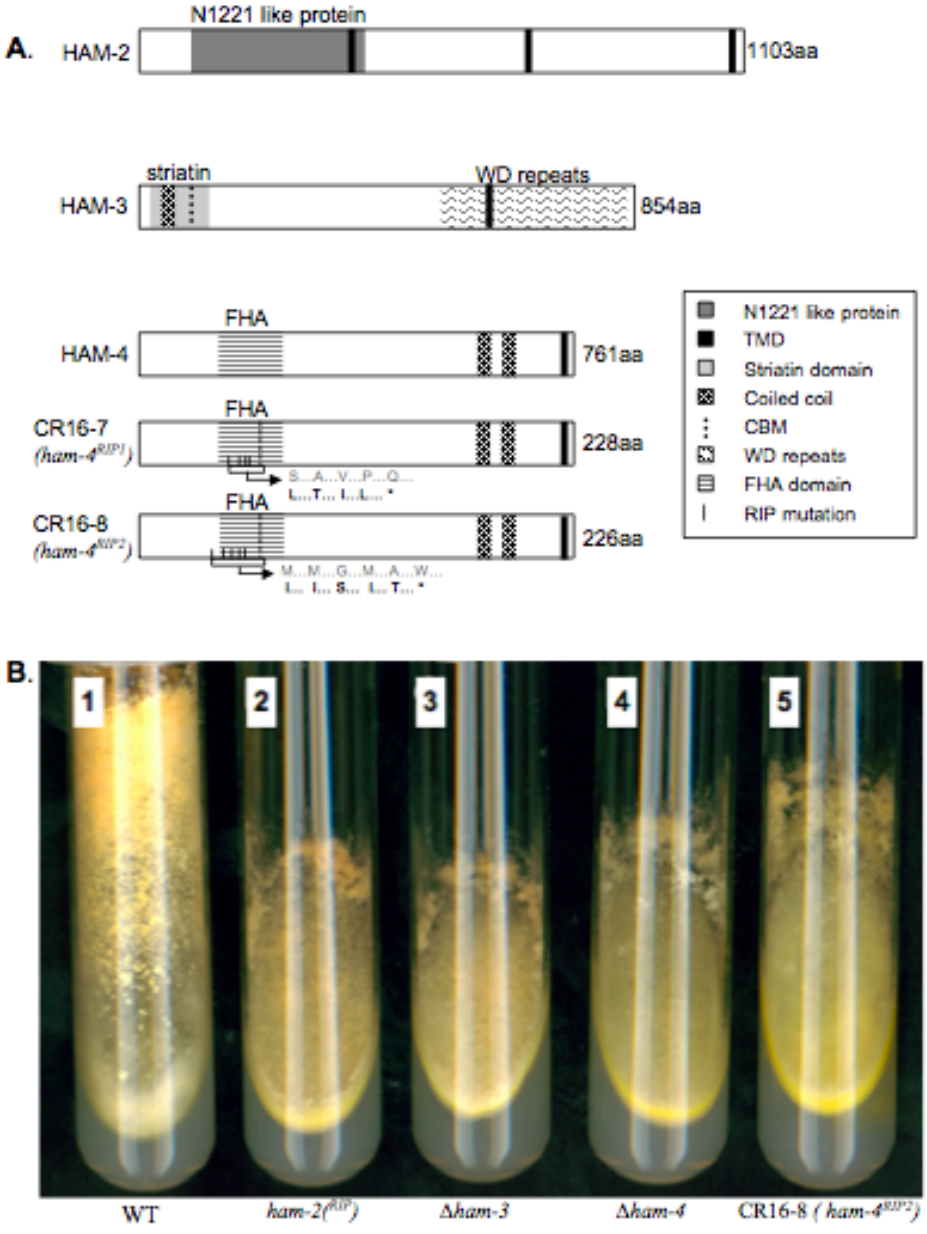
A.
N1221 like protein
HAM-2
1103aa
striatin
WD repeats
HAM-3
854aa
FHA
HAM-4
761aa
CR16-7
(ham-4RIP1)
228aa
CR16-8
(ham-4RIP2)
226aa
N1221 like protein
TMD
Striatin domain
Coiled coil
CBM
WD repeats
FHA domain
RIP mutation
B.
1
2
3
4
5
WT
ham-2(RIP)
Δham-3
Δham-4
CR16-8 ( ham-4RIP2)

Figure 2-2.

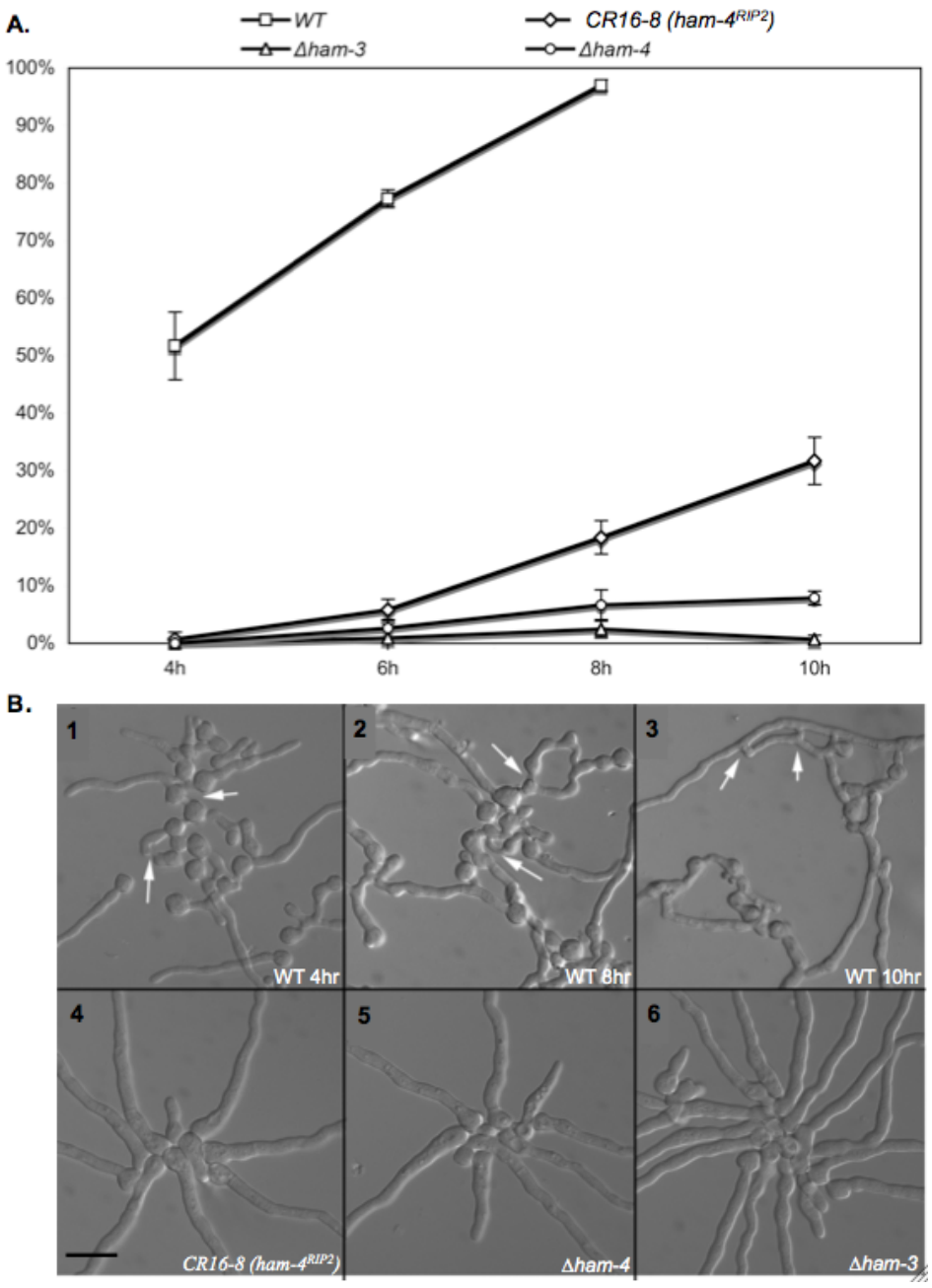
A.
WT
CR16-8 (ham-4RIP2)
Δham-3
Δham-4
100%
90%
80%
70%
60%
50%
40%
30%
20%
10%
0%
4h
6h
8h
10h
B.
1
WT 4hr
2
WT 8hr
3
WT 10hr
4
CR16-8 (ham-4RIP2)
5
Δham-4
6
Δham-3

Figure 2-3.

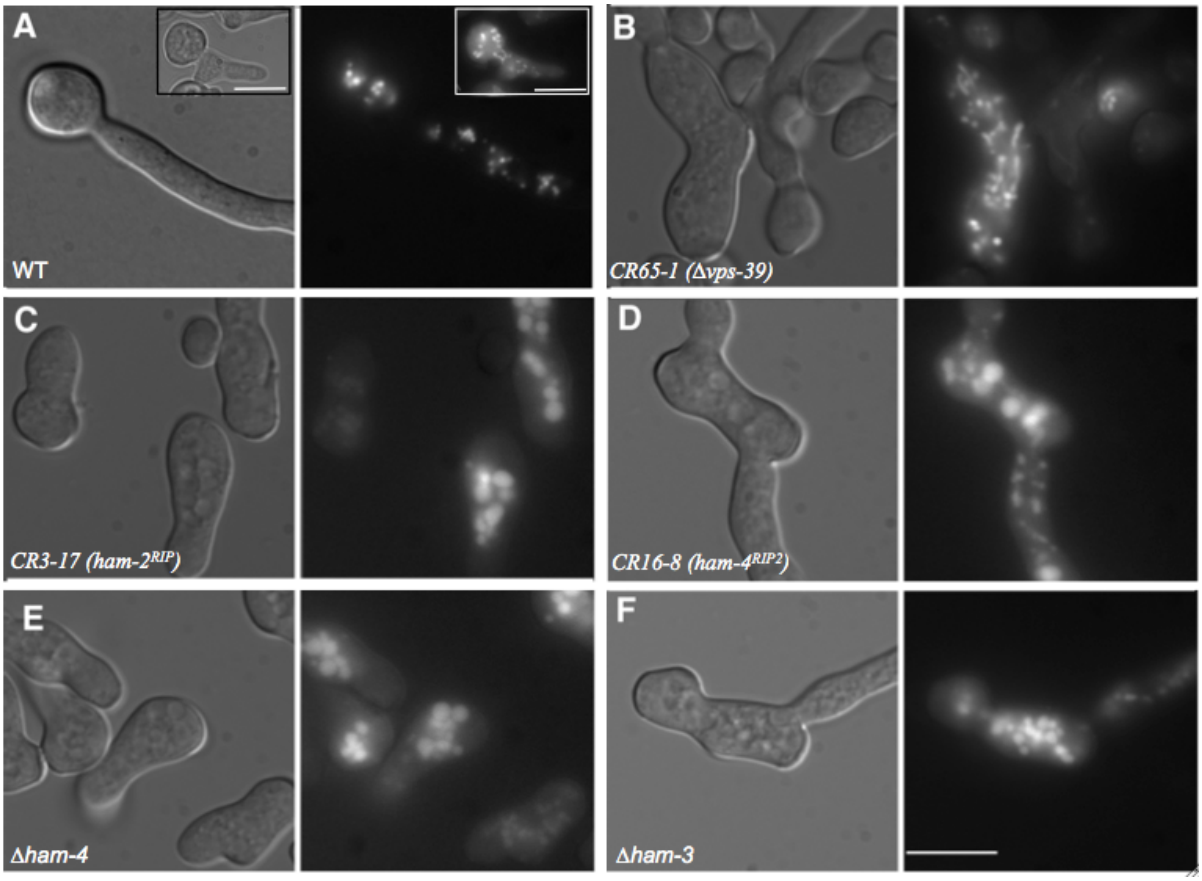
A
WT
B
CR65-1 (Δvps-39)
C
CR3-17 (ham-2RIP)
D
CR16-8 (ham-4RIP2)
E
Δham-4
F
Δham-3

Figure 2-4.

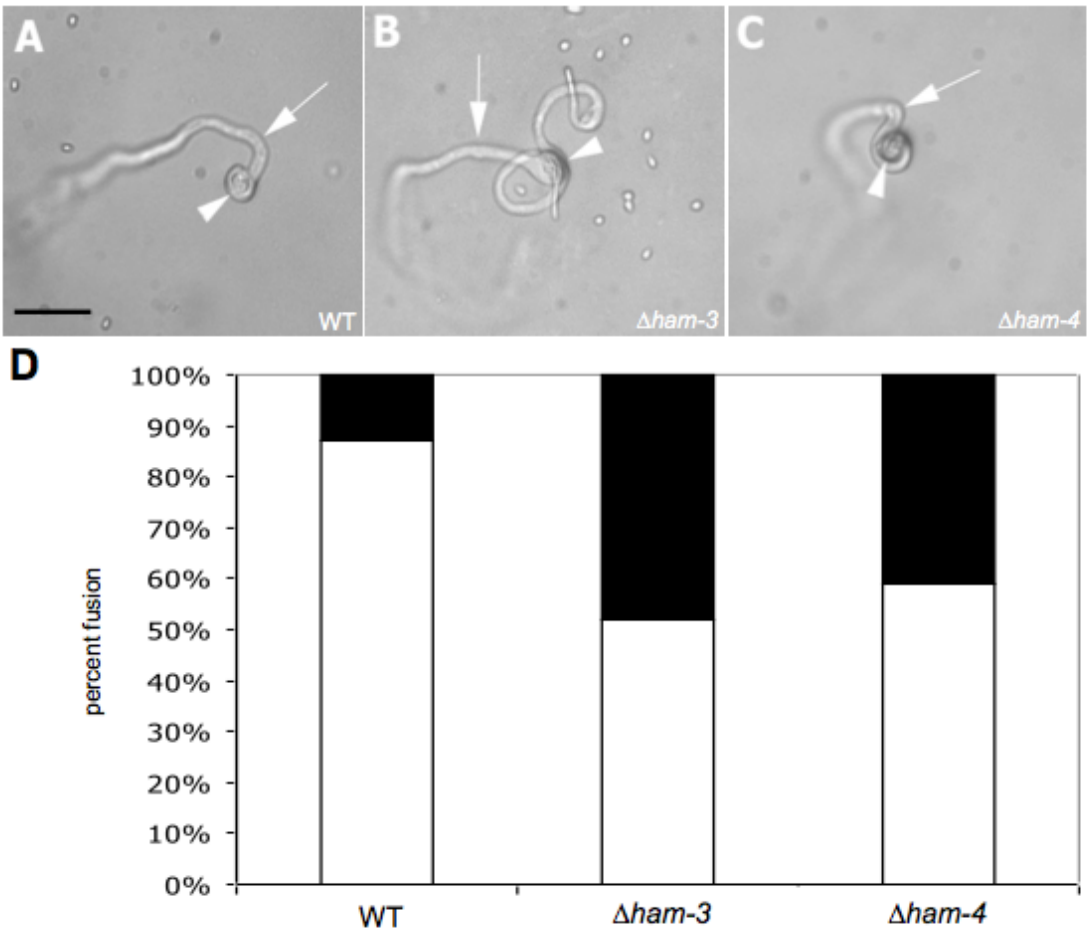
A
WT
B
Δham-3
C
Δham-4
D
percent fusion
100%
90%
80%
70%
60%
50%
40%
30%
20%
10%
0%
WT
Δham-3
Δham-4

Figure 2-5

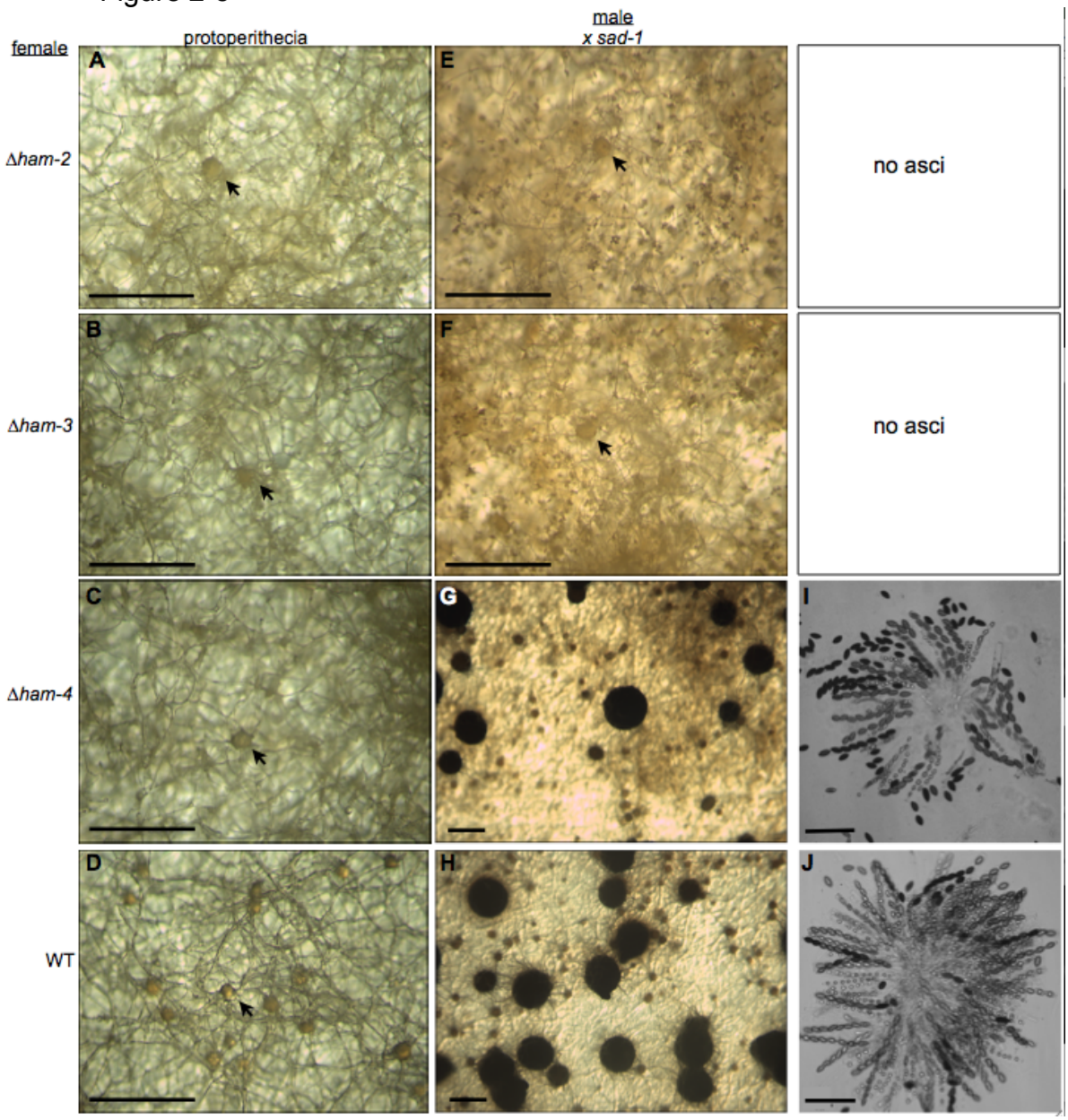
female
protoperithecia
male
x sad-1
Δham-2
Δham-3
Δham-4
WT
A
B
C
D
E
F
G
H
I
J
no asci
no asci

Figure 2-6.

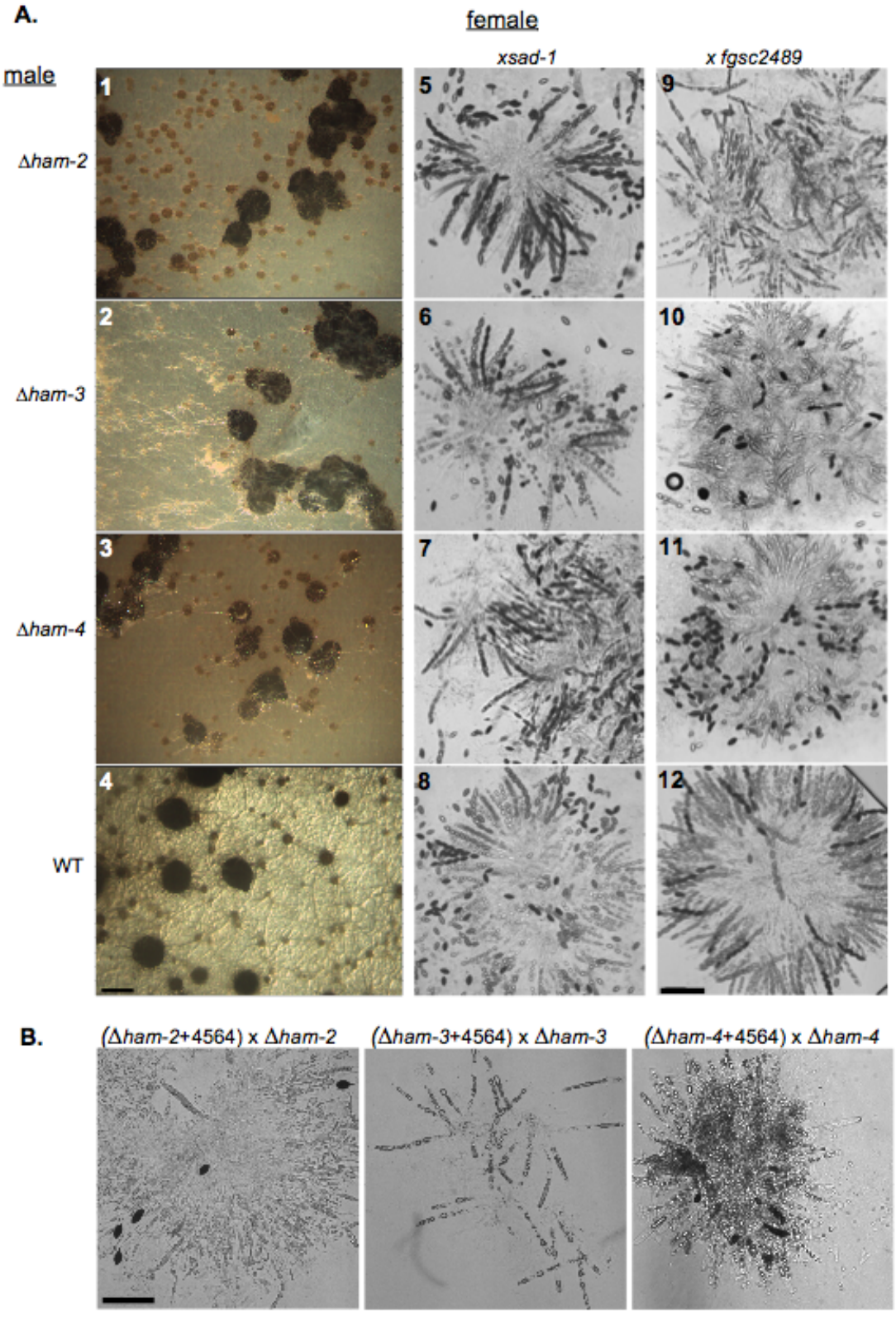
A.
female
xsad-1
x fgsc2489
male
Δham-2
Δham-3
Δham-4
WT
1
2
3
4
5
6
7
8
9
10
11
12
B.
(Δham-2+4564) x Δham-2
(Δham-3+4564) x Δham-3
(Δham-4+4564) x Δham-4

Figure 2-7.

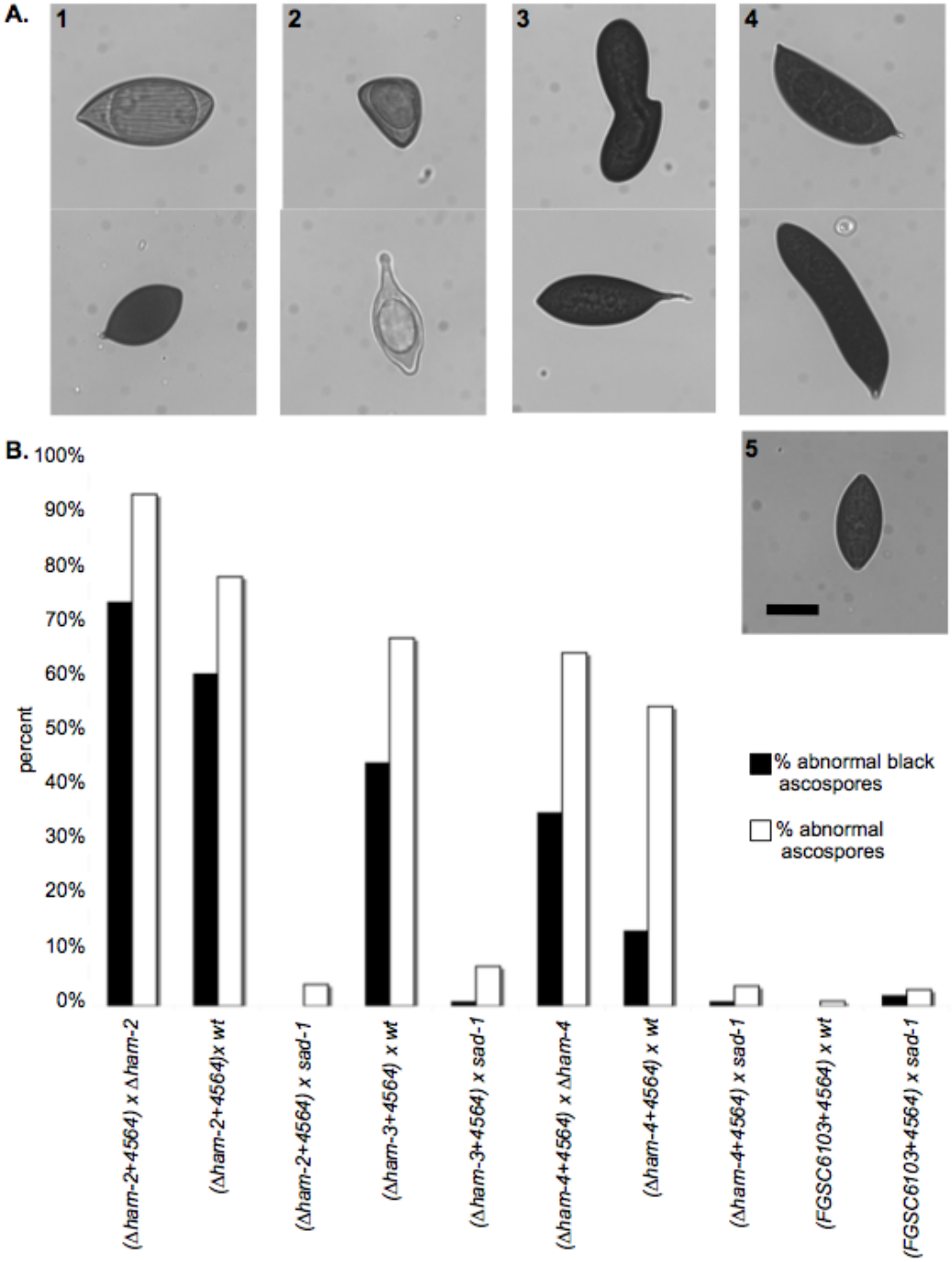
A.
1
2
3
4
5
B.
100%
90%
80%
70%
60%
50%
40%
30%
20%
10%
0%
percent
% abnormal black ascospores
% abnormal ascospores
(Δham-2+4564) x Δham-2
(Δham-2+4564)x wt
(Δham-2+4564) x sad-1
(Δham-3+4564) x wt
(Δham-3+4564) x sad-1
(Δham-4+4564) x Δham-4
(Δham-4+4564) x wt
(Δham-4+4564) x sad-1
(FGSC6103+4564) x wt
(FGSC6103+4564) x sad-1

Figure 2-8.

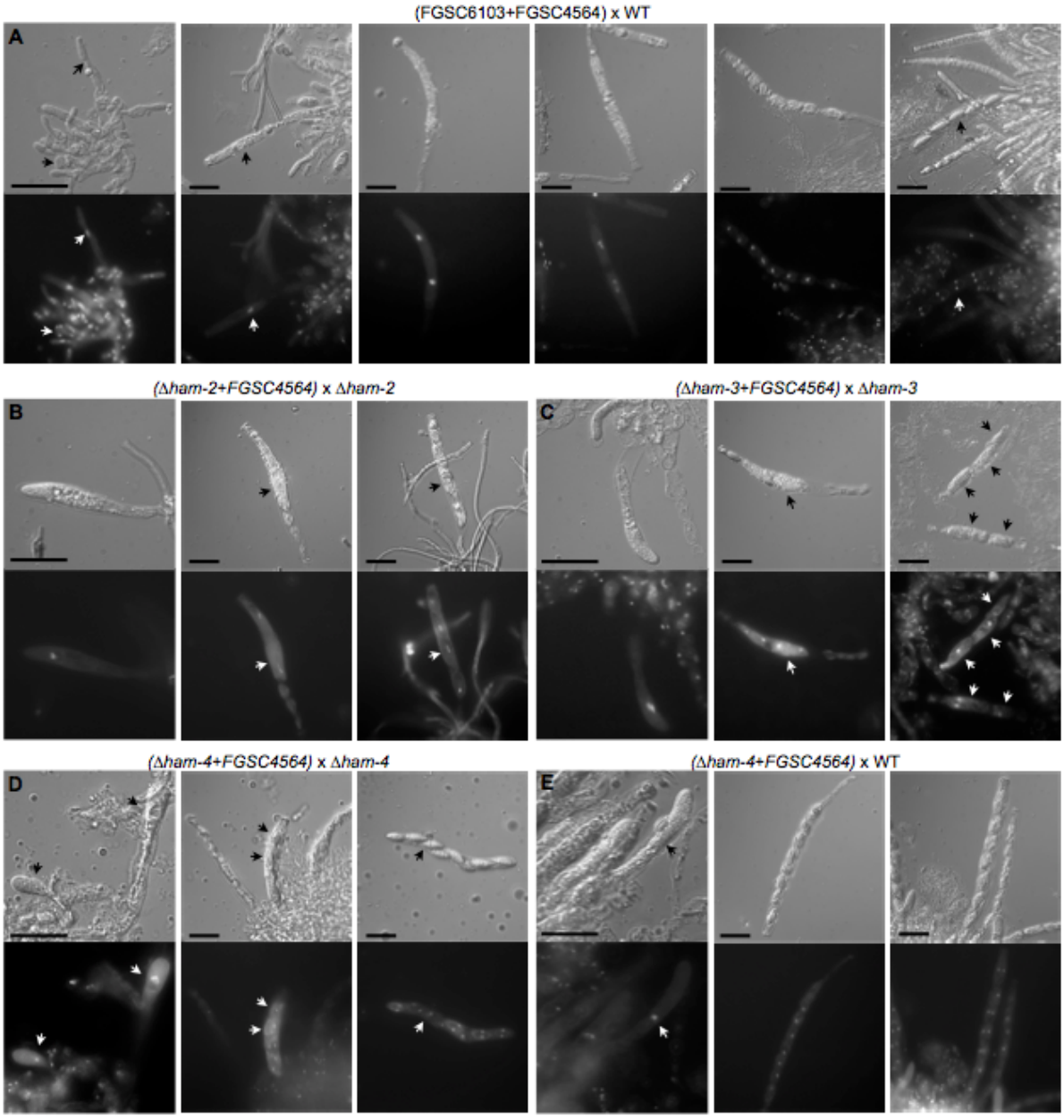
(FGSC6103+FGSC4564) x WT
A
(Δham-2+FGSC4564) x Δham-2
B
(Δham-3+FGSC4564) x Δham-3
C
(Δham-4+FGSC4564) x Δham-4
D
(Δham-4+FGSC4564) x WT
E

Figure 2-9.

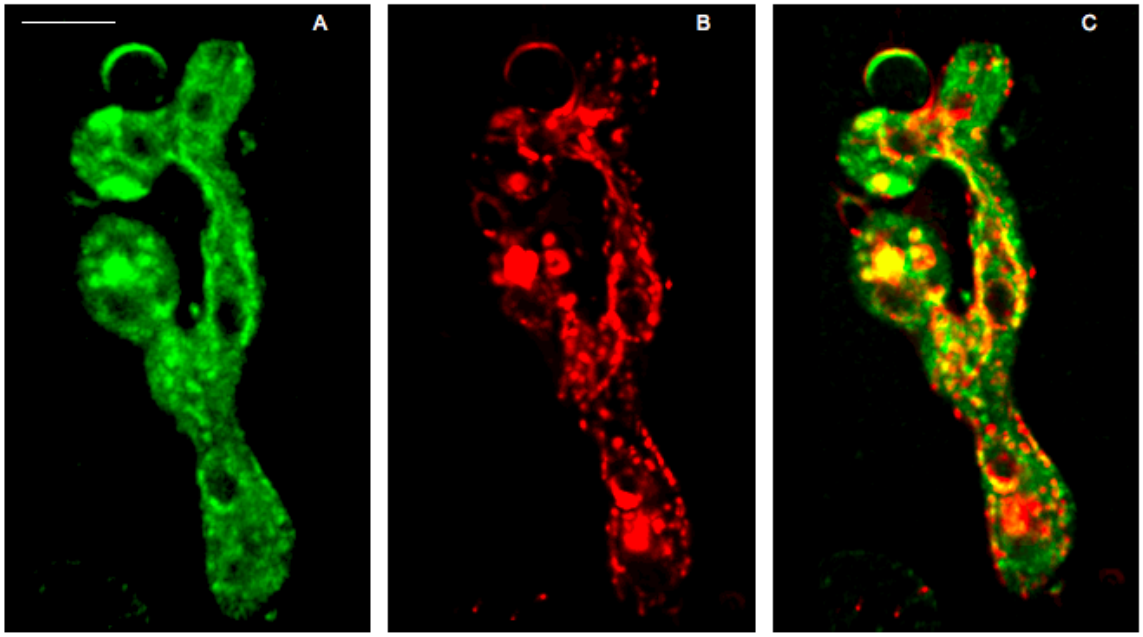

**Chapter 3**: Nuclear movement, genomic mixing and colony architecture in *Neurospora crassa*

This chapter was done in collaboration with Dr. Marcus Roper who contributed data analysis, programming skills, ideas, and mentoring to the project.

**Abstract:**

The multinucleate cells of filamentous fungi are able to harbour genetically different nuclei. This intra-mycleial genetic richness is known to contribute to the ability of these organisms to exploit heterogeneous environments and contributes to the virulence of pathogenic fungi. However, few studies have investigated the spatial and temporal development of genetic diversity within a single organism. In particular the dynamics of tip growth are known to lead to segregation of different genetic lineages at the boundary of a colony, creating genetically homogeneous sectors. Here we show that the hidden architecture of tipward flows actively mixes genetically diverse nuclei within a fungal colony. By directly measuring nuclear movement in the model ascomycete fungus *Neurospora crassa,* we show that new genomes rapidly disperse through an entire colony and that a mature *N. crassa* colony can incorporate nuclei from conidia of another strain into its mycelium. This dispersal and nuclear velocities are driven by spatially coarse pressure gradients between the edge of the colony and the growing tips. We also show that although wild type and the hyphal fusion mutant *soft* have similar average nuclear velocities, they have different profiles of nuclear flow. In addition to explaining how fungal colonies are adapted to preserve genetic richness during growth, our results suggest that many aspects of reproduction and dispersal in multinucleate organisms may be constrained by the need to ensure participation of the different genomes present within the organism.

## 1. Introduction

Genetic diversity between individuals is important to the function and resilience of ecosystems, communities, and species (for example Reusch et al. 2005). Genetic diversity is most often measured within and between conspecific populations assuming that each individual has a single karyotype, with exceptions such as chimeras, germ lines, and cancer cells containing mutations. This assumption is made because multicellular individuals arising from a single fertilization event generally have restricted nuclear flow due to the delineation of cells or septa that prevent mixing and translocation of nuclei. By contrast, organisms such as filamentous fungi, myxomycetes (Dussutour et al. 2010), and hydra can harbor multiple nuclei in a common cytoplasm (Stoner and Weissman 1996) introducing a new paradigm of genetic diversity. This paradigm includes the possibility of both competition and complementation between different genomes within a single organism (James et al. 2008). Although dynamic shifts in the populations of genetically different nuclei endow these organisms with additional phenotypic plasticity, harbouring defective nuclei can reduce overall fitness and introduces the possibility for conflict and competition between nuclei.

Filamentous fungi, with their branched, reticulated, and interconnected hyphae, are examples of organisms that harbour many millions of nuclei within a shared cytoplasm. Unlike multi-celled plants or animals, nuclei within a fungal colony appear to be both totipotent and able to migrate through the connected cytoplasmic space, though the extent of migration is dependent on the morphology or architecture of the species. Both aspects of colony architecture, such as hyphal size, density, branching, and fusion frequency, as well as the internal physiology of a fungus are thought to influence the motility of nutrients and organelles such as nuclei. For example, the type of septa, the cytoskeleton, and the hyphal connectivity of a colony could all affect translocation of organelles in a mycelium (Fischer et al. 2008, Plamann 1996, Gladfelter and Berman 2009, Bebber et al. 2007). The general body plan of *Neurospora crassa,* a model filamentous ascomycete fungus, has been described as an interconnected branching and fusing mesh-like network in the interior of the colony, while fusion is suppressed in the foraging periphery (Hickey et al. 2002). Many vegetative hyphal fusion mutants have been identified in *N. crassa* (Fleissner et al. 2005, Xiang and Glass 2004, Fleissner et al. 2008, Pandey and Glass 2002, Simonin et al. 2010). These mutants are unable create an interconnected network through hyphal fusion and instead maintain multiple series of branches that lead back to single founding hypha. One previously identified fusion mutant, *soft* (Fleissner et al. 2005), has a similar maximum growth rate to wild type making it an ideal mutant to use to compare nuclear movement in a connected (wild type) versus unconnected (*soft*) system and further explore the role of hyphal architecture in nuclear movement.

Mobile nuclei within shared cytoplasm may be genetically different, creating potential for conflicts between lineages. Although in many fungal species, degrees of genetic difference are regulated by heterokaryon incompatibility loci, both single nuclear isolations from lab strains and micro-satellite studies in wild fungi have shown that filamentous fungi are tolerant of internal genetic diversity (Maheshwari 1999, Pawlowska and Taylor 2004, James et al. 2008). New genomes are continually introduced within a colony by mutation, parasexuality, and by the exchange of genetic material following vegetative fusion with neighbouring colonies.

Harboring multiple genetic lineages within the same individual can lead to different outcomes due to competition between the nuclei, external environmental factors, and the architecture/morphology of the individual colony. In colonial yeast and in some filamentous fungi, nuclear competition leads to segregation of different genomes Hallatschek et al. 2007, Wang et al. 2005). Nuclei present at the tips tend to remain there, and divide preferentially to nuclei in the interior, leading to genetically homogeneous sectors. In the colonies of many filamentous ascomycete species, nuclei are mobile within a shared cytoplasm and nuclear ratios can be altered to reflect changing environments. Previous studies using filamentous fungi such as *Penicillium cyclopium* and *N. crassa* indicate that these colonies are able to maintain dynamic, well-mixed, heterogeneous nuclear ratios that change rapidly to suit exterior environmental conditions (Jinks 1952, Pittenger et al. 1955, Davis 1960). It is unclear how some fungi are able to maintain dynamic well-mixed multi-genomic nuclear ratios yet others break down into genetically different sectors arising from a common colony.

We used colonies of *N. crassa* containing *histone-1::gfp-* and *histone-1::dsRED-* labelled nuclei to further quantify and explore the dynamics of nuclear movement within a colony and to determine the fate of different genomes in this multigenomic organism. In addition we compared nuclear movement in wild type colonies that can create an interconnected network with nuclear movement in the fusion mutant *soft*, which is unable to create an interconnected network. *Soft* is a filamentous ascomycete-specific gene that is necessary for vegetative hyphal fusion (Fleissner et al. 2005). The resulting colony architecture in a *soft* mutant is a branched network with no fusions or interconnections. By comparing nuclear velocity profiles between wild type and *soft* colonies, we will obtain a better understanding of how hyphal architecture influences nuclear flow and dispersal within *N. crassa* colonies.

## 2. Materials and Methods

### *2.1 Strains and growth media*

Strain R15-07 (*his-3 a*) was grown in 250 ml ehrlenmeyer flasks containing 100 mls of Vogels (Vogel 1956) minimal media plus histidine for 1 week then transformed via electroporation with the following vectors, pMF280 (Freitag et al. 2004) *his-3*$^{+}$*::Pccg1-hH1-sgfp* (H1gfp) and pMF332 *his-3*$^{+}$*::Pccg1-hH1-dsRed* and an empty pBM61vector. Electroporation was performed according to (Margolin et al., 1997) with 1.5kV setting. Transformants that recovered the

ability to grow on minimal media with no supplements were selected and screened for nuclear fluorescence. One strain from each transformation was selected, MR1-4 (*H1-gfp*), MR2-4 (empty vector, wild type), and MR3-6 (*H1-dsRed*). In addition we also used a *soft*-H1-GFP strain, to measure nuclear velocities in a fusion mutant. *Soft* is unable to undergo fusion to create an interconnected network

*2.2 Microscopy*

Microscopy was performed using a Zeiss Axioskop II microscope and a Zeiss dissecting microscope. Micrographs were captured using a Hamamatsu digital C4742-95 CCD camera (Hamamatsu, Japan) and the Openlab software program (Coventry, United Kingdom). Micrographs taken using a Zeiss dissecting microscope were captured using a Micropublisher 5.0 RTV camera using Q capture image software (Surrey, BC Canada).

*2.3 Nuclear densities at the growth front*

Strain MR1-4 was grown for approximately a week in minimal media slant tubes at 25$^{o}$C in constant light. Conidia from MR1-4 were suspended in water at a concentration of approximately $10^{8}$ condia/ml and 3 ul of conidial suspension was pipetted in a line across one short edge of a rectangular piece of minimal media with 3% agar. The media rectangle was the same size as the 6x4 cm glass slide it was placed on for imaging. The inoculated pieces of media on slides were placed in petri dishes and incubated at 25°C in constant light. The first 8mm of the growing front of the colony was evaluated for nuclear density. Nuclei were counted when they reached 1.0, 1.5, 1.8, and 2.5 cm from the inoculation point to determine changing nuclear densities in the tip region over time and colony age.

*2.4 Inter-colony fusion and nuclear distribution*

We directly measured the fates of new genomes entering an established colony by inoculating fluorescently-labeled conidia onto an unlabeled colony. Genetically compatible germlings readily fuse within older colonies, depositing their genomes into the mature hyphae (Fig. 3-1). Wild type colony MR2-4 was grown on 3% agar minimal media rectangles as described above, until the colonies had grown 12 mm. Then, 3ul of approximately $10^{8}$ conidia/ml of MR3-6 (*H1::dsRed*) was added in a line across the growing MR2-4 colony. Lines of MR3-6 conidia were added at 2, 4, 6, or 8 mm behind the periphery of the MR2-4 colony. Images were taken at the MR3-6 inoculation point after 4 hrs to evaluate fusion events and to observe that *H1::dsRed* nuclei had entered the larger colony. At 8 hrs, images were taken at the periphery of the colonies and the number of fluorescently-labeled nuclei were counted.

*2.5 Particle Image Velocimetry (PIV)*

To measure nuclear velocities and distributions, MR1-4 colonies and *soft*-H1-gfp colonies were grown on rectangles of 3% agar Vogels (Vogel 1956) minimal media inoculated using the same technique and experimental set-up as described above. Movies of these colonies were then taken starting at the tips of

the colony and at 4 mm increments behind the tips, progressing toward the origin of the colony. Once a 20 mm transect was taken behind the growing tips of the colonies, which had grown 3 and 4 cm total, the increment between transects was increased and images were taken every 8 mm. Twenty-five images were taken at 8 locations along each transects with a 100 ms exposure time and a 0.1 s interval between images except for the tips, which were taken with a 0.3 s interval between images. Images were taken in colonies that had grown 2, 3 and 4 cm. Images were analyzed for nuclear direction and velocities using a Mat Lab (Natick MA) program written by Marcus Roper to measure Particle Image Velocimetry (PIV) - particle tracking. This approach allowed us to measure the speed and direction of individual nuclei in an image and develop a profile of nuclear movement within a colony.

To measure distribution of nuclear movement across hyphal transects, we again employed a PIV-Particle tracking scheme. In addition to using a Matlab program developed by M. Roper, we skeletonized hyphal segments, finding both the midline of the hypha and the diameter. We then measured the movement of nuclei within these skeletonized hyphae in 20 consecutive images taken from 8 different locations along a transect 8 mm from the periphery of a 2 cm colony. Essentially each nucleus was given a vector of movement from one image to the next. The vectors were translated into nuclear velocity resulting in a profile of nuclear movement in relation to the midline of the hypha. Over 800 segments of hypha were analyzed. Nuclei in septal areas were identified and removed from the analysis.

### *2.6 Osmotic potential*

Conidia of Mr1-4 were inoculated onto solid minimal media rectangles as described above and grown for approximately 2 cm. Ten ul of 0.6 M sucrose minimal media was added directly behind a 2 cm colony. Images were taken at approximate 8 mm behind the periphery of the colony. Eight spots along this transect were imaged, with 25 images with an exposure time of 100 ms with 0.1 s between image captures taken before osmolyte addition, and the same number of images at the same exposure were taken approximately 1 minute after osmolyte addition. Additional images were taken approximately 4 minutes after osmolyte addition, when the colonies had resumed their tipward flows.

## 3.0 Results

### *3.1 Growth front*

Fungal colonies grow into new habitats by tip extension. A continual tipward flux of vesicles and nuclei provides the new material needed to generate new cell wall and populates the spaces created at hyphal tips (Fig. 3-2A). We measured the rate of tip growth and colony densification in a 2D colony. Specifically, we made a line inoculation of conidia on the edge of a rectangular block of solid

mediamedium, the fungal colony initiated by the germinated and fused conidia spreading across the block, with a single 1D growing front (Fig. 3-2B). We determined that the nuclear density of the colony increases as the colony becomes larger and ages. The colony nuclear density of the growing front of a 1 cm colony was less dense than that of a colony 1.5, 1.8, or 2.5 cm in size. The colonies that were 1.5, 1.8, or 2.5 cm had between 1.2 and 2 nuclei per $mm^2$ and were not statistically different. All three colonies had a slight peak in density around 2 mm behind the tips and then had a drastic decrease in nuclear density from 1.5mm to the tips where nuclear density dropped zero. The colony that was 1cm in length had significantly less nuclear density, an average of 0.5 nuclei per $mm^2$ in the growth front starting 6mm behind the leading edge of the colony. In the 1 cm long colony, there was also a peak of density around 2 mm behind the periphery and then the nuclear density decreased steadily and there were no nuclei at the tips.

*3.2 Nuclear mixing*

New genomes introduced within the colony rapidly disperse over the entire colony. We directly measured the fates of new genomes, by inoculating H1::dsRed- labelled conidia into an unlabeled colony. Genetically compatible germlings readily fuse within older colonies, depositing their genomes into the mature hyphae. Once incorporated into the colony, we saw these genomically-different H1::dsRed nuclei move to the growing tips, covering distances of more than 36 mm (Fig 3-3) in less than 8 hours. This translocation was faster than the hyphal growth rate (approximately 2.6mm/hr at 25 $^{o}$ C). In eight hours, the nuclei not only moved the distance of hyphal growth but additionally moved the distance behind the tips where they had been added. For example the conidia that were added 10 mm behind the tips travelled a total of about 30 mm in eight hours, 10mm of distance from inoculation to the tips and 20mm of hyphal growth. A nucleus from a conidium added 13mm behind the growing tips had to travel 33mm to reach the tips after 8 hrs of growth and nuclei added 16 mm behind the tips had to travel 36mm to reach the tips of the colony. It is possible that the nuclei could have moved even faster than 36mm in 8hrs as the nuclei were already present at the tips after 8hrs, the nuclei could have arrived at the tips earlier.

Four hours after inoculation of H1-dsRed conidia into the interior of the colony, images of hyphae directly next to the inoculation point were taken. The number of red nuclei in these hyphae was counted revealing that when when conidia were 10 and 13mm behind the colony periphery an average of 13.9 and 12.7 red nuclei per image, respectively, were found in the hyphae. The number of red nuclei found in the hyphae next to the inoculation point 16mm behind the periphery was less, having an average of 7.3 nuclei per image. These data gave us an understanding of how many red nuclei were entering the colony at the inoculation point and demonstrated that fusion was not limiting our results.

The number of red nuclei found at the periphery of the colony decreased the further back in the colony conidia were added. When conidia were added 10 mm behind the periphery of the colony, an average of 22.6 nuclei per image were seen at the tips of the colony. This number progressively decreased as conidia were added further back in the colony, at 13 mm behind the periphery an average of 11.3 nuclei per image at hyphal tips were present, while at 16 mm the average was 0.4 nuclei per image at the hyphal tips (Fig. 3-3C).

*3.3 Nuclear Velocities*

To understand nuclear movement and whether hyphal architecture affects nuclear distribution, we directly measured the internal dynamics of nuclei within a colony, using H1::GFP labeled nuclei. A hybrid Particle Image Velocimetry-Particle Tracking (PIV-PT) scheme was used to make simultaneous velocity measurements of several thousand nuclei at different stations within the colony. Mean nuclear velocities were the same for colonies of different ages, and the profile of nuclear flow was the same whether the colony was 3, 4, or 5 cm in length (Fig. 3-4). Nuclear velocities ranged from 0 to just over 30 um/s. Nuclear velocities were binned into 1um/s intervals and the fraction of total nuclei at each velocity interval was calculated and graphed using a log scale. In all of the graphs the fractions of nuclei exponentially decreased from 0 to 34 um/s with the largest fraction of nuclei moving at slow speeds between 0 and 0.5 um/s. The profile of nuclear velocities for the tip regions of colonies was distinctly different than that for hyphae 8 mm and 16 mm behind the periphery of the colony. The tip regions had a smaller fraction of nuclei moving at higher speeds, indicating that a larger fraction or more nuclei were moving at slower speeds than in areas further back in the colony. This can be seen by the parabolic shape of the curve of the velocities of nuclei graphed on a log scale. Essentially nuclei in the tip region are all moving at similar slow speeds, which we hypothesize are being driven by pressure driven bulk flow as a result of tip growth. This is consistent with the nuclei of the tip region being limited by hyphal growth rates (Ramos-Garcia et al. 2009) and a lack of fusion in the tip region.

The nuclear velocity profile of *soft* colonies was compared to that of wild type. *Soft* colonies have no fusion within the colony leading to a branching network lacking fusions, which create loops and redundancies within the network. For example, if a hypha leading to a branch is injured in a *soft* colony, there are no other routes available to move nuclei from one side of the injury to the other and the branch is effectively cut off from the rest of the colony. In wild type, as a result of fusion, there would be multiple routes to circumvent an injured area and maintain nuclear flow through the system. Hyphal fusions also create loops within the colony where nuclei could in theory travel in a circular route. These loops would not be present in *soft* colonies that can't fuse, the route could only be forward toward the tips or back toward the origin, depending on the direction of the pressure gradients in the colony. The velocities of nuclei were graphed against the fraction of nuclei moving at those velocities, on a log/log scale in *soft* and wild type colonies. Velocity was only measured up to speeds of 10 um/s. In

the tip region, *soft* and wild type colonies had similar nuclear velocity profiles, where most nuclei were moving at slower speeds and only a small fraction of nuclei were moving at higher speeds (Fig. 3-5A). At 8 mm and 16 mm behind the colony periphery, *soft* maintained the same S – shaped curve of nuclear velocities. The only difference was an increase in the fraction of nuclei moving at higher speeds. Even though wild type had the same nuclear velocity profile as *soft* at the tips, where no fusion occurs in either colony, wild type had a much different nuclear velocity profile at 8 and 16 mm behind the colony periphery. In these sections of the colony, wild type had a linear decrease in the fraction of nuclei as the velocity increased. This indicates a more consistent distribution of nuclei moving at speeds between 1 and 10 um/s. Wild type and *soft* differ in the fraction of nuclei moving at velocities between about 2 and 9 um/s. Wild type has a significantly larger fraction of nuclei moving at these speeds than in *soft.* Even though the average nuclear velocities are the same, the distribution or profile of nuclear velocities are different.

Velocities of nuclei were measured on transects every 4 mm behind the tips of both wild type and *soft* colonies. Though nuclear velocities were similar (Fig 3-6A), the dispersion of nuclear velocities was very different between the two strains (Fig. 3-6B). Average nuclear velocities were approximately 2.8 um/s for *soft* and 3.4 um/s for wild type measured 4 mm behind the periphery. *soft* maintained an average nuclear velocity between 2.5 and 2.9 um/s from 4 to 20 mm behind the periphery of the colony and then dropped to about 2 um/s from 20 to 30 mm. Wild type average nuclear velocity decreased from 3.4 um/s at 4 mm behind the periphery to about 2.2 um/s at 16 mm behind the periphery and had the same average velocity from 16 mm to 24mm behind the periphery. However the standard deviations were up to 8 um/s for these averages (Fig 3-6B) and there was no significant difference between the strains due to the large variation in nuclear speeds. Because there were such large differences we graphed the standard deviations of the average nuclear velocities over the colony (Fig. 3-6B). We have already shown (above) that nuclear velocities range from 0 to over 30 um/s and that there is less variation in nuclear velocities in the tip region of the colony than at 8 mm and 16 mm behind the periphery of the colony. Differences in standard deviations or dispersion of nuclear velocities would indicate a different profile of flow between the strains, which we believe is due to differences in hyphal architecture. In wild type, there was a large dispersion of velocities between 4 and 16 mm from the tips, approximately 6.5 to 9 um/s, much greater than *soft,* where it was around 4 to 6 um/s. In the interior of the wild type colony there were more uniform nuclear velocities, and the standard deviation of velocities dropped to around 3 um/s. *soft* displayed a more consistent dispersion of nuclear velocities over the entire colony ranging from 4 to 6 um/s. Both *soft* and wild type colonies had standard deviations less than 0.5 um/s and average nuclear velocities less than 0.5um/s at the tips, indicating that nuclei are moving at a consistent, slow, speed with little variance than in the rest of the colony. Thus, hyphal fusion and the architecture of the colony does not change average velocities but does change the distribution of velocities within a colony.

*3.4 Nuclear movement in hyphal segments*

To further explore whether nuclei move by pressure-driven flows we measured nuclear velocities in hyphae in relation to the center of the hypha (Fig 3-7). Figure 3-7 shows measurements of nuclear movement within a hypha. As would be expected of particles moving through a tube driven by a pressure gradient, the result was a parabolic distribution of nuclear movement across a hyphal transect (Fig 3-8). The nuclei in the center of the colony were moving at a faster rate than the nuclei toward the edges of the colony. Nuclear velocities ranged from -4 pixels/s to 6 pixels/s with the majority of nuclei moving at about 1.5 pixels/s. However when we scaled the nuclear velocities to the size of the hypha, we found a parabolic distribution of nuclear movement across the hypha. Hyphae were scaled to a standard diameter and nuclear velocities were scaled to the fraction of the distance from the center line to hyphal edge. This parabolic pattern of flow is consistent with pressure-driven flow through tubes, where friction and resistance decreases the velocity of particles toward the edges of the tube. Interestingly, we found that there is an approximate 2 um zone of exclusion toward the edge of the hyphae where there appear to be no nuclei present in larger hyphae. Small branch hyphae that had a small diameter, which could only support one or two nuclei, were excluded from this measurement.

*3.5 Pressure-Driven Flow*

We suspected that the complex multi-directional flows of nuclei are driven by spatially coarse pressure gradients. In order to test whether we could change the pressure gradients in the colony by creating an osmotic potential, we used a hyper-osmotic sucrose solution to manipulate the turgor pressure at sites within the colony. By decreasing the turgor pressure at a single site within the interior of the colony, we were able to reverse the direction of nuclear flow within the entire local network (Fig 3-9). Immediately after application of the sucrose solution, nuclear flow within the hyphae had reversed direction (Fig. 3-9B).Flows that had previously been tipward were now flowing toward the origin of the colony and flows that had previously been toward the origin of the colony flowed tipward. Reversed flows of nuclei were seen for 1-2 min after the first application of hyper-osmotic treatment. We found that flows within the colony recovered to their initial directions 3-5 min after treatment, which was approximately the same amount of time for recovery from an osmotic shock (Lew and Nasserifar 2009). We graphed the fraction of nuclei moving at specific velocities both forward and reverse, before and after addition of the sucrose solution. The resulting profiles appeared to be almost mirror images of each other with distinct peaks and valleys of the profiles matching when the two graphs were superimposed upon each other (Fig. 3-9 C and D).

## 4.0 Discussion

In this study, we showed that nuclear movement in *N. crassa* is a dynamic event driven by internal pressures and hyphal architecture. The osmotic- and growth-induced pressure gradients and the architectural and morphological

constraints of the system of hyphae in a colony lead to the vigorous mixing and distribution of nuclei throughout the colony. If a population of nuclei enters or arises in an already established colony as a result of fusion or mutation, these nuclei would be spread and become well mixed throughout the original colony. This mechanism of nuclear mixing allows the colony to maintain genetic diversity within the mycelium.

Nuclear heterogeneity is a dynamic event in some ascomycete fungi. Our data show that *N. crassa* has a way of actively dispersing and mixing nuclei within its colony, which could provide the advantage of genetic diversity in hyphae encountering new environments and prevent genetic sectoring. Some filamentous fungi can rapidly change the ratios of nuclei in a colony to respond to the external environment (Pittenger et al. 1955, Davis 1960, James et al. 2008). There are both possible advantages and disadvantages to maintaining a heterokaryon. Usually the unit of selection is an individual and the individual is one genotype. In fungi what we might consider an individual can harbor multiple genotypes that can have changing ratios, making it possible for the unit of selection to be individual nuclei as opposed to the entire mycelium. If the unit of selection in the mycelium is distilled down to a nuclear level, competition can occur within the same organism leading to a decrease in fitness in some instances (James et al. 2008). For example, the negative effects of one genotype are not selected out of the population because they are complemented by nuclear products of another genotype, yet the total fitness of the organism is decreased. The magnitude of this process is largely dependent on the fitness of the individual genotypes, the interactions between the two genotypes, the ratios of genotypes in the hyphae, and the ability to maintain a heterokaryon. For a fast-growing fungus such as *N. crassa,* which quickly colonizes recently burned substrate, the advantage of harboring and actively mixing genetically different nuclei within a colony might allow for quick colonization and adaptability to utilize different substrates, leading to an increase in fitness.

We show that a larger *N. crassa* colony can overtake and incorporate the nuclei of germlings into its nuclear pool. These nuclei are fated to be mixed throughout the larger mycelium and incorporated into the larger nuclear pool. A similar distribution of genetically different nuclei occurs when two monokaryotic basidiomycete mycelia fuse (reviewed in (Gladfelter and Berman 2009)) and a dikaryon is formed. In a rapid manner, new genomes are exposed to the foraging front of the colony. The incorporation of nuclei from *N. crassa* germlings into a larger colony is restricted in nature by genetic compatibility (reviewed in Glass 2006), but it is not unthinkable that a larger colony will sporulate and eventually overtake its own asexual progeny. These progeny have had an opportunity to sample the surrounding environment before being re-accepted back into the fold of the larger colony via cell fusion events.

There appeared to be a length-scale limiting mixing of nuclei from conidia fusing into already existing larger colonies. Very few nuclei entering the colony at 16 mm behind the growth front were found at the tips of the colony within eight hours. There was almost a 50% decrease in the number of H1-dsRed nuclei in the hyphae directly next to the H1-dsRed conidia when the inoculation was 16

mm behind the periphery instead of at 10 mm (Fig. 3 C). The decrease in nuclear input into the system in combination with both a larger distance to travel and a larger area of hyphae to populate might lead to the decrease in nuclei seen at the tips of the colony when conidia were added to the colony 16 mm from the periphery.

Nuclei move in all directions within individual hyphae, but the majority bulk flow of the nuclei is toward the periphery of the colony. Our data provides multiple lines of evidence that nuclear movement is pressure-driven, which has been previously suggested for internal hyphal cytoplasm and organelle movement at hyphal tips (Lew 2005, Ramos-Garcia et al. 2009). Evidence for a pressure-driven flow in *N. crassa* hyphae includes that direction of flow is reversed with addition of osmotic pressure, nuclei move faster in the center of a hyphal transect and that *soft* and wild type have different flow profiles.

The absence of hyphal fusion within a colony does not change the average velocity of nuclei within the system, but changes the pattern of flow. *soft* colonies show a larger variation of nuclear velocities in interior of the colony than do wild type colonies and also show a smaller proportion of nuclei moving at faster speeds. Nuclear velocities and dispersion of nuclear velocities was the same in hyphae at the periphery of both *soft* and wild type colonies. Wild type colonies have no fusion in the tip region and both strains have nuclear velocities limited by tip growth (Ramos-Garcia et al. 2009). *Soft* colonies consist of multiple branches originating from feeder hyphae in the interior of the colony. This results in much higher rates of nuclear flow as only a small number of hyphae supply nuclei to the growing tips of the colony. As a result, *soft* colonies have fewer nuclei moving at higher speeds than in wild type, yet still the same average nuclear velocity throughout the colony, indicating that some of the nuclei in *soft* colonies must be moving at very high speeds while others are moving very slowly. Also *soft* has a higher dispersion of nuclear velocities further back in the colony than in wild type, supporting this theory. Wild type colonies, in contrast, have a more even distribution of nuclear velocities. The fraction of nuclei moving at a given velocity exponentially decreases as nuclear velocity increases in wild type colonies. This more even distribution of nuclear velocities could reflect a connection of multiple hyphae able to feed growing tips. The limitation on nuclear flow in wild type colonies could be factors such as hyphal conductance, colony mesh size, and fusion frequency whereas in *soft* the limitation would more likely be the number of tips being fed by internal hyphae and the amount of branching.

Nuclei in *N. crassa* move at different speeds and directions, but the ultimate product is a population of well-mixed nuclei with a pressure-driven bulk flow toward the tips of a colony. An already established colony can incorporate new nuclei through fusion with conidia, and these nuclei become spread throughout the colony. The velocities and movement of nuclei are influenced by the hyphal architecture of the colony and are driven by coarse pressure gradients that can be altered by environmental changes. This research will eventually lead to a comprehensive model of nuclear movement within an entire colony of *N.crassa.*

## 5.0 References


Bebber, Daniel P, Juliet Hynes, Peter R Darrah, Lynne Boddy, and Mark D Fricker. (2007). “Biological solutions to transport network design.” *Proceedings Of The Royal Society B-Biological Sciences* 274 (1623): 2307-2315.

DAVIS, RH. (1960). “ADAPTATION IN PANTOTHENATE-REQUIRING NEUROSPORA .2. NUCLEAR COMPETITION DURING ADAPTATION.” *American Journal Of Botany* 47 (8): 648-654.

Dussutour A, Latty T, Beekman M, Simpson SJ. (2010). Amoeboid organism solves complex nutritional challenges. Proc Natl Acad Sci USA 107:4607–4611.

Fischer, Reinhard, Nadine Zekert, and Norio Takeshita. (2008). “Polarized growth in fungi – interplay between the cytoskeleton, positional markers and membrane domains.” *Molecular Microbiology* 68 (4) (May): 813-826.

Fleissner, A., Sarkar, S., Jacobson, D.J., Roca, M.G., Read, N.D., and Glass, N.L. (2005). The *so* locus is required for vegetative cell fusion and postfertilization events in *Neurospora crassa*. Eukaryot Cell *4*, 920-930.

Fleissner, A, S Diamond, and N L Glass. (2008). “The Saccharomyces cerevisiae PRM1 Homolog in Neurospora crassa Is Involved in Vegetative and Sexual Cell Fusion Events but Also Has Postfertilization Functions.” *Genetics* 181 (2) (November 24): 497-510.

Fleissner, Andre, and N Louise Glass. (2007). “SO, a Protein Involved in Hyphal Fusion in Neurospora crassa, Localizes to Septal Plugs .” *Eukaryotic Cell* 6 (1) (January 1): 84-94.

Freitag, M, PC Hickey, NB Raju, EU Selker, and ND Read. (2004). “GFP as a tool to analyze the organization, dynamics and function of nuclei and microtubules in Neurospora crassa.” *Fungal Genetics And Biology* 41 (10): 897-910.

Gladfelter, Amy, and Judith Berman. (2009). “Dancing genomes: fungal nuclear positioning.” *Nature Reviews Microbiology* 7 (12): 875-886.

Hallatschek, Oskar, Pascal Hersen, Sharad Ramanathan, and David R Nelson. (2007). “Genetic drift at expanding frontiers promotes gene segregation.” *Proceedings Of The National Academy Of Sciences Of The United States Of America* 104 (50): 19926-19930.

Hickey, PC, DJ Jacobson, ND Read, and NL Glass. (2002). “Live-cell imaging of vegetative hyphal fusion in Neurospora crassa.” *Fungal Genetics And Biology* 37 (1): 109-119.

James, Timothy Y, Jan Stenlid, Ake Olson, and Hanna Johannesson. (2008). “Evolutionary significance of imbalanced nuclear ratios within heterokaryons of the basidiomycete fungus Heterobasidion parviporum.” *Evolution* 62 (9): 2279-2296.

JINKS, JL. (1952). HETEROKARYOSIS - A SYSTEM OF ADAPTATION IN

WILD FUNGI. *Proceedings Of The Royal Society Of London Series B-Biological Sciences* 140 (898): 83-&.
Lew, Roger R, and Shanar Nasserifar. (2009).Transient responses during hyperosmotic shock in the filamentous fungus Neurospora crassa. *Microbiology-Sgm* 155: 903-911
Lew, RR. (2005). Mass flow and pressure-driven hyphal extension in Neurospora crassa. *Microbiology-Sgm* 151: 2685-2692. doi:10.1099/mic.0.27947-0.
Maheshwari, R. 1999. “Microconidia of Neurospora crassa.” *Fungal Genetics And Biology* 26 (1): 1-18.
Maheshwari, R. (1999) Microconidia of Neurospora crassa. Fungal Genet. Biol. 26, 1–18.
Margolin, B.S., Freitag, M., and Selker, E.U. (1997). Improved plasmids for gene targeting at the *his-3* locus of *Neurospora crassa* by electroporation. Fungal Genet Newslett *44*, 34-36.
Pandey, A, and L Glass.(2002). Activation of MAP kinases during mating-type mediated vegetative incompatibility and germination in Neurospora crassa. *Molecular Biology Of The Cell* 13: 156A-156A.
Pawlowska, TE, and JW Taylor.(2004).Organization of genetic variation in individuals of arbuscular mycorrhizal fungi. *Nature* 427 (6976): 733-737.
PITTENGER, TH, AW KIMBALL, and KC ATWOOD. (1955). CONTROL OF NUCLEAR RATIOS IN NEUROSPORA HETEROKARYONS. *American Journal Of Botany* 42 (10): 954-958.
Plamann, M. (1996). Nuclear division, nuclear distribution and cytokinesis in filamentous fungi. *Journal Of Genetics* 75 (3): 351-360.
Ramos-Garcia, Silvia L, Robert W Roberson, Michael Freitag, Salomon Bartnicki-Garcia, and Rosa R Mourino-Perez. (2009). Cytoplasmic Bulk Flow Propels Nuclei in Mature Hyphae of Neurospora crassa. *Eukaryotic Cell* 8 (12): 1880-1890. doi:10.1128/EC.00062-09.
Reusch, T.B.H., Ehlers, A., Hammerli, A. & Worm, B. (2005). Ecosystem recovery after climatic extremes enhanced by genotypic diversity. Proc. Natl. Acad. Sci. USA, 102, 2826–2831.
Simonin, Anna R, Carolyn G Rasmussen, Mabel Yang, and N Louise Glass. (2010). Genes encoding a striatin-like protein (ham-3) and a forkhead associated protein (ham-4) are required for hyphal fusion in Neurospora crassa. *Fungal Genetics And Biology* 47 (10) (October): 855-868.
Stoner, D.S. & Weissman, I.L. (1996). Somatic and germ cell parasitism in a colonial ascidian: possible role for a highly polymorphic allorecognition system. *Proc Natl Acad Sci U S A* 93, 15254-15259.
Vogel, H.J. (1956). A convenient growth medium for *Neurospora*. Microbiol Genet Bull *13*, 42-46.
Wang, CS, TM Butt, and RJ St Leger. (2005). Colony sectorization of Metarhizium anisopliae is a sign of ageing. *Microbiology-Sgm* 151 (Pt 10): 3223-3236.
Xiang, QJ, and NL Glass. (2004). Chromosome rearrangements in isolates that escape from het-c heterokaryon incompatibility in Neurospora crassa. *Current Genetics* 44 (6): 329-338.

**Figure Legend:**

Figure. 3-1 Image of genetically different nuclei in a common mycelium. A) A heterokaryon of H1::gfp (MR1-4) and H1::dsRed (MR3-6). B) Nuclear distribution of in an H1::gfp colony. C) Nuclei from MR1-4 conidia migrating into a MR3-6 colony after hyphal fusion. The nuclei are moving from the conidia into the larger colony.

Figure. 3-2 Nuclear density in the tip region of colonies of different sizes. Inset shows the distance of the colony from the inoculation point. Clouds around each line indicate standard deviation. Dark blue represents a 1 cm long colony, light blue represents a 1.5 cm colony, yellow represents a 1.8 cm colony and red represents a 2.5 cm colony.

Figure. 3-3 Images of H1-ds red nuclei in a MR3-6 colony A) entering a MR2-4 colony and B) at the tips of an MR3-6 colony. C) Graph showing the average number of nuclei per image in hyphae next to the H1-dsRed inoculation point 4hrs post inoculation at different distances behind the periphery of the colony and nuclei at the growing front of the colony taken 8hrs after inoculation with H1-dsRed conidia.

Figure. 3-4 Nuclear velocities in colonies 3, 4, and 5 cm long at A) the tips, B) 8mm behind the tips, and C) 20mm behind the tips.

Figure. 3-5 Fraction of nuclei moving at a given velocity in 3cm wild type (blue) and *soft* colonies (red) at A) the tips of the colonies, B) 8mm behind the tips, and C)16mm behind the tips. Standard deviations shown for selected points along the graph.

Figure. 3-6 A) Average nuclear velocities within a 3cm colony at different transects within the wild type (blue) and *soft* colonies (red). B) Standard deviations of wild type and soft nuclear velocities in a 3cm colony.

Figure. 3-7 A) Image of nuclear movement between two frames taken 0.1s seconds apart. Pink is the location of the nucleus in the first image, green indicates the nucleus in the second image and white indicates overlap of the two. The blue lines represent a vector of movement. B) A graph of movement of all the nuclei in a series of 25 images taken 0.1s apart. velocities are ranked as follows from fastest to slowest: red, yellow, green, light blue, dark blue. black circled nuclei have been removed due to their proximity to septa.

Figure. 3-8  A) Velocities of nuclei within hyphae graphed against their location in the colony. B) Adjusted streaming velocities scaled to the size of hypha standardizing the distance from the center of the hypha of all different sizes this is all noise from variation in hyphae diameters?

Figure. 3-9 A) Profile of nuclear velocities for an area 5mm behind the tips before addition of sugar solution (blue) and after addition of sugar solution (red). B) A replicate of the same experiment. C) The before and after sucrose solution flow profiles of A. the ‘after’ profile has been flipped and aligned with the ‘before’ profile.  D) before and after profiles of B super imposed upon each other and aligned.

Figure. 3-1

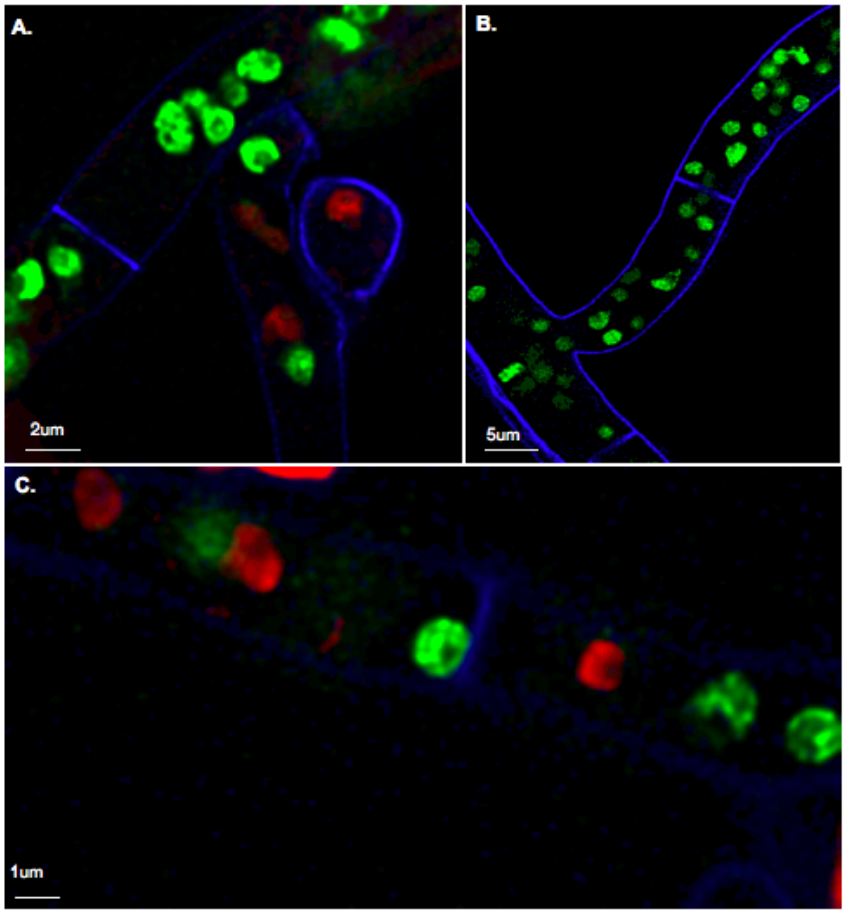

Figure. 3-2

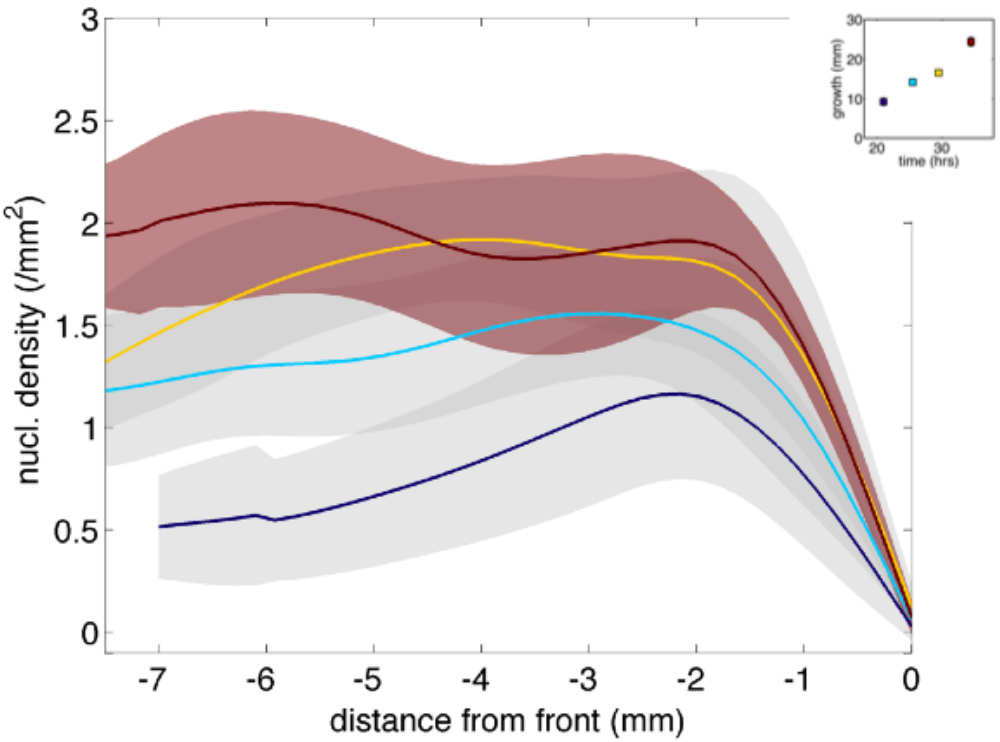

Figure. 3-3

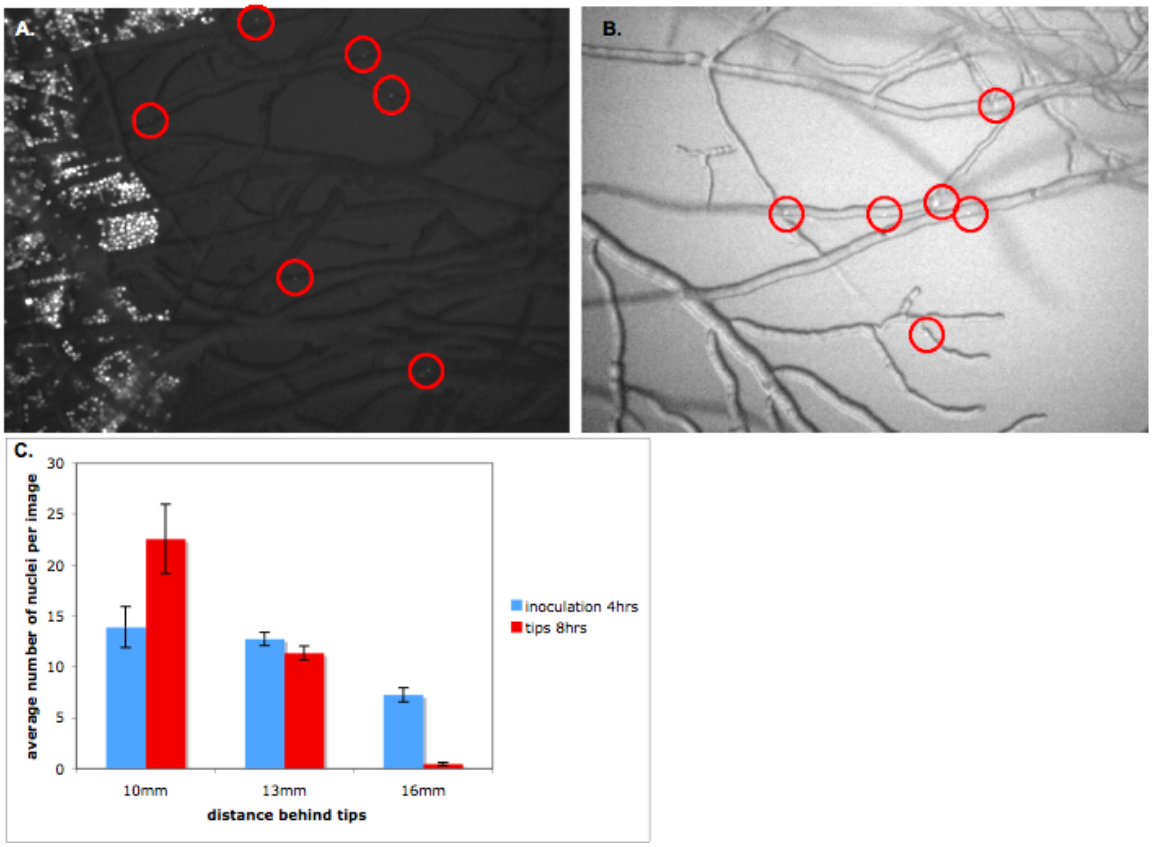
A.
B.
C.
average number of nuclei per image
30
25
20
15
10
5
0
10mm
13mm
16mm
distance behind tips
inoculation 4hrs
tips 8hrs

Figure. 3-4

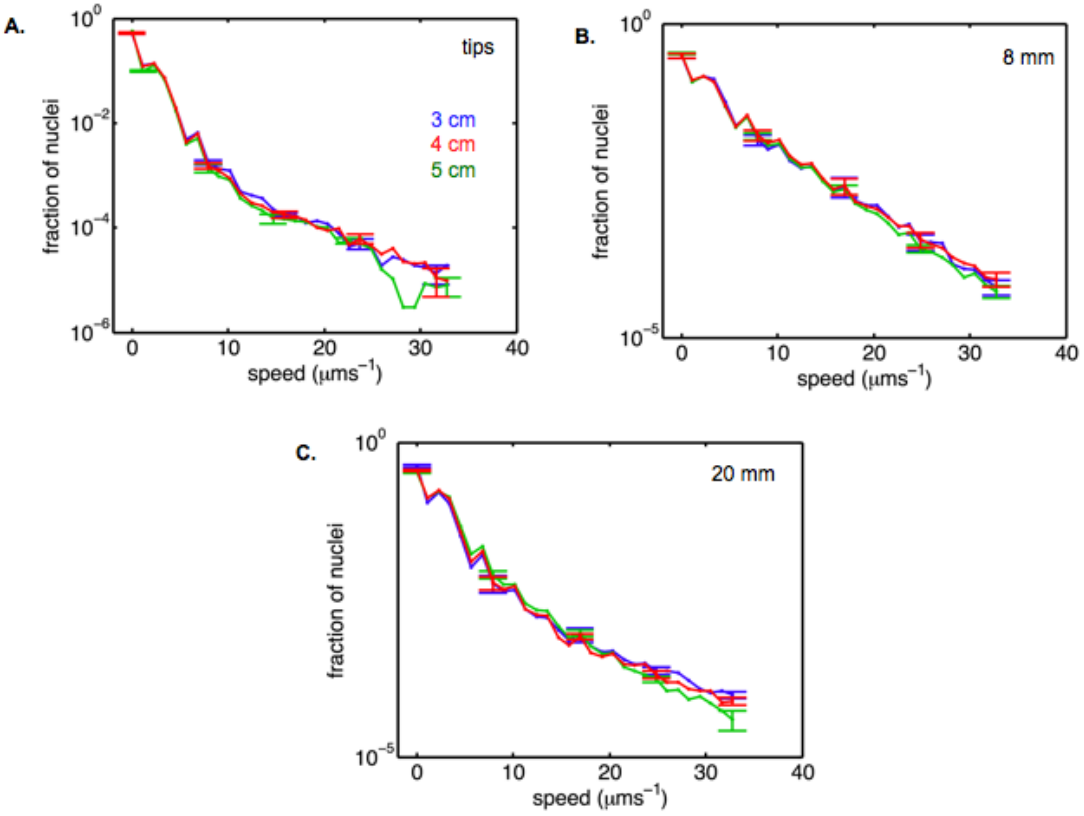
A.
tips
3 cm
4 cm
5 cm
fraction of nuclei
speed (μms$^{-1}$)
B.
8 mm
fraction of nuclei
speed (μms$^{-1}$)
C.
20 mm
fraction of nuclei
speed (μms$^{-1}$)

Figure 3-5

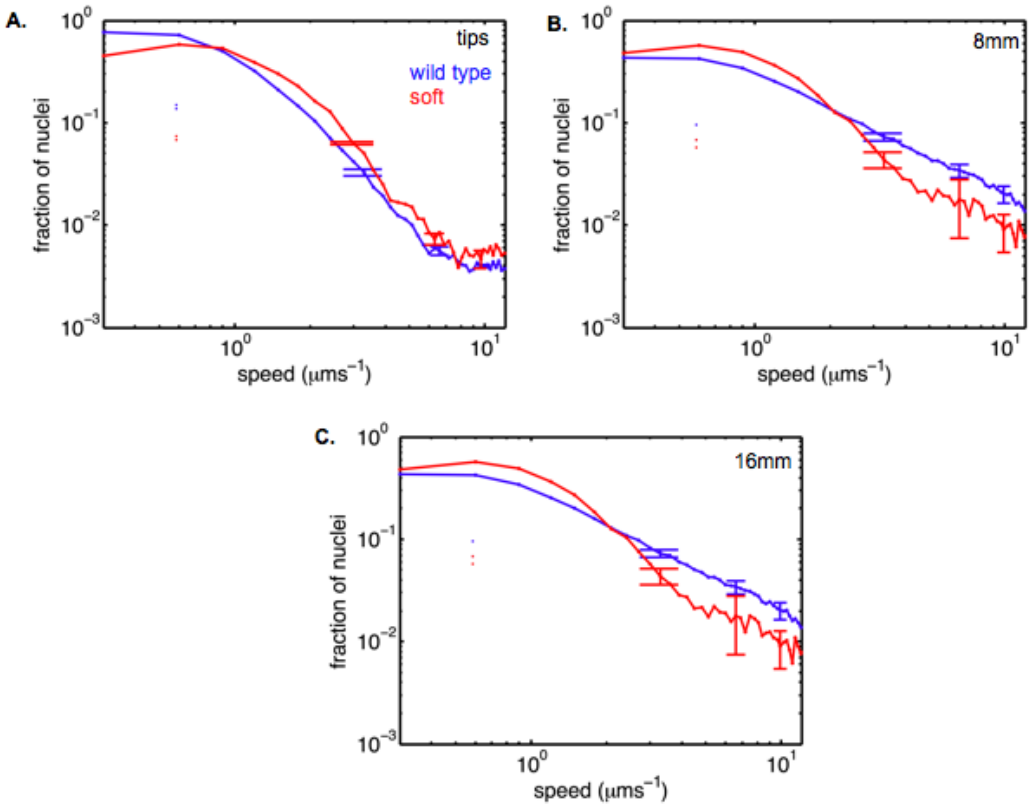
A.
tips
wild type
soft
fraction of nuclei
speed (μms$^{-1}$)
B.
8mm
fraction of nuclei
speed (μms$^{-1}$)
C.
16mm
fraction of nuclei
speed (μms$^{-1}$)

Figure. 3-6

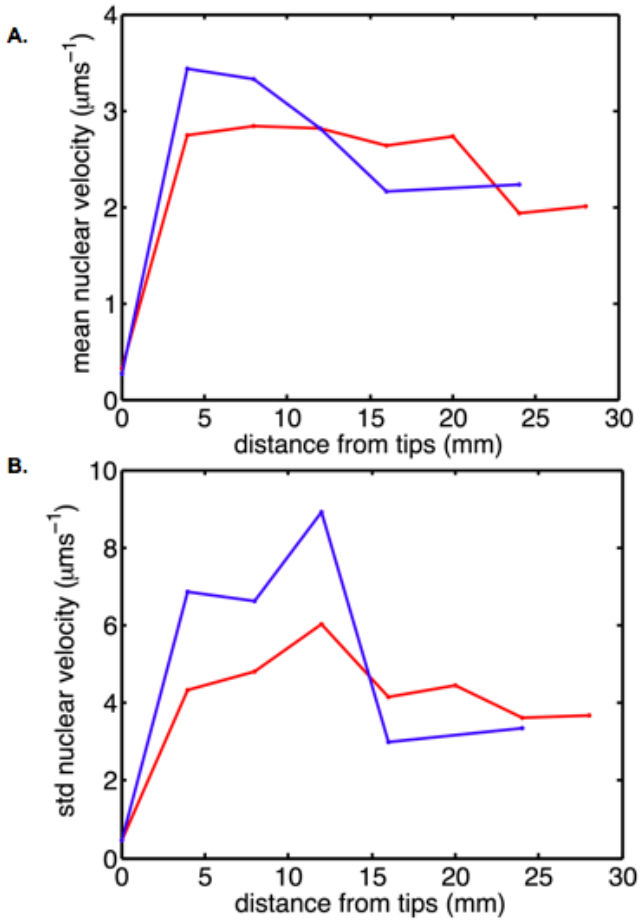
A.
mean nuclear velocity (μms$^{-1}$)
0
1
2
3
4
0
5
10
15
20
25
30
distance from tips (mm)
B.
std nuclear velocity (μms$^{-1}$)
0
2
4
6
8
10
0
5
10
15
20
25
30
distance from tips (mm)

Figure 3-7

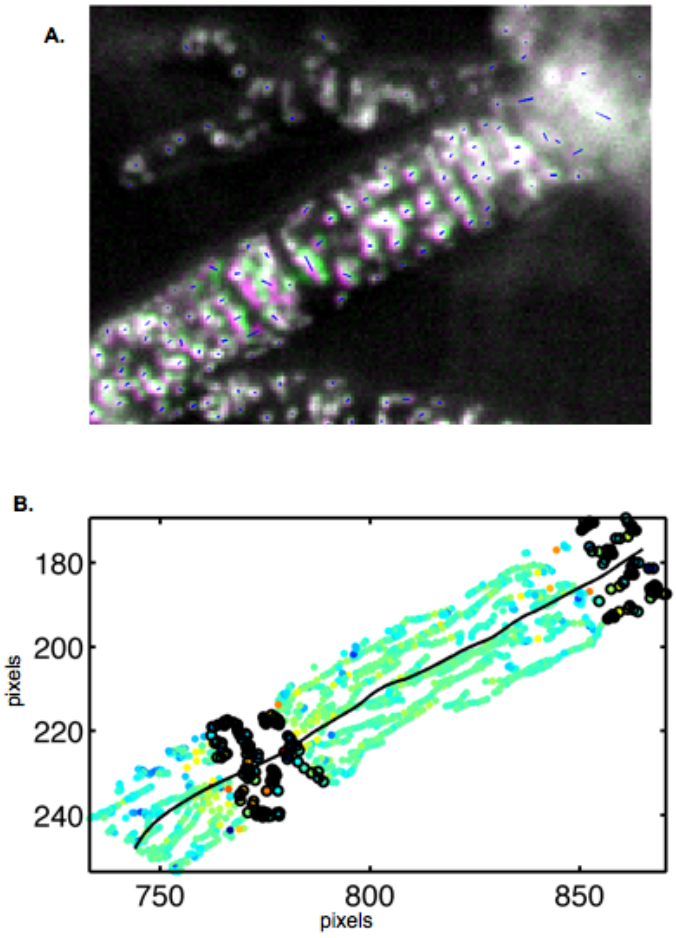

Figure. 3-8

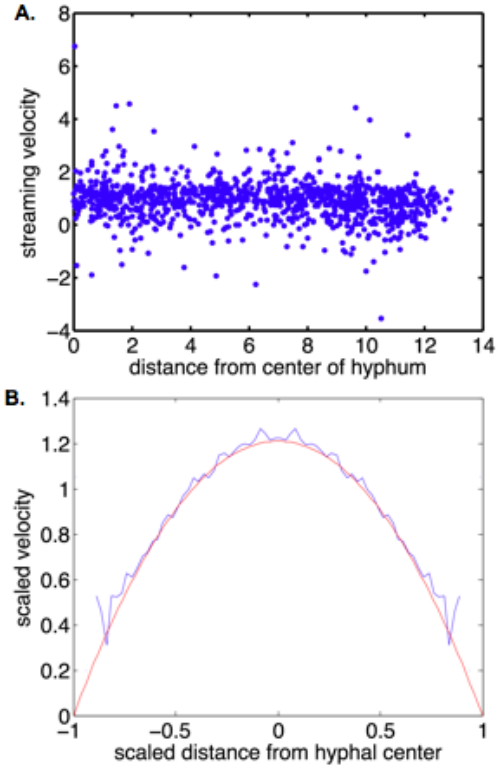
A.
streaming velocity
distance from center of hyphum
B.
scaled velocity
scaled distance from hyphal center

Figure. 3-9

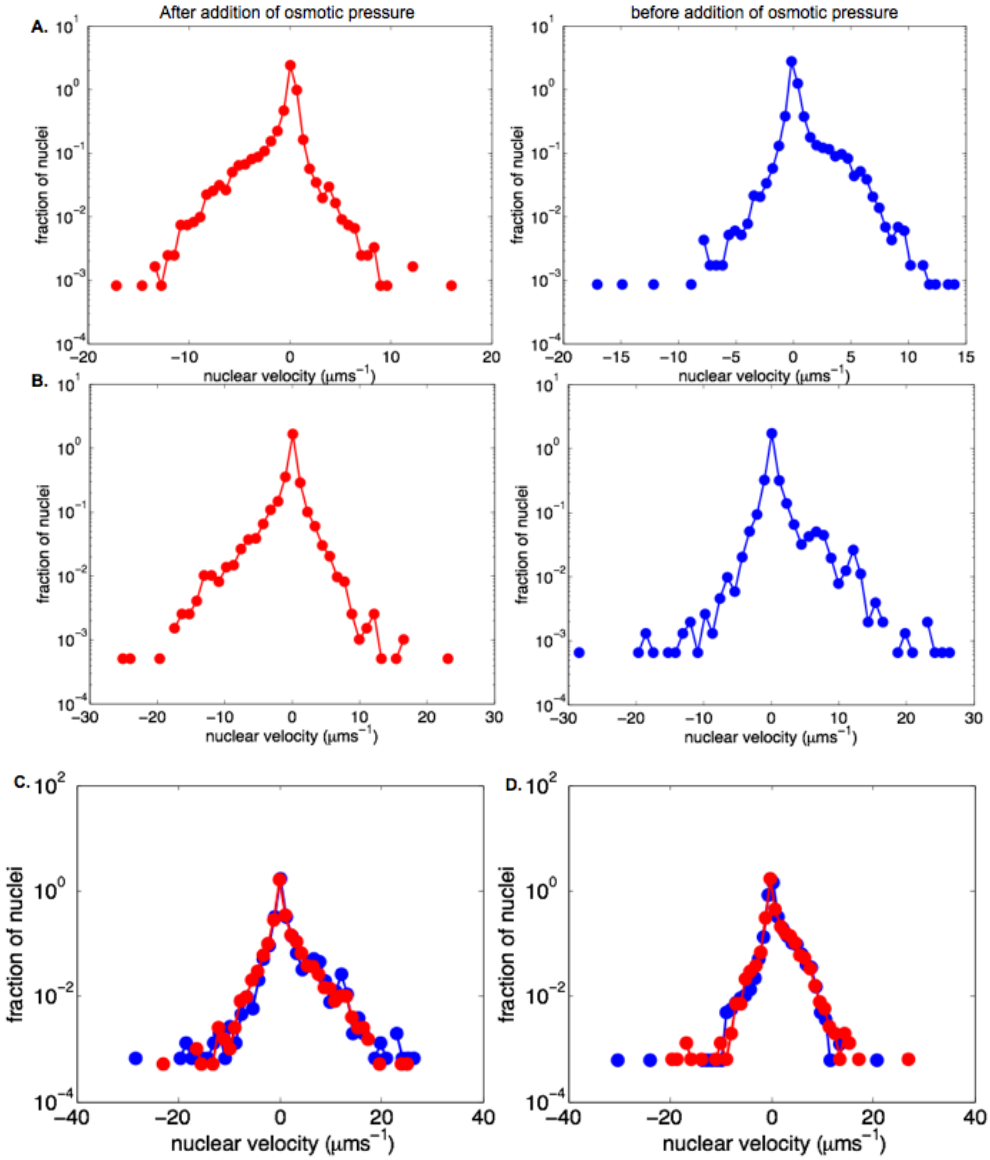
A.
After addition of osmotic pressure
before addition of osmotic pressure
B.
C.
D.
fraction of nuclei
nuclear velocity (μms$^{-1}$)

**Chapter 4**: Network merger, development, and vegetative hyphal fusion influence resource translocation within and between *Neurospora crassa* colonies

**Abstract:**

Nutrient translocation in fungal colonies is essential for processes such as nutrient cycling and distribution in forest ecosystems, mycorrhizal symbioses in agricultural systems, and substrate reduction in industrial systems. Fungi across all phyla have been shown to translocate resources from the origin of the colony to growing hyphal tips, and there is evidence that some fungi can translocate resources between colonies. Fusions between vegetative hyphae help create a distinctive mycelial architecture that can be described as an interconnected network. It is thought that the morphology and architecture of a colony will greatly influence the ability to translocate resources, but this hypothesis has never directly been tested. To test this hypothesis, we measured translocation of 2-amino [1-$^{14}$C] isobutyric acid ($^{14}$C AIB) and 2-aminoisobutyric -$^{15}$N acid ($^{15}$N AIB) in the *Neurospora crassa* hyphal fusion mutants *soft* (no fusion) and *prm-1* (50% fusion frequency), in comparison to wild type colonies. We found that the *soft* mutant is severely reduced in its ability to translocate both AIB tracers and has a lower natural abundance of $\delta^{13}$C than do *prm-1* and wild type. All three strains (*soft, prm-1,* and wild type), have higher levels of N in hyphal tips than elsewhere in the mycelium. We also tested the ability of wild type colonies to share nutrients at different developmental ages through inter-colony fusions. Upon hyphal fusion, wild type colonies will share nutrients as germlings and as small colonies, but different colonies cease to share nutrients when they reach 0.5 cm in diameter. This study highlights that hyphal fusion is necessary for efficient nutrient translocation within a *N. crassa* colony, but also shows that established *N. crassa* colonies do not share resources.

## 1.Introduction

Fungi are important as mycorrhizal symbionts, saprobic decomposers, pathogens, and as substrate degraders in the production of biological enzymes for industry. Filamentous fungi are unique in their ability to create an interconnected hyphal network allowing the entire colony to maintain uninterrupted cytoplasmic continuities. There are presumed to be many advantages for the formation of an interconnected network, such as increased communication, maintaining homeostasis, and distribution of water and nutrients (Rayner 1991). Filamentous fungi can act as conduits to take up and redistribute resources in forest ecosystems; some fungi, such as *Serpula lacrimins,* can translocate nitrogen (N) and carbon (C) across distances as great as meters (Boddy 1995). Bidirectional distribution of resources is necessary for mycorrhizal fungi to bring nutrients such as N or phosphate (P) to the plant and to transport C from the plant to growing hyphal tips (Smith and Read 1997). In pathogenic fungi, such as rusts, transport occurs from the site of plant infection to the rest of the fungal colony (Staples 2001, Voegele and Mendgen 2003). Although morphology of fungal colonies have been studied since the 1930's (Buller 1933), only recently have there been studies linking morphology to hyphal transport (Cariney 2005, Bebber et al. 2007). The morphology of a fungal network presumably affects its ability transport and distribute nutrients, which is essential in biomass degradation. It is difficult to predict fungal metabolic function because the link between fungal cell physiology and colony morphology/development is unknown. It is also unknown how colony architecture affects metabolite transport within aggregates, productivity, growth, and cell physiology. In industrial systems for enzyme production, colony translocation efficiency could have a large effect on substrate colonization and aggregation, and in maintaining the correct ratio of nutrients for adequate growth (Grimm et al. 2005).

Many techniques have been used to image and quantify transport within fungal colonies including tracing with radioactive or stable isotopes. Recently a live cell imaging technique, Photon Counting Scintillation Imaging (PCSI), has been used to image the translocation of radioisotope-labeled tracers moving through growing fungi (Tlalka et al 2002, 2003, and 2007, Fricker et al. 2008). In particular, a non-protein non-metabolizable radioactively labeled tracer, 2-amino [1-$^{14}$C] isobutyric acid ($^{14}$C-AIB), has been used to image and measure translocation in cord-forming fungi (Boddy et al 2009, Tlalka et al. 2002, Olsson 1998). $^{14}$C-AIB is taken up through amino acid transporters (Ogilviella et al. 1981) and accumulates in the free amino acid pool where it is moved at similar rates through hyphae (Tlalka et al. 2002, Olsson et al 1998). This tracer has been used to label cord-forming fungi and to show bidirectional transport of amino acids, movement of amino acids from distal parts of a colony to hyphae colonizing a new carbon source, and coordinated pulsatile movement of amino acids within and between colonies (Tlalka et al 2002, 2003, and 2007, Fricker et al. 2008). In addition to $^{14}$C-AIB, other radioactively- labeled substrates have been used to

track translocation in fungi, for example $^{32}P$ in AM fungi, and $^{86}Rb$ in *N. crassa* (Thain and Girvin 1987). There is also evidence that colonies of AM fungi will fuse and mediate the translocation of a $^{32}P$ tracer from one host plant to another (Mikkelsen et al. 2008) through a connected mycorrhizal network. Enriched stable isotope tracers are also a valuable tool for tracking the translocation of nutrients both within a colony and between presumably fusing colonies (for example (Mikkelsen et al. 2008) (Jacobs et al. 2004) (Philip and Simard 2008) (Leigh et al. 2009)) For example, *Rhizoctonia solani* will translocate $^{13}C$ from a glucose-rich source to an area of the colony growing over a carbon free substrate. Additionally, transfer of $^{13}C$ occurs through ectomycorrhizal (EM) common mycorrhizal networks (for example (Philip and Simard 2008)), but in arbuscular mycorrhizal (AM) common mycorrhizal netoworks carbon remains in the fungal mycelium and is rarely shared plant to plant (Pfeffer et al. 2004).

There are a number of environmental factors that influence the flow of nutrient dynamics within a colony. Nutrient sources and sinks greatly alter the direction and magnitude of flow in hyphae (Tlalka et al. 2008, Jacobs et al. 2004). Fusion between colonies of cord-forming fungi can alter the oscillation of pulsatile nutrient movement resulting in the synchronization of the oscillations of merging colonies (Tlalka et al. 2007). Mycoheterotrophic plants can draw carbon away from both photosynthetic plants and mycorrhizal fungi by tapping into and exploiting a common mycorrhizal network (reviewed in Leake 1994). In addition, water availability and water potential gradients can greatly affect nutrient translocation and bulk flow within hyphae (Jennings et al. 1987, Allen et al. 2009).

Despite the large body of research on nutrient translocation in fungi, one of the great unknown aspects in this field is the influence of hyphal fusion and network morphology on the movement of resources through a colony. Although an interconnected fungal mycelium is believed to be important for fungi to exploit heterogeneous resources (Rayner 1991), this has not been tested directly and there is little understanding of how fusion affects nutrient dynamics. Network models based on nutrient translocation in a cord-forming fungus indicates that there is a trade off between redundancy (i.e. multiple loops) in a colony and the efficiency of translocation (Bebber et al. 2007), which can be altered by reinforcement (cord formation) of important pathways. However, little empirical data exists supporting the idea that an altered network affects nutrient translocation.

Hyphal fusion has been studied extensively in the filamentous ascomycete fungus *Neurospora crassa* (Fleissner et al. 2008) and therefore it is an ideal model system to explore the dynamics of nutrient distribution in fungal colonies. Many hyphal fusion mutants have been identified (for example (Xiang et al. 2002) (Pandey et al. 2004) (Fleissner et al. 2005) (Simonin et al. 2010) (Aldabbous et al. 2010)), allowing for the study of resource distribution in these underdeveloped networks. Fusion occurs when two hyphae grow toward each other through chemotropic communication, then contact and adhere to each other, followed by cell wall breakdown and membrane merger to create a pore through which cytoplasm and organelles can move.

Two fusion mutants have been identified that, despite exhibiting a decreased frequency of fusion, maintain a maximal growth rate similar to those of wild type colonies. The *soft* locus encodes a filamentous ascomycete-specific protein necessary for hyphal fusion, dynamic communication between germlings, and septal plugging after injury. Although both *soft* and *prm-1* have maximal growth rates similar to those of wild type, the *soft* mutant shows a lag in reaching this maximal growth rate (Fleissner 2005, F. Richards, N.L. Glass and A. Pringle in preparation), presumably due to an inability to cooperate during germination via fusion events. The *prm-1* mutant has not yet been analyzed for this trait. The *prm-1* mutant shows a 50% reduction in germling and hyphal fusion (Fleissner et al. 2009), and only rare germling and hyphal fusions occur between strains that contain a deletion mutation of the *soft* gene (Fleissner et al. 2005). The *N. crassa prm-1* locus encodes a putative transmembrane protein that has been shown to be important for plasma membrane merger during hyphal fusion (Fleissner et al. 2009). These mutants are a superb tool by which to evaluate how the frequency of fusion within a colony can affect translocation of resources across a colony, and how the failure (*soft* mutants) or the reduction (*prm-1* mutants) of fusion frequency affects the ability of a fungal colony to respond to the presence of a exploitable resource in a heterogenous environment. Here we use a combination of techniques such radioisotope and stable isotope tracers, as well as fluorescently-labeled proteins to quantify and visualize nutrient translocation within and between wild type *N. crassa* colonies and colonies of fusion mutants.

## 2. Materials and Methods

### *2.1 Strains and media*

The strains used in this study were *soft* (FGSC 508), Δ*soft::hph A* (FGSC 11293) , Δ*prm-1::hph A* (A32, (Fleissner et al. 2009)), and wild type (FGSC 2489). We also used *H1*::dsRed and *his-3::Prdi1-rdi-1-sgfp A* (P6103-5, Rasmussen et al. 2007). Strains were grown on Vogel's minimal medium (Vogel, 1956) with required supplements. Strains were obtained from the Fungal Genetics Stock Center (FGSC) (Colot et al. 2006, McCluskey 2003) or from the referenced people who made the strains. To obtain inoculum plugs and strips, strains were grown from conidia on plates of Vogel's (Vogel 1956) minimal media. The one-tenth sucrose media used for stable isotope experiments contained 2 g/L sucrose and 1.5% agar. The media used for sucrose bait plugs in the radioisotope experiments contained 20 g/L sucrose and 1.5% agar. Strains used for nanoSIMS analysis were shaken in media containing 20 g/L sucrose and the appropriate stable isotope tracer. The conidia were washed and then plated on silica chips covered in 10 ul of water agar (water with 1.5% agar).

### *2.2 Radioisotope experiments*

We tested the ability of wild type and the fusion mutant strains to transport 2-amino [1-$^{14}$C] isobutyric acid from the center of a colony to hyphae at the periphery as the colony grew out from an inoculation plug. Two 8 mm diameter, 3 mm thick, minimal media agar plugs cut from just behind the tip region of a

growing colony were placed in opposite corners on scintillation screens lining 12 cm x 12 cm square Petri plates (Fig. 4-1A). The plugs were approximately 4 cm from the side of the plate and approximately 3 cm from the top or bottom of the plate, and approximately 7.2 cm away from each other on a diagonal. An 8 mm diameter glucose and agar plug, which we termed a "bait plug", was placed approximately 4 cm opposite each inoculation plug, resulting in a total of 4 plugs on the plate (Fig. 1A). Water soaked pieces of paper towel were placed in the corners of the plates off the screen to maintain air humidity in the plates. To each inoculation plug 10 ul of 0.9 mM of 2-amino [1-$^{14}$C] isobutyric acid ($^{14}$C-AIB) was added at the time of placement on the scintillation screen. The microcosms were then imaged using a photon counting camera over three days to observe the movement of the $^{14}$C-AIB through the colonies as they grew. Specifics on imaging techniques can be found in (Tlalka et al. 2002). To test whether the different strains would transport AIB from the periphery of a colony toward the interior, we used the same experimental design as described above, except that $^{14}$C-AIB was added to the uninoculated bait plugs instead of the inoculation plugs (Fig. 4-1B).

Finally, we tested the transport of $^{14}$C-AIB from one colony to another genetically identical colony via hyphal fusion events. Six 8 mm diameter inoculation plugs taken from just behind the tip region of the same colony were placed in two rows of three approximately 3 cm apart on a scintillation screen lining a 12 cm x 12 cm square petri plate (Fig. 4-1C). $^{14}$C-AIB was added to three of the inoculation plugs in a checker-board pattern and photon emission was counted as described in (Tlalka et al. 2002).

*2.3 Stable isotope experiments*

Colonies of *soft, prm-1*, and wild type were grown for approximately one week in Vogel's (Vogel 1956) minimal media slant tubes at 25$^{o}$C in constant light. Conidia were harvested by adding 1ml of sterile water to a tube and vortexing for 30 s. Twenty ul of conidial suspension was streaked in a line across the middle of a 24 x 24 cm Petri plate filled with minimal media. Two mm wide x 2 mm deep x 22 cm long sections of colony were taken approximately 2-6 mm behind the tips of the colony and were removed from the plates to be used as inoculum strips. These strips were then placed on glass slides placed on top of non-ionized Nytran nylon membrane (Whatman) on top of Vogels 2% sucrose agar prepared as described above. This experimental design is similar to that used by (Thain and Garvin 1987). Ten replicates of each strain were prepared. To 4 plates of each strain, 300ul of 2-aminoisobutyric -$^{15}$N acid ($^{15}$N-AIB) (Sigma-Aldrich) at a concentration of 1 ug/ul for a total of 300ug of $^{15}$N-AIB were added evenly along the inoculum strip. Three hundred ul of water were added to one plate of each strain as a control. All colonies were grown linearly for 3 cm, and the same amount and concentration of $^{15}$N-AIB was added to four replicates of each strain that had not yet been labeled. All colonies were then grown until they were 5 cm in linear length. Colonies were grown at 25$^{o}$C in constant light for the entire experiment.

The colonies were cut with clean razor blades into three regions that were 1.67 cm wide (Fig. 1D). Region A is the closest to the inoculum plug, but did not

include any biomass on the glass slides or from the inoculation strip. Region B is the middle section of the colony from 1.67 cm to 3.34 cm and region C is the outermost region including the colony periphery from 3.34 cm to 5 cm. Hyphal biomass was scraped off the membrane covering the media for each region, placed in pre-weighed 5 X 9 mm tin cups (Costech Analytical Inc.) in a 96 well plate. All biomass was dried for 2 days at 60$^{o}$C and was checked between day one and two to make sure weights hadn't changed, indicating that the samples had been desiccated. All samples were then weighed and the weight of the tin cup was subtracted from the final weight to give the weight of the fungal biomass. The cups were balled and sent to the Colorado plateau Stable Isotope Center for C and N analysis with a Isotope Ratio Mass Spectrometer at the Colorado Plateau Stable Isotope Laboratory (see following website for instrument details: www. isotope.nau.edu).

*2.4 NanoSIMS experiments*

Wild-type conidia were harvested from FGS 2489 grown in minimal media slant tubes for approximately a week. The conidial suspension was filtered through cheese cloth to remove the majority of hyphal fragments. The resulting suspension was split into three equal parts into eppendorf microcentrifuge tubes, centrifuged for 2 minutes and re-suspended in either 300 ul of 1 ug/ul $^{15}$N-AIB, 300 ul of 20 ug/ul $^{13}$C glucose, or sterile water as a control. Each tube was then shaken at 30$^{o}$C for 2 hours. The conidia were centrifuged and then washed with water three times to remove any residual tracer, and finally re-suspended in 300 ul of water. The two isotopically labeled suspensions were then mixed together and vortexed to mix the conidia well. Ten ul of the mixed conidia were plated onto a 3 silica chips with a small coating of water agar. This same procedure was done with the non-labeled conidia as a negative control. The chips were then placed in a 30$^{o}$C incubator for 3 - 4 hrs until conidia had germinated and started to fuse. The samples were desiccated for 24 hrs at 50$^{o}$C. The resulting dried chips were analyzed using an epifluoresence microscope to determine regions of interest to be analyzed using nano Secondary Ion Mass Spectrometry (nanoSIMS) methods described in (Finzi-Hart et al. 2009). NanoSIMS was performed by Jennifer Pett-Ridge at Lawrence Livermore National Laboratory using a Cameca NanoSIMS 50 instrument.

*2.5 Microscopy and Developmental Age Experiments*

The radioisotope experiments revealed little nutrient sharing between established wild type colonies, and as such we designed an experiment to test the age at which colonies stopped sharing resources. Two different strains with fluorescently labeled proteins were used, *H1*-dsRed and *rdi*-gfp. Histone 1-dsRED localizes to nuclei and RDI-GFP localizes to the cytoplasm (Rasmussen and Glass 2007). These strains were grown for approximately 1 week in minimal media slant tubes. The conidia from these strains were harvested as described above. Three ul of approximately $10^{8}$/ml conidia of each strain were inoculated in a line either 5 mm or 1.0 mm apart on the center of a rectangle of minimal media agar on a 6 x 4 cm glass slide. The colonies were kept in a 25$^{o}$C constant light

room. The two colonies then each had a linear growing front, one growing toward the other colony which we called the inner portion of the colony and one growing front away from the other colony which we called the outer portion of the colony. The colonies inoculated 5 mm apart were grown until the outer portion of the colony had grown 5 mm. The colony was then imaged on the following transects: 1) the center of the inner portions of the colonies where the two colonies had met and fused (2.5 mm from both inoculation lines), 2) directly next to the inoculation lines on the inner portion of the colony, 3) at the tips of the outer portion of each colony (5 mm from the inoculation line). These measurements were then repeated when the colony had grown to 10 mm. Additional transects were imaged on the outer portions of the colonies every 5 mm.

The colonies that were inoculated 10 mm apart were grown for 7.5 mm from the inoculation point, allowing the two inner parts of the colonies to meet and fuse. The colony was then imaged along the following transects: 1) the center of the inner portions of the colonies where the two had met and fused (5mm from both inoculation lines), 2) 2.5mm from each inoculation line toward the inner portion of the colony, 3) directly next to the inoculation lines on the inner portion of the colony, 4) 5 mm on the outer portion of each colony, and 5) 7.5 mm at the tips of the outer portion of each colony. These measurements were then repeated at 10 mm, and 20 mm of growth. Additional transects were imaged on the outer portions of the colonies in 1 cm increments.

Images were taken at 10 different points along each transect, at each point an image was taken with a GFP filter and an image was taken with a dsRed filter. Three replicates were performed for each experiment. Micrographs were taken with a Hamamatsu digital C4742-95 CCD camera (Hamamatsu, Japan) using the Openlab software program (Coventry, United Kingdom) and a Zeiss Axioskop II microscope. Micrographs taken using a Zeiss dissecting microscope were captured using a Micropublisher 5.0 RTV camera using Q capture image software (Surrey, BC Canada).

## 3. Results

### *3.1 $^{14}$C-AIB distribution within wild type, prm-1, and soft colonies*

We found distinctly different patterns of distribution in wild type, *prm-1*, and *soft* when $^{14}$C-AIB was added to plugs at the time of inoculation. In the wild type colonies, the majority of the $^{14}$C-AIB was distributed toward the periphery of the colony and only a small amount of tracer remained in the interior of the colonies around the inoculation points. The presence of a sucrose bait plug appeared to make no difference in the localization of the tracer, as there did not appear to be a higher density of tracer near the sucrose bait plug compared to the rest of the colony tips (Fig. 4-2A).

*prm-1* colonies had a distinctly different pattern of $^{14}$C-AIB distribution. Though there was evidence of the tracer reaching the tips of the colony, more $^{14}$C-AIB remained in the interior of the colonies than in wild type colonies (Fig. 4-2B). Similar to wild type, the sucrose bait plugs did not appear to influence the concentration and distribution of tracer in the colonies.

*soft* colonies were severely deficient in the ability to transport $^{14}$C-AIB to the periphery of the colonies. Instead the majority of the tracer was concentrated around the original inoculum plug with little being transported further into the colony. Again, the sucrose bait plugs did not seem to influence the distribution of $^{14}$C-AIB within soft colonies (Fig. 4-2C).

*3.2 $^{14}$C-AIB reverse transport from bait plugs in wild type, prm-1, and soft colonies*

To determine whether colonies of wild type and the fusion mutants could transport $^{14}$C-AIB from a bait plug in a retrograde manner from colony tips toward the interior of the colony, we added $^{14}$C-AIB to the bait plugs instead of the inoculum plugs. We found that in all three strains there was minimal reverse translocation from the bait plug to the interior of the colony after almost 3 days of growth. In some of the colonies from all three strains, there appeared to be a small amount of reverse flow in a very localized area (Fig. 4-3).

*3.3 $^{15}$N-AIB distribution in wild type, prm-1, and soft colonies from inoculation point*

We wanted to quantify the differences in AIB translocation that we observed in wild type, *prm-1,* and *soft* strains. We therefore used an enriched stable isotope tracer, $^{15}$N-AIB, and subsequently measured the $\delta^{15}$N, in different regions of the colonies. $^{15}$N-AIB was added to inoculum strips of wild type, *soft* and *prm-1* at the time of inoculation. After 5 cm of growth, 1.67 cm wide sections of the colony were analyzed for $\delta^{15}$N as well as $\delta$13C and total N and C. Regions A (interior), B (middle), and C (tips) were analyzed. We found that region A of all the strains had similar $\delta^{15}$N levels. Wild type colonies had an average $\delta$15N of 2299.6 o/oo ($\pm$ 530.7 o/oo), *prm-1* had an average of 2390.3 o/oo ($\pm$ 487.4 o/oo), and *soft* had an average of 2563.4 o/oo ($\pm$ 248.7 o/oo). $\delta^{15}$N slightly increased in wild type and *prm-1* colonies from region A to region B and region B to region C. As a result, region C had significantly higher $\delta^{15}$N than region A, but neither were significantly different than region B. Wild type and *prm-1* were not statistically different from each other in any of the regions. *Soft* colonies, however, had much lower $\delta^{15}$N in regions B and C as compared to region A. *Soft* colonies had an average of 1638.6 o/oo ($\pm$ 126.2 o/oo) in region B and an average of 1204.5 o/oo ($\pm$38.2o/oo) in region C, significantly lower $\delta^{15}$N than section A and wild type and *prm-1* (Fig. 4-4A ).

*3.4 $^{15}$N-AIB Distribution in wild type, prm-1 and soft colonies after 3 cm of growth*

To determine if the movement of $^{15}$N-AIB from the inoculation strip to the tips of the colony was due to growth or active translocation, we repeated the same experiment but added the $^{15}$N-AIB tracer was added to the inoculation strip after 3cm of colony growth. When the tracer was added after 3 cm of growth, the *prm-1* and *soft* colonies showed a similar $\delta^{15}$N in region A, *prm-1* (2120.8 $\pm$232.5) and *soft* (2195.49 $\pm$405.88). These levels of $^{15}$N in region A were similar to the level of $^{15}$N in region A of wild type, *prm-1*, and *soft* colonies where the

tracer had been added prior to growth from the inoculum strip (see above). However, wild type colonies had significantly higher levels of $^{15}N$ in region A (2880.07 ±124.08) when the tracer was added after 3cm of growth. These data possibly indicate that wild type colonies initially took up more AIB than the other two strains. In all three colonies we found that there is a decrease in $^{15}N$ from section A to section B, but this decrease is significantly greater in the *soft* colonies as compared to wild type and *prm-1*. Wild type and *prm-1* had similar levels of $^{15}N$ in region B (1868.7 ±661.39) and (1451.76 ±492.95) respectively, while *soft* had a very low level of $^{15}N$ in region B (315.6 ±129.7) but was still enriched above background. The average natural abundance $^{15}N$ for unenriched negative control colonies was ~+4.5o/oo (data not shown). Interestingly, $^{15}N$ levels slightly increased in region C of *prm-1* colonies compared to wild type colonies, in which $^{15}N$ levels decreased from region B to region C. *Soft* colonies also had the lowest levels of $^{15}N$ in region C (118.9 ±38.2) (Fig. 4-4 B).

*3.5 Comparison of $\delta^{15}N$ in different parts of the colony*

To better visualize and compare the changes in translocation of $^{15}N$ AIB between different regions of the colonies in the three strains, we analyzed our results by calculating the ratio of change in $\delta^{15}N$ between the colony sections. This was done by taking the ratio of region A to region B, region B to region C, and region A to region C. If the ratio is above one, the amount of $^{15}N$ is increasing from one region to the next, and conversely if the ratio is below one, the amount of $^{15}N$ is decreasing from one region to the next. When the tracer was added before any growth occurred, both wild type and *prm-1* colonies had increasing amounts of $^{15}N$ from regions A to B to C, except that *prm-1* decreased from region B to region C. All of the *soft* colonies showed decreasing amounts of $^{15}N$ from regions A to B to C, with the largest decrease between regions A and C, which is representative of the total decrease in $^{15}N$ across the colony (Fig. 4-4 C).

When the tracer was added to the colonies after 3cm of growth, all of the colonies had a decreasing amount of $^{15}N$ from region A to region B and region A to region C (Fig. 4-4D). Wild type and *soft* had colonies had decreasing levels of $^{15}N$ from region B to region C, but *prm-1* had increasing levels of $^{15}N$ from region B to region C, however overall levels of $^{15}N$ decreased from inoculum to tips across the colony. Also, *soft* had a much larger change in $^{15}N$ between regions when the tracer was added after 3 cm of growth than when it was added at the time of inoculation. These data suggest that the *soft* mutant is defective in its ability to transport the tracer over distances, and not that it just has a decreased ability to translocate tracer as it grows into new environments.

There was a significantly larger change between the sections of *soft* colonies than between the sections of wild type and *prm-1* colonies. The change is due to a large decrease in amount of $^{15}N$ in the middle and tip regions of the *soft* colonies as compared to the section closest to the inoculation point. When the tracer was added at the time of inoculation, $^{15}N$ levels increased in the middle and tip regions as compared to the section closest to the inoculation point in both wild type and *prm-1* colonies. When the tracer was added after 3 cm of growth, the levels of $^{15}N$ either decrease or remain the same in wild type and *prm-1*

colonies. In wild type and *prm-1*, the trend of translocation changes from increasing if the tracer was added at the time of inoculation to decreasing if the tracer was added after the colony has grown 3cm. In *soft* colonies the trend remained the same whenever the tracer was added, the only difference was the magnitude of decrease in levels of $^{15}N$ in the peripheral sections.

*3.6 Total C/N ratios change throughout wild type, prm-1, and soft colonies*

We also found differences in total C/N ratio in the three different strains, and between the different sections sampled within each strain. Interestingly, we found that *soft*, in all sections sampled and in both experiments, had a higher C/N ratio than *prm-1* and wild type. In this circumstance C, N, or the synergy of both C and N could be driving change in C/N ratios between the three strains. We therefore analyzed C and N separately and found no statistically significant trends in total C amounts in our sampling. Total C amounts were extremely variable in all of our replicates. However, we did find differences in strain and location of total N percentages in the colonies. In the *soft* mutant colonies, all treatments showed significantly lower total N levels than in wild type and *prm-1* colonies. These data led us to conclude that total N was driving the differences in C/N ratios. In addition, the tip region of all the colonies, regardless of strain or experimental regime, had a lower C/N driven by higher total N in the tip region (Fig 4-5).

Because we did not use an enriched $^{13}C$ tracer, we were able to analyze $\delta$ $^{13}C$ natural abundance in our samples. We found that these ratios were very consistent and had little variability between replicates. *Soft* had a significantly more negative $\delta^{13}C$ than either *prm-1* or wild type colonies. In conclusion, *soft* is stoichiometrically different from *prm-1* and wild type, but it unclear whether this might be a result of decreased translocation abilities (Fig. 4-6).

*3.7 Using nanoSIMS to determine nutrient sharing between germlings*

Cytoplasmic mixing in germlings in has been previously shown but not quantified. To quantify nutrient sharing between germlings that have fused, we labeled two different populations of conidia and analyzed fusion pairs using nanoSIMS. With this method we were able to image and measure the amount of translocation of $^{15}N$-AIB and $^{13}C$ glucose from one conidium into another, post fusion. After fusion, it was obvious that the $^{15}N$ tracer had moved into the previously unlabeled colony and there was an even distribution of $^{15}N$ in both conidia. This result was different than for conidia that did not fuse, where one germling had much higher levels of $^{15}N$ than the other germling. In this image the highest levels of $^{15}N$ were in the original conidia and less in the germ tube.

$^{13}C$ was also translocated from one conidium to its fusion partner, but not nearly as evenly as the$^{15}N$-AIB. It was easy to identify the germling that had originally been labeled with the $^{13}C$ glucose, because it had the highest levels of $^{13}C$ concentrated in the original conidia of the germling fusion pair. The amounts of $^{13}C$ in the germ tube were much less than the fusion partner. From this experiment we determined that germlings do share nutrients, and readily merge

their cytoplasmic content. This result has been shown previously with dyes and fluorescently labeled proteins, but not using isotopically-enriched nutrients (Fig 4-7).

*3.7 Translocation of $^{14}$C-AIB from labeled colonies to unlabeled colonies*

When 6 inoculation plugs were placed in two rows of three approximately 2.5 cm apart from each other and $^{14}$C-AIB was added to alternating plugs in one row such that essentially every other plug was labeled, we found a striking pattern emerge. The colonies grew into almost perfect rectangles as can be seen by the area of growth of the labeled colonies, resulting in a visual pattern was that of a checker-board of labeled and unlabeled colonies. The colonies did not appear to grow into each other or translocate the label a distinguishable distance into neighboring colonies. In addition, there was very little growth of one colony into another. The lack of translocation of nutrients from one established colony into another is consistent with the lack of reverse translocation we observed in *N. crassa* colonies (see above). The fact that germlings readily share nutrients but mature colonies do not suggested that a developmental time point occurred at which colonies fail to share nutrients and cytoplasmic contents with other colonies (Fig. 4-8).

*3.8 Translocation of a cytoplasmic GFP marker and dsRed nuclear marker from labeled to unlabeled colonies*

To determine at what developmental time point colonies cease to share nutrients, we measured the amount of cytoplasmic and nuclear mixing between colonies that were inoculated in lines at either 10 or 5 mm apart. The colonies were inoculated onto rectangles of solid media such that there would be two linear growth fronts per colony. Images were taken at transects throughout both colonies and also at the area where the two colonies met. For each image three lines were drawn across the image and hyphae were scored as to whether it was green, red, or both green and red. 10 images for each transect were analyzed and averaged, this experiment was repeated 3 times for each distance. We found that wild type colonies shared cytoplasm when they were inoculated 5 mm apart, such that they had grown approximately 2.5 mm from their inoculation point when they encountered another colony. After the outer regions of the colonies had grown to 1 cm from the inoculation line, GFP fluorescence could be detected in hyphae and tips of both colonies (Fig. 4-9A). Fluorescently labeled nuclei were not detected in the opposite RDI::GFP labeled colony. Nuclei did not appear to migrate much from one colony to another where as cytoplasm moved easily from one colony to another.

When colonies were plated 10 mm apart there was little to no mixing of cytoplasm or nuclei from one colony to another, such that the colonies had grown approximately 5 mm from the inoculation point when they encountered another colony. Measurements were taken after the outer portion of the colony had grown 2 cm. There was mixing of cytoplasm and nuclei in the center area where the two colonies met but mixing was limited to the interaction zone. It appears that there is little mixing between colonies when they encounter another colony after 5 mm

of growth (Fig. 4-9B), and that the colonies have reached a developmental age at which resource sharing ceases and is potentially no longer advantageous.

## 4. Discussion

This study used multiple techniques, such as radioisotope tracers, stable isotope tracers, and fluorescently labeled proteins to visualize and quantify nutrient movement within and between *N. crassa* colonies. Using fusion mutants *soft*, and *prm-1*, we were able to show that hyphal fusion influences nutrient distribution within *N. crassa* colonies. The fusion mutant *soft,* which lacks hyphal fusion (Fleissner et al. 2005), is severely decreased in its ability to transport resources as compared to *prm-1* mutants (50% fusion frequency) (Fleissner et al. 2009) and wild type colonies. These results imply that vegetative hyphal fusion is important for nutrient translocation. It appears that *soft* is also stoichiometrically different than *prm-1* and wild type, but it is unclear whether this is a result of the lack of hyphal fusion and reduced ability to translocate nutrients. In addition, we show that wild type colonies larger that 5 mm in diameter cease to share resources even though germlings and small colonies readily merge resources.

### *4.1 Nutrient movement within colonies*

Nutrient translocation and rates of movement in individual fungal species is of particular interest in many fields but research linking network morphology to measured nutrient movement is scarce. Grazing by *Collembola* on cord-forming colonies of *P. velutina* did not decrease transport efficiency (Rotheray et al. 2008) implying that networks are resilient, which might be dependent on alternate routes of transport in connected systems. An efficient translocation network can be modeled by reinforcing pathways and introducing crosslinking pathways, analogous to fusions, adding robustness to the system (Bebber et al. 2007). By using fusion mutants, we removed or reduced the fusion component of an *N. crassa* colony through genetic manipulation. Our results indicate that fusion is necessary for effective nutrient translocation in non-cord- forming fungal colonies, and in some cases a 50% reduction in fusion frequency will also result in decreased nutrient translocation. It should be taken into account that our study does not preclude any pleiotropic affects *soft* and *prm-1* mutations might have on other colony functions that in turn could have an indirect affect on nutrient translocation. However, *prm-1* and *soft* have similar growth rates as wild type, suggesting that any pleiotropic effects of the mutations are minimal.

There were differences in nutrient distribution patterns between the $^{14}C$ AIB tracer experiments and $^{15}N$-AIB tracer experiments. The radioisotope tracer experiments showed that *prm-1* colonies maintain more tracer in the middle area of the colonies , unlike in wild type, where most of the tracer localized to the tips of the colonies. One explanation for this difference is that environmental conditions were different between the two experiments. In the radioisotope tracer experiments, the colonies were growing across a dry scintillation screen with no medium. Microscopic evaluation of a colony growing in similar conditions revealed desiccated hyphae, leading us to believe that the dry conditions were not very favorable for growth. In contrast, the colonies in the stable isotope

experiments were well hydrated and had a small carbon source available as they grew across a membrane above sucrose and agar medium. Water availability can greatly affect nutrient dynamics in fungal colonies (Jennings 1987) and therefore might be the source of the differences we observed between the two experiments. Thus, in favorable conditions perhaps a 50% decrease in fusion does not affect translocation abilities but in dry conditions a 50% reduction has a greater affect on colony translocation. Another explanation for the discrepancies in these data is simply that our sampling methods were not sensitive enough. The regions sampled in our stable isotope experiments might have been too large to detect subtle differences in nutrient distribution between *prm-1* and wild type, whereas the radioisotope experiment allowed us to visualize these differences.

Based on our results it appears colonies can more easily translocate a tracer when labeled from an inoculation point, but it is more difficult to move nutrients through an already established colony. This has been shown previously in *R. solanii,* where C translocation was slower in already established colonies in heterogeneous environments (Jacobs et al. 2004). As the interior of a colony uses up available nutrients and ages it become more and more vacuolated and in some fungi, septa become plugged, effectively shutting off the interior of the colony. Our results show that *N. crassa* after 5 cm of growth still has an active interior that is connected to the rest of the colony. When tracer is added at the time of inoculation, the amount of tracer steadily increased toward the tips of the colony but when the tracer was added after 3 cm of growth, the amount of tracer decreased from the inoculation point to the tips of the colony. It should be noted that even though the trend was a reduction of tracer toward the tips, there was still a high amount of enrichment at the tips of wild type and *prm-1,* indicating the ability to effectively translocate the tracer.

Mycorrhizal fungi need to have the ability for bidirectional transport from tips to roots and roots to tips. This requires metabolic activity throughout the entire colony as it grows and forages in order to maintain and benefit from a symbiotic relationship with its host (Cruz et al. 2007). Bidirectional transport does not occur in *N. crassa* under the conditions of our experiments. Our results show that when encountering a carbon-rich 'bait' plug under nutrient poor conditions, *N. crassa* colonies did not transport resources from the 'bait' plug to the interior of the colony but instead sent these resources outwards toward foraging tips. This could again be the result of a dry, nutrient poor environment or perhaps the tips of a colony are more of resource sink than the interior of the colony. Our data show that the tips of *N. crassa* colonies have a higher percentage of N than the interior of the colony, suggesting that resources are translocated to areas of high N to promote growth. It is possible that in fast growing, fast colonizing, non-cord-forming fungi, retrograde translocation is not necessary or the pressure gradients increasing toward hyphal tips are greater than in sinks in other parts of the colony.

*4.2 Nutrient movement between colonies*

Germlings readily share cytoplasm and nuclei when they fuse (for example (Roca et al. 2010, Fleissner et al. 2009)). We confirmed and quantified this cytoplasmic mixing using nanoSIMS technology to create a map of $^{15}N$ and $^{13}C$ isotope ratios over two fusing germlings. nanoSIMS has previously been used in other biological systems such as corals and cyanobacteria to measure $^{15}N$ and $^{13}C$ levels (Clode et al. 2007, Wagner 2009), but is just recently being used to study fungi. We used this technology to show that two fusing germlings with different stable isotope tracers share cytoplasm. This experiment was essentially a proof of principle and also one of the first experiments using nanoSIMS to analyze $^{15}N$ in fungi.

Despite showing that germlings readily fuse and share cytoplasm, our results also show that genetically identical ~ 5 mm colonies that are physically interacting do not share cytoplasm and nutrients. Presumably there is some developmental or physiological change that occurs when a colony reaches approximately 5 mm of growth. There are quite a few developmental differences between germlings and mature colonies. For example, the transcriptional profile of germlings is much different from that of older colonies (Kasuga et al. 2008) (Kasuga et al. 2005). Some hyphal fusion mutants are merely delayed in fusion, but will resume fusion after they have grown for a certain distance. Wild type conidia fuse via Conidial Anastomosis Tubes (CATs) almost immediately after germination (Roca et al. 2005). An example of a mutant that exhibits this delay in fusion is CR16-8, a strain that has a mutation in a gene, *ham-4*, resulting in the truncation of the HAM-4 protein (Simonin et al. 2010). *ham-4* deletion mutants are defective in hyphal fusion but CR16-8 mutants regain their ability to fuse after approximately 10 hrs post germination, whereas wild type conidia start to fuse after 2 hrs. Other functions such as heterokaryon incompatibility are suppressed in germlings, and do not resume until after the conidia have already fused and created a colony (Hutchison, pers. comm). *N. crassa* germlings lack a defined Spitzenkorper and a nuclear exclusion zone in the hyphal apex, but once these germlings grow to 150 um they have acquired both (Araujo-Palomares et al. 2007). Though exact physiological differences that lead to changes in resource sharing are unknown, it is clear that germlings and young colonies are developmentally distinct from mature colonies.

Fusion readily occurs between two mature *N. crassa* colonies. Sections taken from the same colony of wild type *N. crassa* after 4hrs of separation can pass cytoplasm and organelles through fusion points, but the extent of translocation was not measured (Hickey et al. 2002). We also observed fusion points between mature colonies but these fusion points did not lead to resource sharing. The inability to translocate resources between mature colonies, as is seen in *N. crassa,* is not always seen in other fungi. Fusion between two, non-germling, genetically different AM fungal colonies, also resulted in cytoplasm and organelles passing through these fusion points (Giovannetti et al. 1999). In contrast to our results, AM fungal colonies can fuse and act as conduit for P translocation from one host plant to another (Mikkelsen et al. 2008). Basidiomycete fungi can also fuse to create larger communicating and nutrient

sharing networks (Tlalka et al. 2007 and 2008) and to create dikaryons (Gladfelter and Berman 2009, James et al. 2008).

We have shown that *N. crassa* doesn't transport nutrients from the tips of the colony to the interior of the colony when it encounters a nutrient rich source. The inability to translocate resources in retrograde could limit the ability for *N. crassa* to share and translocate resources between colonies as well. Perhaps the fast growth rate and non-cord-forming architecture of *N. crassa* results in the highest pressure source being the periphery of the colony. A pressure-driven flow toward the tips might be overcome by a strong enough sink elsewhere in the colony, but in our experiments the sinks were not great enough to effectively overcome the sink of the growing periphery. Interestingly, we showed in chapter 3 that conidia can fuse with a larger mature colony and nuclei from the conidia can be transported through out the colony. Perhaps one partner that is developmentally competent to share resources is sufficient to induce resource sharing between partners. Alternatively maybe mixing ability is a matter of pressure differences between two colonies. Two mature colonies with linear growth fronts that meet might have well matched turgor pressures and bulk flows, resulting in no resource flow between the two. Conidia would not have high tip driven bulk flow and once fused with a larger colony the conidial contents would be drawn toward the tips of the larger colony.

## 5. Conclusion

We found that hyphal fusion within colonies is necessary for efficient nutrient transport, which also supports the assumption that an interconnected network is important for colony communication and homeostasis. However, translocation of nutrients/organelles via hyphal fusion between mature colonies does not appear to play a large role in resource allocation in *N. crassa.* Inter colony mergers hold many risks; mycoviruses can be transferred, resource plundering can occur, foreign nuclei can take over and effectively exterminate the genotype of the original colony. However there are also benefits to fusing with another colony, such as synergistic complementation resulting in a more robust colony, nutrient sharing with a larger foraging area, and increased germination rates. Further investigation will reveal the mechanisms and physiology behind the cessation of inter colony resource translocation in *N. crassa colonies.*

## 6. References

Aldabbous, M S, M G Roca, A Stout, I C Huang, N D Read, and S J Free. 2010. The ham-5, rcm-1 and rco-1 genes regulate hyphal fusion in Neurospora crassa. *Microbiology* 156 (9) (September 1): 2621-2629.

Allen, Michael F. 2009. Bidirectional water flows through the soil-fungal-plant mycorrhizal continuum. *New Phytologist* 182 (2): 290-293.

Araujo-Palomares, Cynthia L, Ernestina Castro-Longoria, and Meritxell Riquelme. 2007. Ontogeny of the Spitzenkörper in germlings of Neurospora crassa. *Fungal Genetics And Biology* 44 (6) (June): 492-503.

Bebber, Daniel P, Juliet Hynes, Peter R Darrah, Lynne Boddy, and Mark D

Fricker. 2007. Biological solutions to transport network design. *Proceedings Of The Royal Society B-Biological Sciences* 274 (1623): 2307-2315.
Boddy, Lynne, Juliet Hynes, Daniel P Bebber, and Mark D Fricker. (2009) Saprotrophic cord systems: dispersal mechanisms in space and time." Mycoscience 50 (1): 9-19. doi:10.1007/s10267-008-0450-4.
Boddy, L. & Watkinson, S. C. WOOD DECOMPOSITION, HIGHER FUNGI, AND THEIR ROLE IN NUTRIENT REDISTRIBUTION. (1995) Canadian Journal of Botany-Revue Canadienne De Botanique 73, S1377-S1383.
Buller, A. H. R. (1933) *Researches on Fungi,* vol. 5. Longman, London.
Cairney, JWG. (2005) Basidiomycete mycelia in forest soils: dimensions, dynamics and roles in nutrient distribution. *Mycological Research* 109: 7-20.
Clode, Peta L, Richard A Stern, and Alan T Marshall. 2007. Subcellular imaging of isotopically labeled carbon compounds in a biological sample by ion microprobe (NanoSIMS). *Microscopy Research And Technique* 70 (3): 220-229.
Colot, H. V., Park, G., Turner, G. E., Ringelberg, C., Crew, C. M., Litvinkova, L., Weiss, R. L., Borkovich, K. A., and Dunlap J. C. (2006) A high-throughput gene knockout procedure for *Neurospora* reveals functions for multiple transcription factors. *Proc. Natl. Acad. Sci. U.S.A*. 103**,** 10352–10357.
Cruz, C, H Egsgaard, C Trujillo, P Ambus, N Requena, M A Martins-Loucao, and I Jakobsen. 2007. "Enzymatic Evidence for the Key Role of Arginine in Nitrogen Translocation by Arbuscular Mycorrhizal Fungi." *PLANT PHYSIOLOGY* 144 (2) (April 28): 782-792. doi:10.1104/pp.106.090522.
Finzi-Hart, Juliette A., Jennifer Pett-Ridge, Peter K. Weber, Radu Popa, Stewart J. Fallon, Troy Gunderson, Ian D. Hutcheon, Kenneth H. Nealson, and Douglas G. Capone. 2009. Fixation and fate of C and N in the cyanobacterium Trichodesmium using nanometer-scale secondary ion mass spectrometry. *Proceedings Of The National Academy Of Sciences Of The United States Of America* 106 (15): 6345-6350.
Fleissner, A, S Sarkar, DJ Jacobson, MG Roca, ND Read, and NL Glass. 2005. The so locus is required for vegetative cell fusion and postfertilization events in Neurospora crassa. *Eukaryotic Cell* 4 (5): 920-930..
Fleissner, A, S Diamond, and N L Glass. 2008. The Saccharomyces cerevisiae PRM1 Homolog in Neurospora crassa Is Involved in Vegetative and Sexual Cell Fusion Events but Also Has Postfertilization Functions. *Genetics* 181 (2) (November 24): 497-510.
Fleissner, Andre, Anna R Simonin, and N Louise Glass. 2008. Cell fusion in the filamentous fungus, Neurospora crassa. *Methods in molecular biology (Clifton, N.J.)* 475: 21-38.
Fleissner, Andre, Spencer Diamond, and N Louise Glass. 2009. The Saccharomyces cerevisiae PRM1 Homolog in Neurospora crassa Is Involved in Vegetative and Sexual Cell Fusion Events but Also Has Postfertilization Functions. *Genetics* 181 (2): 497-510.
Fricker, M D, J A Lee, D P Bebber, M Tlalka, J Hynes, P R Darrah, S C Watkinson, and L BODDY. 2008. Imaging complex nutrient dynamics in

mycelial networks. *Journal Of Microscopy-Oxford* 231 (2): 317-331.
Giovannetti, M, D Azzolini, and AS Citernesi. 1999. Anastomosis formation and nuclear and protoplasmic exchange in arbuscular mycorrhizal fungi. *Applied and Environmental Microbiology* 65 (12): 5571-5575.
Gladfelter, Amy, and Judith Berman. 2009. Dancing genomes: fungal nuclear positioning. *Nature Reviews Microbiology* 7 (12): 875-886..
Grimm, L H, S Kelly, R Krull, and D C Hempel. 2005. "Morphology and productivity of filamentous fungi. *Applied Microbiology and Biotechnology* 69 (4) (November 17): 375-384.
Hickey, PC, DJ Jacobson, ND Read, and NL Glass. 2002. Live-cell imaging of vegetative hyphal fusion in Neurospora crassa. *Fungal Genetics And Biology* 37 (1): 109-119.
Jacobs, H, GP Boswell, CM Scrimgeour, FA Davidson, GM Gadd, and K Ritz. 2004. Translocation of carbon by Rhizoctonia solani in nutritionally-heterogeneous microcosms. *Mycological Research* 108: 453-462..
James, Timothy Y, Jan Stenlid, Ake Olson, and Hanna Johannesson. 2008. Evolutionary significance of imbalanced nuclear ratios within heterokaryons of the basidiomycete fungus Heterobasidion parviporum. *Evolution* 62 (9):
JENNINGS, DH. 1987. Translocation of Solutes in Fungi. *Biological Reviews of the Cambridge Philosophical Society* 62 (3): 215-243.
Kasuga, T, JP Townsend, CG Tian, LB Gilbert, G Mannhaupt, JW Taylor, and NL Glass. 2005. Long-oligomer microarray profiling in Neurospora crassa reveals the transcriptional program underlying biochemical and physiological events of conidial germination. *Nucleic Acids Research* 33 (20):
Kasuga, T, and N L Glass. 2008. Dissecting Colony Development of Neurospora crassa Using mRNA Profiling and Comparative Genomics Approaches." *Eukaryotic Cell* 7 (9) (September 5): 1549-1564.
Leake JR. 1994. Tansley review: the biology of myco-heterotrophic ('saprophytic') plants. New Phytologist 127: 171–216.
Leigh, Joanne, Angela Hodge, and Alastair H Fitter. 2009. Arbuscular mycorrhizal fungi can transfer substantial amounts of nitrogen to their host plant from organic material. *New Phytologist* 181 (1): 199-207.
McCluskey, K. (2003). The Fungal Genetics Stock Center: from molds to molecules. Adv Appl Microbiol *52*, 245-262.
Mikkelsen, Bolette L, Søren Rosendahl, and Iver Jakobsen. 2008. Underground resource allocation between individual networks of mycorrhizal fungi." *New Phytologist* 180 (4) (December 2): 890-898.
OGILVIEVILLA, S, RM DEBUSK, and AG DEBUSK. 1981. CHARACTERIZATION OF 2-AMINOISOBUTYRIC ACID TRANSPORT IN NEUROSPORA-CRASSA - A GENERAL AMINO-ACID PERMEASE-SPECIFIC SUBSTRATE. *Journal Of Bacteriology* 147 (3): 944-948.
Olsson S, Gray SN. 1998. Patterns and dynamics of 32P-phosphate and labelled 2-aminoisobutyric acid (14C-AIB) translocation in intact basidiomycete mycelia. FEMS Microbiology Ecology 26: 109–120.
Pandey, A, MG Roca, ND Read, and NL Glass. 2004. Role of a mitogen-

activated protein kinase pathway during conidial germination and hyphal fusion in Neurospora crassa. *Eukaryotic Cell* 3 (2): 348-358.
Pfeffer, Philip E, David D Douds, Heike Bucking, Daniel P Schwartz, and Yair Shachar-Hill. 2004. The fungus does not transfer carbon to or between roots in an arbuscular mycorrhizal symbiosis. *New Phytologist* 163 (3) (September): 617-627.
Philip, Leanne J, and Suzanne W Simard. 2008. Minimum pulses of stable and radioactive carbon isotopes to detect belowground carbon transfer between plants. *Plant And Soil* 308 (1-2) (May 1): 23-35.
Rasmussen, Carolyn G, and N Louise Glass. 2007. Localization of RHO-4 indicates differential regulation of conidial versus vegetative septation in the filamentous fungus Neurospora crassa. *Eukaryotic Cell* 6 (7): 1097-1107.
Rayner, ADM. 1991. THE CHALLENGE OF THE INDIVIDUALISTIC MYCELIUM. *Mycologia* 83 (1): 48-71.
Roca, M G, H C Kuo, A Lichius, M Freitag, and N D Read. 2010. Nuclear Dynamics, Mitosis, and the Cytoskeleton during the Early Stages of Colony Initiation in Neurospora crassa. *Eukaryotic Cell* 9 (8) (August 3): 1171-1183.
Roca, MG, J Arlt, CE Jeffree, and ND Read. 2005. Cell biology of conidial anastomosis tubes in Neurospora crassa. *Eukaryotic Cell* 4 (5): 911-919. doi:10.1128/EC.4.5.911-919.2005.
Rotheray, T D, T H Jones, M D Fricker, and Lynne Boddy. 2008. Grazing alters network architecture during interspecific mycelial interactions. *Fungal Ecology* 1 (4) (November): 124-132.
Simonin, Anna R, Carolyn G Rasmussen, Mabel Yang, and N Louise Glass. 2010. Genes encoding a striatin-like protein (ham-3) and a forkhead associated protein (ham-4) are required for hyphal fusion in Neurospora crassa.. *Fungal Genetics And Biology* 47 (10) (October): 855-868.
Smith, S. E. & Read, D. J. (1997) in *Mycorrhizal symbiosis* (Academic Press, San Diego, CA.
Staples, RC. 2001. Nutrients for a rust fungus: the role of haustoria. Trends in Plant Science 6 (11): 496-498.
Thain, J. F. & Girvin, D. TRANSLOCATION THROUGH ESTABLISHED MYCELIUM OF NEUROSPORA-CRASSA ON A NUTRIENT-FREE SUBSTRATE. Transactions of the British Mycological Society 89, 45-49 (1987).
Tlalka, M, SC WATKINSON, PR Darrah, and MD Fricker. 2002. Continuous imaging of amino-acid translocation in intact mycelia of Phanerochaete velutina reveals rapid, pulsatile fluxes. *New Phytologist* 153 (1): 173-184.
Tlalka, M, D Hensman, P R Darrah, S C Watkinson, and M D Fricker. 2003. Noncircadian oscillations in amino acid transport have complementary profiles in assimilatory and foraging hyphae of Phanerochaete velutina. *New Phytologist* 158 (2) (May): 325-335. doi:10.1046/j.1469-8137.2003.00737.x.
Tlalka, M, D P Bebber, P R Darrah, S C Watkinson, and M D Fricker. 2007. Emergence of self-organised oscillatory domains in fungal mycelia. *Fungal*

*Genetics And Biology* 44 (11) (November): 1085-1095.
Tlalka, M, D P Bebber, P R Darrah, S C Watkinson, and M D Fricker. 2008. Quantifying dynamic resource allocation illuminates foraging strategy in Phanerochaete velutina. *Fungal Genetics And Biology* 45 (7): 1111-1121.
Tlalka, M, M Fricker, and S Watkinson. 2008. Imaging of Long-Distance - Aminoisobutyric Acid Translocation Dynamics during Resource Capture by Serpula lacrymans. *Applied and Environmental Microbiology* 74 (9) (May 2): 2700-2708.
Voegele, RT, and K Mendgen. 2003. Rust haustoria: nutrient uptake and beyond. *New Phytologist* 159 (1): 93-100.
Vogel, H.J. (1956). A convenient growth medium for *Neurospora*. Microbiol Genet Bull *13*, 42-46.
Wagner, Michael. 2009. Single-Cell Ecophysiology of Microbes as Revealed by Raman Microspectroscopy or Secondary Ion Mass Spectrometry Imaging. *Annual Review Of Microbiology* 63: 411-429.
Xiang, QJ, C Rasmussen, and NL Glass. 2002. The ham-2 locus, encoding a putative transmembrane protein, is required for hyphal fusion in Neurospora crassa. *Genetics* 160 (1): 169-180.

**Figure legend**:

Figure 4-1.
Experimental design of radioisotope and stable isotope experiments. The first three diagrams show placement of inoculum plugs (I) and sucrose bait plugs (B) on 12 cm x 12 cm Petri dishes covered in scintillation screen. Asterisks (*) indicate $^{14}$C-AIB label was added to a plug. A) inoculum plugs were labeled B) sucrose bait plugs were labeled and C) half of the inoculum plugs were labeled. D) A diagram of plates used for stable isotope translocation experiments, sucrose agar covered in cellophane with glass slides placed at the edge of one plate. An inoculum strip was placed on the edge of the glass slides. Letters indicate the 1.67cm regions from which the colony biomass was harvested.

Figure 4-2.
Images of photon emission at 4, 8, 16, 32 and 64 hrs from wild type, *prm-1*, and *soft* colonies where $^{14}$C-AIB has been added to inoculation plugs prior to growth of the colony.

Figure 4-3.
Images of photon emission at 4, 8, 16, 32 and 64 hrs from wild type, *prm-1*, and *soft* colonies where $^{14}$C-AIB has been added to a sucrose bait plug.

Figure 4-4. A) d$^{15}$N in regions of wild type, *prm-1*, and *soft* colonies when a $^{15}$N-AIB tracer was added at the time of colony inoculation. B) $\delta^{15}$N in regions of wild type, *prm-1* and *soft* colonies when a $^{15}$N-AIB tracer was added after 3 cm of growth. C) Comparisons of $\delta^{15}$N between regions of wild type, *prm-1* and *soft* expressed as ratios when tracer was added at inoculation. D) Comparisons of $\delta^{15}$N between regions of wild type, *prm-1* and *soft* expressed as ratios when tracer was added after 3 cm of growth.

Figure 4-5. Total percent nitrogen found in different regions of wild type, *prm-1*, and *soft* colonies when $^{15}$N AIB tracer was added A) at inoculation and B) after 3 cm of growth. Total percent carbon found in different regions of wild type, *prm-1*, and *soft* colonies when $^{15}$N AIB tracer was added C) at inoculation and D) after 3 cm of growth.

Figure 4-6. Total C/N ratios found in different regions of wild type, *prm-1*, and *soft* when $^{15}$N AIB tracer was added A) at the time of inoculation B) after 3 cm of growth. Comparisons of total C/N within strains both when tracer was added at the time of inoculation and after 3 cm of growth in C) wild type, D) *prm-1* and E) *soft* mutants.

Figure 4-7. $\delta^{13}$C natural abundance levels in wild type, *prm-1*, and *soft* colonies when $^{15}$N-AIB tracer was added A) at the time of inoculation and B) after 3 cm of growth.

Figure 4-8.
Photon emission images of wild type colonies grown for 64 hours from inoculation plugs taken from the same colony on a scintillation screen. U's indicate unlabeled colonies and L's indicate labeled colonies.

Figure 4-9
Images of SEM and nanoSIMS analysis of fused, unfused, and unlabeled control conidia. Column A is SEM, column B shows $\delta^{15}N$ levels, and column C shows $\delta^{13}C$ levels.

Figure 4-10. Percentage of hyphae containing green fluorescence, red fluorescence, or both in A) colonies inoculated 5 mm apart, images taken after the outer part of the colony had grown 10 mm from the line of inoculation and B) colonies inoculated 10 mm apart, images taken after outer part of the colony had grown 20 mm from line of inoculation.

Figure. 4-1.

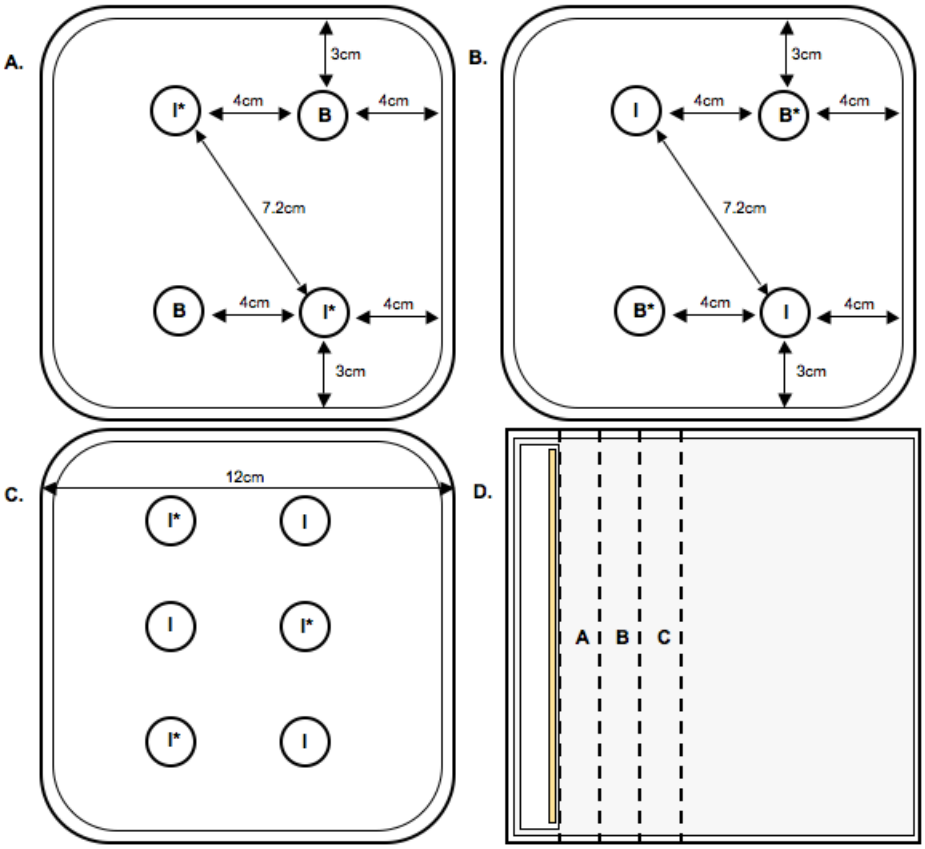
A.
3cm
I*
4cm
B
4cm
7.2cm
B
4cm
I*
4cm
3cm
B.
3cm
I
4cm
B*
4cm
7.2cm
B*
4cm
I
4cm
3cm
C.
12cm
I*
I
I
I*
I*
I
D.
A
B
C

Figure. 4-2.

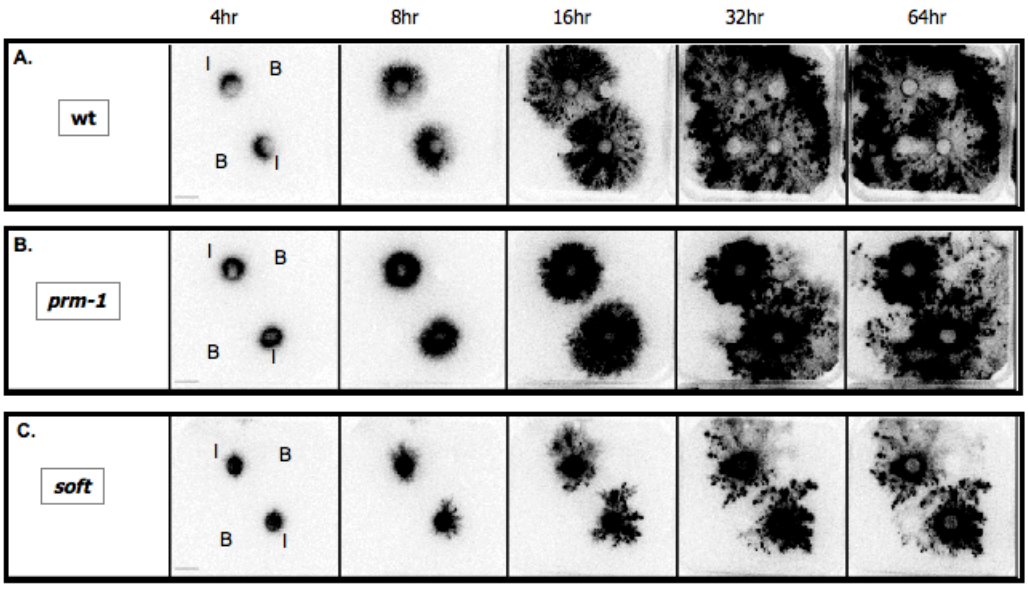

Figure. 4-3.

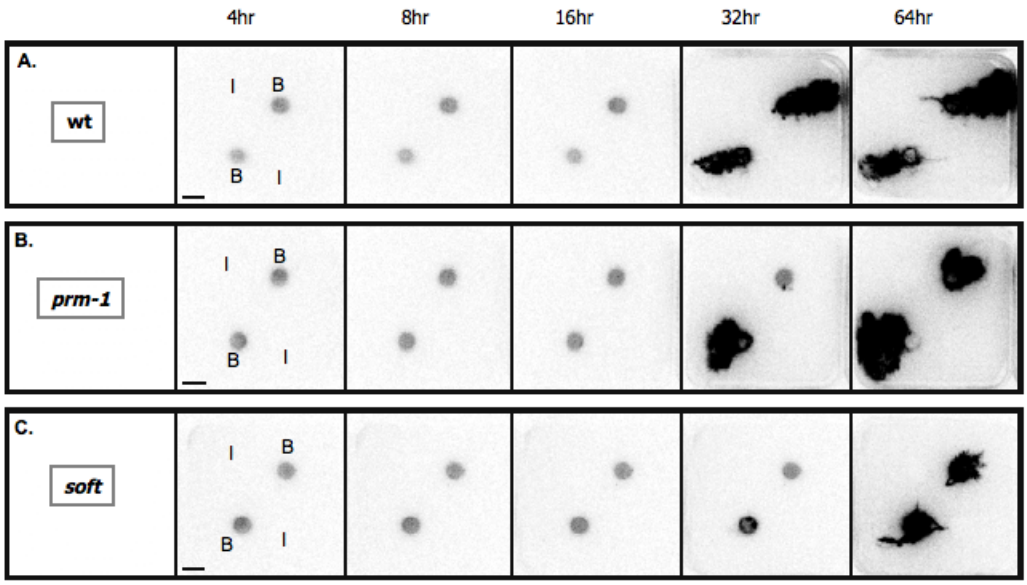

Figure. 4-4

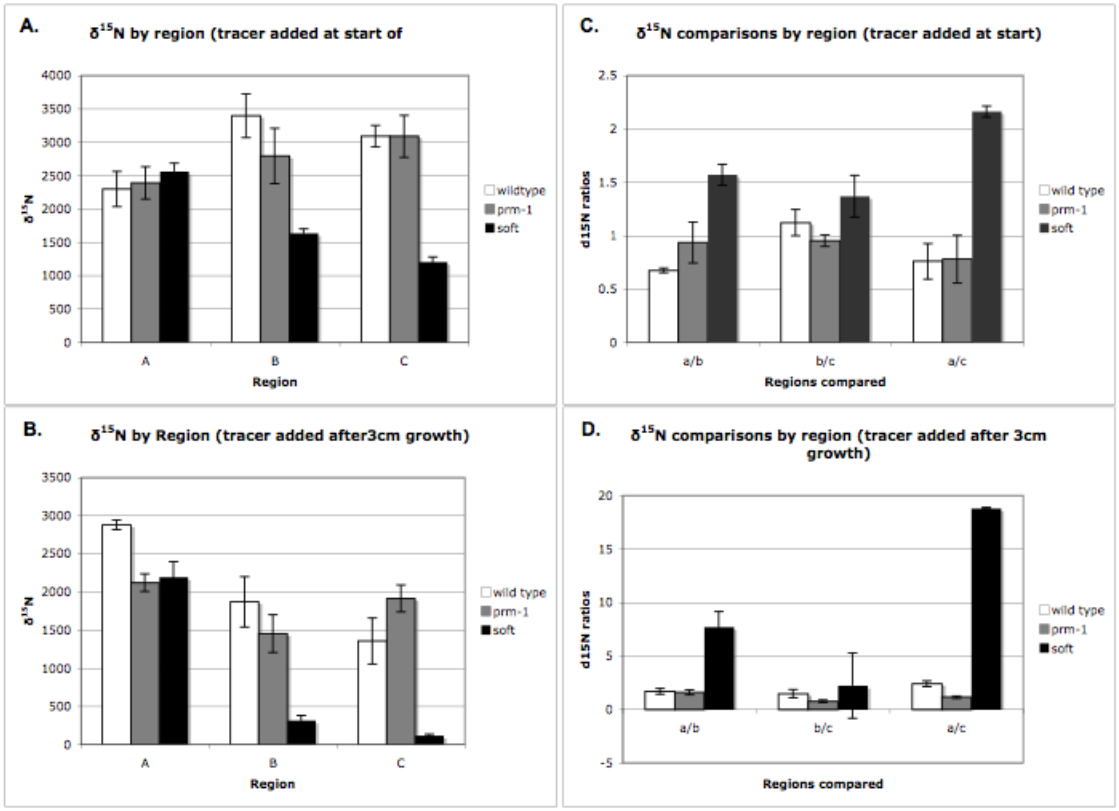
A.
δ15N by region (tracer added at start of
δ15N
Region
A
B
C
wildtype
prm-1
soft
B.
δ15N by Region (tracer added after3cm growth)
δ15N
Region
A
B
C
wild type
prm-1
soft
C.
δ15N comparisons by region (tracer added at start)
d15N ratios
Regions compared
a/b
b/c
a/c
wild type
prm-1
soft
D.
δ15N comparisons by region (tracer added after 3cm growth)
d15N ratios
Regions compared
a/b
b/c
a/c
wild type
prm-1
soft

Figure. 4-5

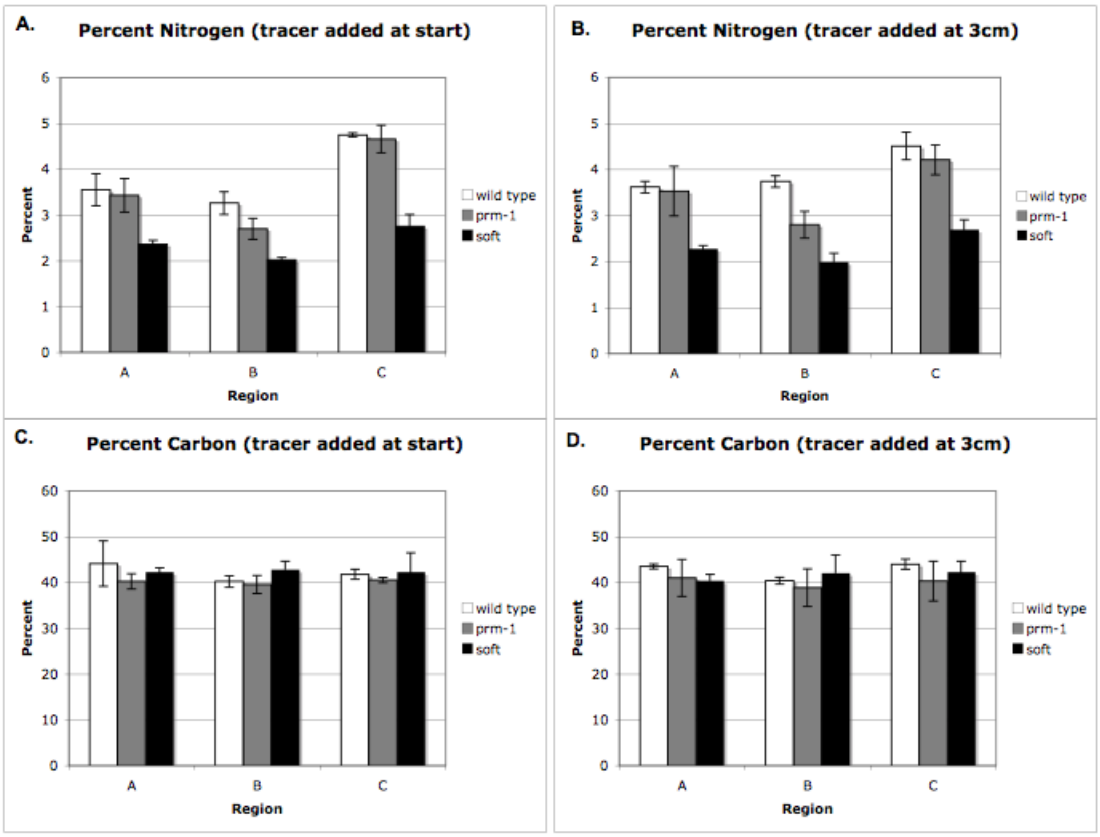
A.
Percent Nitrogen (tracer added at start)
B.
Percent Nitrogen (tracer added at 3cm)
C.
Percent Carbon (tracer added at start)
D.
Percent Carbon (tracer added at 3cm)
Percent
Region
A
B
C
wild type
prm-1
soft

Figure. 4-6

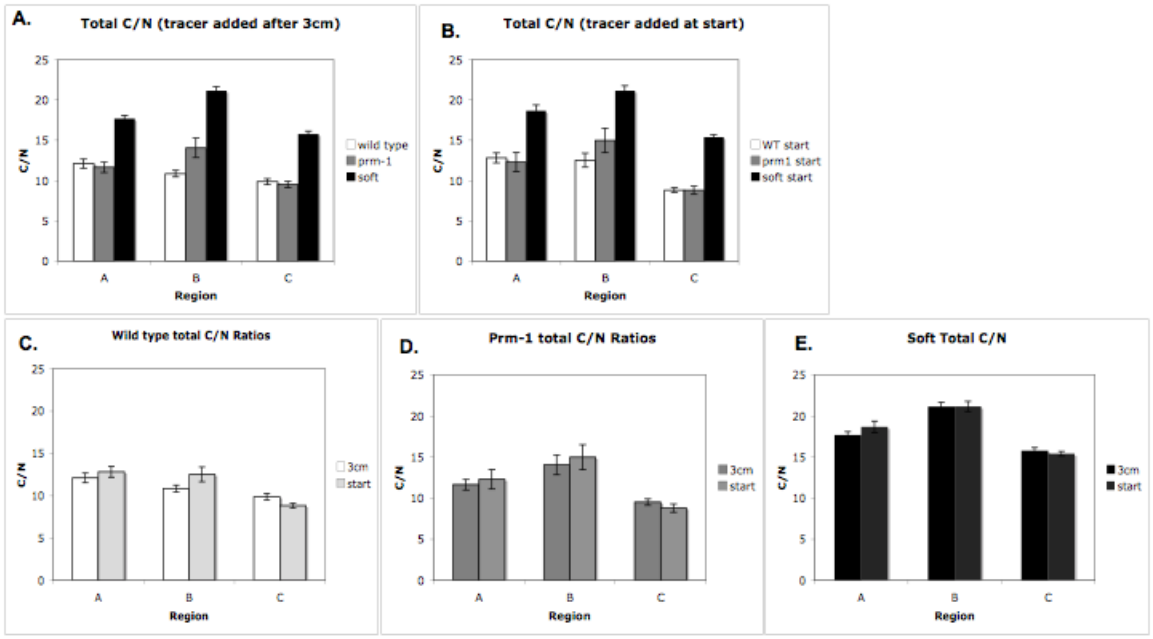
A.
Total C/N (tracer added after 3cm)
C/N
Region
A
B
C
wild type
prm-1
soft
B.
Total C/N (tracer added at start)
WT start
prm1 start
soft start
C.
Wild type total C/N Ratios
3cm
start
D.
Prm-1 total C/N Ratios
E.
Soft Total C/N

Figure. 4-7

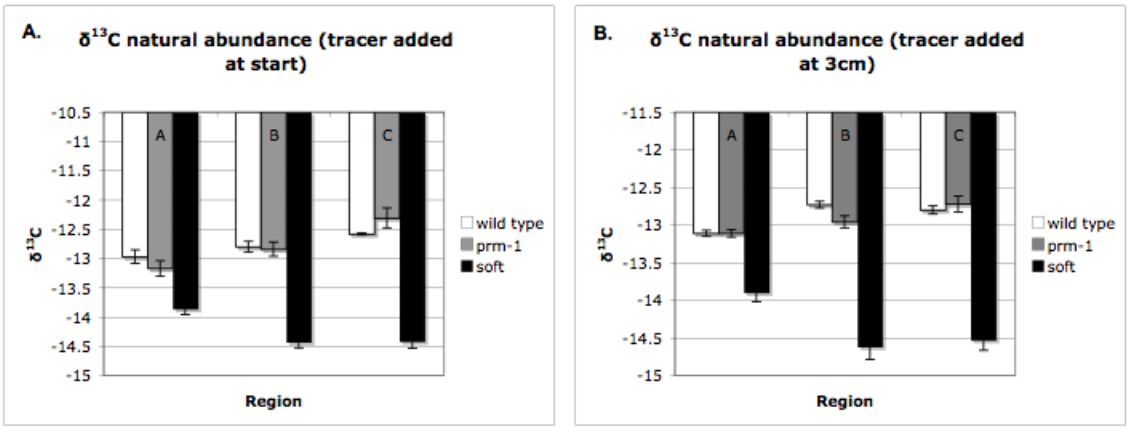
A.
δ13C natural abundance (tracer added at start)
-10.5
-11
-11.5
-12
-12.5
-13
-13.5
-14
-14.5
-15
δ13C
A
B
C
wild type
prm-1
soft
Region
B.
δ13C natural abundance (tracer added at 3cm)
-11.5
-12
-12.5
-13
-13.5
-14
-14.5
-15
δ13C
A
B
C
wild type
prm-1
soft
Region

Figure. 4-8

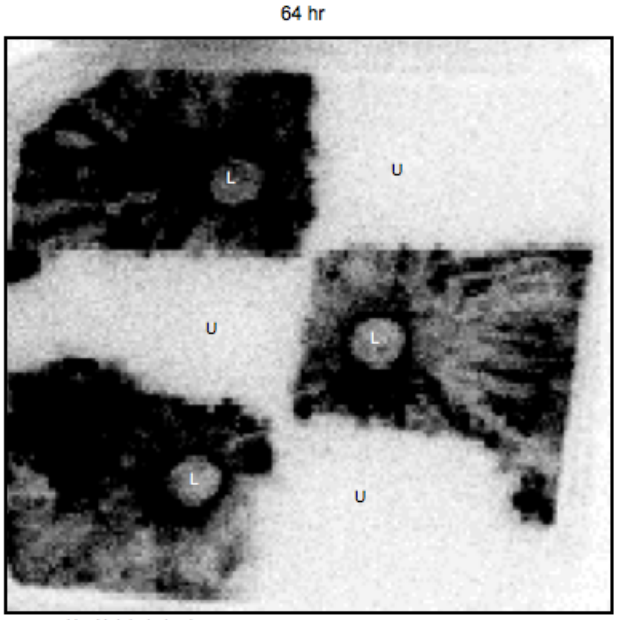


U = Unlabeled colony
L = $^{14}$C AIB labeled colony

Figure. 4-9

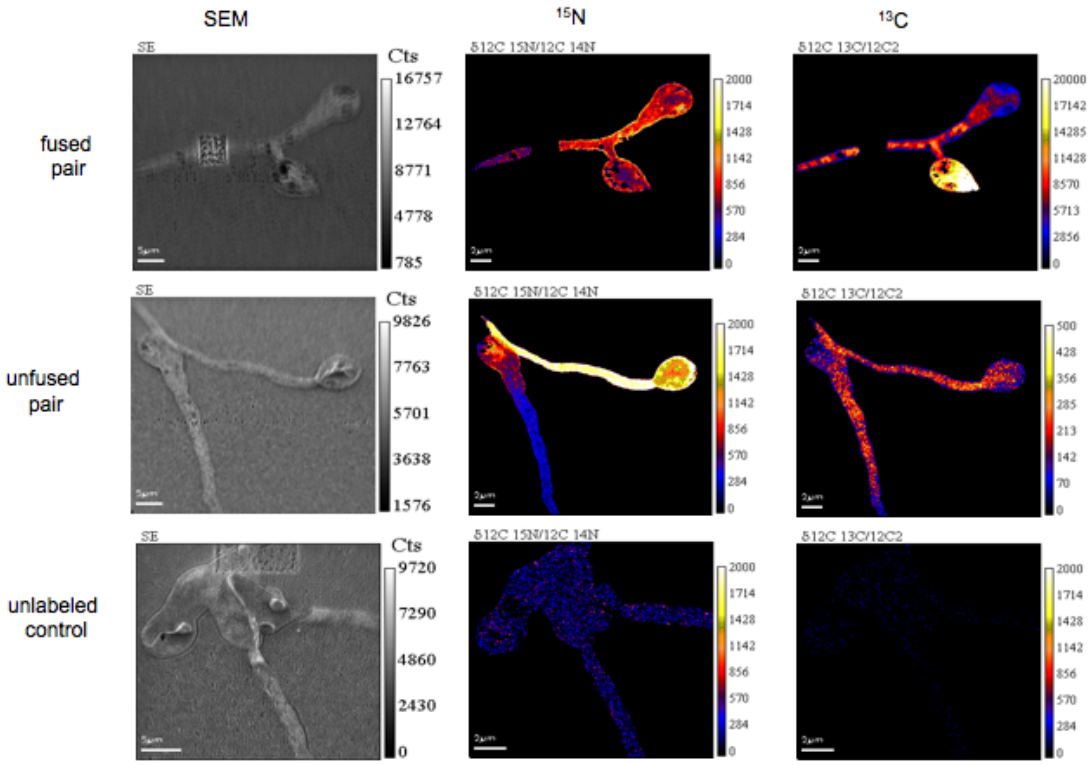
SEM
15N
13C
fused pair
unfused pair
unlabeled control
SE
Cts
δ12C 15N/12C 14N
δ12C 13C/12C2
16757
12764
8771
4778
785
9826
7763
5701
3638
1576
9720
7290
4860
2430
0
2000
1714
1428
1142
856
570
284
20000
17142
14285
11428
8570
5713
2856
500
428
356
285
213
142
70

Figure. 4-10

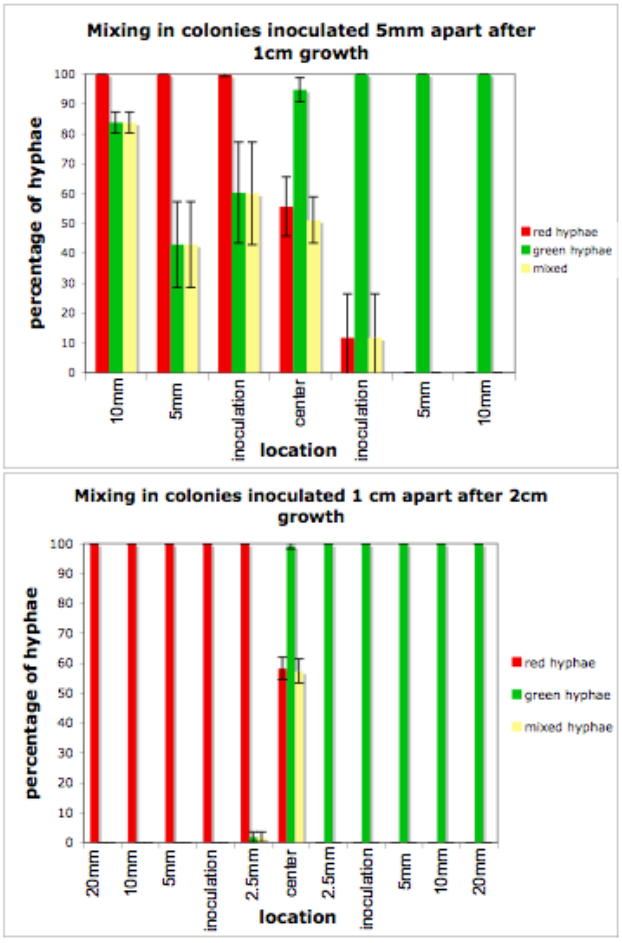
Mixing in colonies inoculated 5mm apart after 1cm growth
percentage of hyphae
100
90
80
70
60
50
40
30
20
10
0
10mm
5mm
inoculation
center
inoculation
5mm
10mm
location
red hyphae
green hyphae
mixed
Mixing in colonies inoculated 1 cm apart after 2cm growth
percentage of hyphae
20mm
10mm
5mm
inoculation
2.5mm
center
2.5mm
inoculation
5mm
10mm
20mm
location
red hyphae
green hyphae
mixed hyphae